STUDY OF FIRE SMOKE FILLING IN BUILDINGS

BY HELIUM SMOKE TESTS

Guanchao Zhao

A Thesis

in

The Department

of

Building, Civil and Environmental Engineering

Presented in Partial Fulfillment of the Requirements
for the Degree of Master of Applied Science (Building Engineering) at
Concordia University
Montreal, Quebec, Canada

August 2012

© Guanchao Zhao, 2012

CONCORDIA UNIVERSITY

School of Graduate Studies

This is to certify that the thesis prepared

By: Guanchao Zhao

Entitled: Study of Fire Smoke Filling in Buildings by Helium Smoke Tests

and submitted in partial fulfillment of the requirements for the degree of

Master of Applied Science (Building Engineering)

complies with the regulations of the University and meets the accepted standards with respect to originality and quality.

Signed by the final examining committee:

_____Samuel Li_____Chair

_____Fariborz Haghighat_____Examiner

_____Hoi Dick Ng_____ Examiner

_____Liangzhu Wang____ _____ Supervisor

Approved by_____

                              Chair of Department or Graduate Program Director

_____2012   _____

                                            Dean of Faculty

ABSTRACT

Study of Fire Smoke Filling in Buildings by Helium Smoke Tests

Guanchao Zhao

One of the commissioning methods for building fire management systems is hot smoke test, in which liquid fuel is burnt to generate a buoyant plume mixed with artificial tracer smoke to model a fire smoke. The method is costly and often causes safety concerns. This thesis proposes an alternative method of "helium smoke test", in which pure helium is supplied to create the buoyant plume. Helium smoke test does not involve burning fuel and it is therefore safer than hot smoke test. This study developed a theoretical model of helium plume, conducted computational fluid dynamics (CFD) simulations to model smoke filling process for helium smoke test, validated the CFD model by the experiments in a full-size and a sub-scale building model, and then applied it to simulations of fire smoke propagations in an actual building and a scaled road tunnel.

Based on the theory of ideal fire smoke plume, the theoretical model was developed to determine the flow rate of helium necessary to achieve the same buoyancy effect as that of the corresponding hot smoke test. An original method was developed in the CFD model, fire dynamics simulator (FDS), to track the smoke layer height based on species concentrations. The FDS model was validated by measured data in a full-size atrium in the literature. To better validate the theoretical and the FDS models of helium smoke test, experiments were conducted in a 1:26.5 sub-scale building model. The smoke was illuminated by laser sheet optics and clear smoke layer height was then recorded. Helium concentrations were measured by a helium analyzer. It is found that helium smoke test can predict smoke layer heights as reasonably well as the corresponding hot smoke test with various fire sizes. The applications of helium smoke test are demonstrated by the simulations in a full-size building test facility and a sub-scale road tunnel at the Institute for Research in Construction of National Research Council Canada (NRC-IRC).

iii

ACKNOWLEDGMENT

Table of Contents

LIST OF FIGURES

LIST OF TABLES

NOMENCLATURE

Cp Specific heat of air at constant pressure, j/K

D Pool diameter, m

g Acceleration due to gravity, m/s^2

l Geometric length scale, m

m Mass burning rate, kg/s

H_f Flame height, m

P Pressure of air, Pa

Q Heat release rate of fire, kW

q_s Smoke flow rate, m^3/s

q_h Helium flow rate, m^3/s

S Area of burning tray, m^2

T_s Smoke temperature, K

T_a Air temperature, K

X_R Radiation fraction

X_a Air ratio of the mixture, %

X_h Helium ratio of the mixture, %

Acronyms

CFD   Computational Fluid Dynamics

FAA   Federal Aviation Administration

FDS   Fire Dynamics Simulator

HeST   Helium Smoke Test

HRR   Heat Release Rate

HST   Hot Smoke Test

LES   Large Eddy Simulation

1. INTRODUCTION

1.1 Background

Fire has long been a common threat to the social safety and property. In Canada, there are many deaths and injuries every year as a result of accidental fires. Table 1.1 shows the summary of fire incidents, deaths, injuries and financial losses in Canada from 1986 to 2000.

Table 1.1 Summary of fire deaths, injuries and losses in Canada 1986-2000 [1].

	Total	Annual Average	Annual Average of First five years	Annual Average of second five years	Annual Average of last five years
Number of Fires	954,331	63,622	68,083	66,199	56,584
Fire Deaths	6,408	427	506	397	379
Fire Injuries	51,212	3,414	3,722	3,581	2,890
Fire Losses in CND (billions)	17.2	1.1	1.0	1.1	1.2

It was observed that the overall trend of fires decreased during this period. In the last five years of the period, the fire incidents average declined by 16% to 56,584 which is below the period average of 63,622; the fire deaths average declined by 25 % to 379 which is below the period average 427; and the fire injuries average declined by 23% to 2,890 which is below the period average of 3,414 [1]. Better building fire smoke management system has helped a lot in preventing the fire hazard, but cost more for modern building structures and materials.

It is also important to note that the major causes of fires are heating equipment, cooking equipment, electrical distribution system and smoking. Failures of mechanical systems and electrical systems are leading factors for fire incidents in building environment. For a metropolitan city like Montreal, there are occasions that no smoke detection system is installed in residences; emergency exits of a building are illegally locked to avoid thefts; fire escapes are blocked by renovations or new constructions. The lack of smoke detection system or its malfunction is found to double the fatalities during fires in Quebec [2].

1.2 Commissioning of Fire Smoke Management System

1.2.1 Overview of Commissioning Method

In buildings, smoke or toxic gases are considered the major cause of fatalities instead of fire burns [3]. Fire smoke management system, often referred to as smoke control or smoke exhaust system, plays an important role as a component in building's fire protection and life safety system [4]. An effective smoke management system could limit the spread of fire, provide smoke free stair shafts and other tenable conditions for people evacuating from building during a fire. Due to its great importance, the reliability of smoke management system needs to be validated by special commissioning methods.

Commissioning is one of the most important prevention procedures to assess the performance of a whole smoke management system, which includes smoke detection, functionality of emergency exits and fire escapes, and where available, sequence of control, ventilation operation, and smoke layer heights for safe escape. A proper

commissioning should begin with design phase, and then to be demonstrated during construction and operation [5].

Once the smoke management system has been installed, there would be ideally three components of testing [4]:

Functional testing: The goal of functional testing is to confirm the whole system works as intended, especially, when and how the fans and dampers will operate.

Performance testing: In performance testing, testing personnel focus on the achievement of expected air flow rate, air velocity and pressure difference are achieved.

Demonstration testing: In demonstration testing, airflow patterns caused by smoke management system are shown by using visible smoke such as theatrical smoke or smoke bombs. Visible smoke could clearly show the air movement. With a good understanding of its advantages and disadvantages, visible smoke could provide valuable lessons about modification and improvement of the smoke management system on both design and operation.

1.2.2 Hot Smoke Test

In conventional demonstration testing, unheated theatrical smoke (so-called "cold smoke") provides a means to visualize the flow pattern, but cannot simulate a real fire smoke. The Commonwealth Scientific and Industrial Research Organization (CSIRO) and the South Australian Metropolitan Fire Services (SAMFS) developed a commissioning method called hot smoke test (HST) in the early 1990s [6]. The hot smoke test uses simulated fire

conditions to assess the functionality of the completed building and the installed smoke management system. The standardized test procedure uses a small clean burning liquid fire, e.g. methylated spirit, to provide buoyant plume and artificial smoke is introduced into the plume as a tracer to identify the location of the smoke plume and hot gas layer. One of the current editions of hot smoke test standard is Australian Standard, Smoke management systems - Hot smoke test AS 4391-1999 [7].

1.2.2.1 Test Apparatus and Data Measurement

A typical set of test apparatus in a hot smoke test is shown in Figure 1.1, followed by detailed description of each part of apparatus.
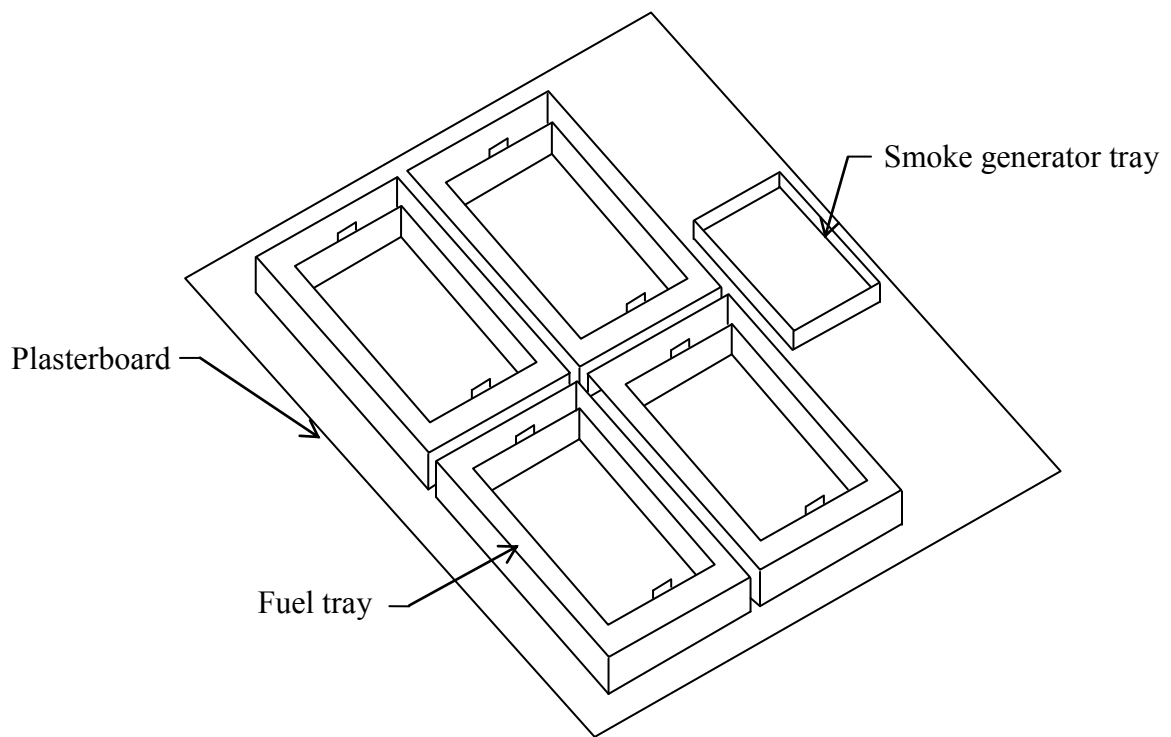
Figure 1.1 Typical set of hot smoke test apparatus, without smoke distribution system release to center of hot plume.

- Non-combustible base

4

A non-combustible base should be no less than 13 mm thick plasterboard. The plasterboard should be large enough that all equipment resting on that would keep a minimum of 1.5 m to the edge of the base.

- Fire trays

The fire trays should be constructed with steel and welded to be watertight during the whole test. Size of fire trays are based on ISO international paper sizes.

- Water bath

The water bath should be constructed with galvanized steel sheet and welded to be watertight during the whole test. Steel rod handles with 10 mm diameter should be welded to the inside wall of tray.

- Heat sensor

Thermocouples or temperature sensors act as heat sensors. Type K thermocouples are highly recommended when ceiling temperatures to be logged with respect to time.

- Tracer smoke

Tracer smoke shall be non-toxic, non-reacting, neutral PH and white in color. The heat from the fire shall have a minimal effect on the tracer smoke. The tracer smoke system could include a distribution system or a smoke generator located adjacent to the fire trays.

- Fuel

To achieve a steady state of burning time no less than 10 minutes, quantities of methylated spirit for different fire tray sizes are recommended by the standard [7].

During a hot smoke test, static photograph, video recording and ceiling temperature are mandatory to be recorded. Plume temperature, smoke obstruction, mass loss of the fuel and radiated heat intensity are often recorded too.

1.2.2.2 Applications

For real commissioning work, there have been a number of applications of hot smoke test. CISRO conducted a series of hot smoke test in many Australian tunnels [6]. Hot smoke tests successfully demonstrated the performance of smoke management system in these tunnels, for example, make-up air provision, pressurization system, smoke baffles and adverse effect of external wind for natural ventilated tunnels.

Figure 1.2 Hot smoke test in city link road tunnel, Melbourne [6].

In scientific research field, people use full-scale test facilities to study the smoke filling process in buildings with large interior spaces, for instance, atria [8]. Due to its large vertical space, the smoke plume in atria is much bigger than that in tunnels and other longitudinal spaces. Thus the study is more challenging and need to be carefully examined. The lesson learned from these tests could help to study of natural smoke filling process and other design parameters for smoke management system.

Because full-scale testing is often costly and involves much time and effort, sub-scale or laboratory-scale testing are preferred by many researchers [9, 10, 11]. Note that when sub-scale model is applied, the scaling laws for each parameter need to be examined to keep certain consistency to full-scale test. Detailed discussion of scaling laws will be presented in Chapter 3.

Besides experimental studies, numerical studies of hot smoke tests are also well received by fire safety engineers and researchers [12, 13, 14]. Among different approaches, Fire Dynamic Simulator (FDS) models developed by the US National Institute of Standards and Technology (NIST) are widely used. FDS is a large eddy simulation (LES) computational fluid dynamics (CFD) model, which numerically solves the Navier-Stokes equations for heat transfer and smoke from fire [15]. The numerical model was found to predict smoke flow pattern, pressure and temperature well, but such model still calls for validations by field test data [10].

1.2.3 Limitations

Because of a real fire involved to simulate an actual fire, hot smoke test has several limitations:

a). The smoke temperature must be safe so that no damages will happen to the building structures. Temperatures in the ceiling jet above the fire must be limited to less than the sprinkler's activation temperature [7]. The smoke temperatures are often about 55°C, which is therefore much lower than those expected in a real fire, even for a fire plume cooled by sprinkler spray fire where temperatures are typically still in the vicinity of 100°C or more.

b). The fire growth is close to instantaneous, which is not consistent with a typical fire growth. Smoke exhaust systems activated by smoke detection designed for early occupant warning would typically activate at an early stage of a fire. In hot smoke test, smoke exhaust activation may occur in 30 seconds with a substantial smoke layer already moving through a space.

c). Besides the high expenditure of the test itself, the necessary risk assessment measures and insurance coverage increase the total cost of hot smoke test.

1.3 Objectives and Thesis Outline

As a result of the limitations abovementioned, building owners are often not in favor of hot smoke test, which is also not mandatory by most of the building codes. Given the fact that the use of fire in a hot smoke test is not to establish real fire conditions but to generate thermally buoyant smoke [7], many researchers started to think of alternative ways to simulate this buoyant smoke with reduced density, for instant, using helium or helium-air mixture. This non-toxic, non-reactive neutral gas is the second lightest gas been found in the universe, while the lightest gas, hydrogen, has a very unstable chemistry properties.

In this thesis, a method called helium smoke test (HeST) using pure helium as buoyant source is proposed. To directly and conveniently correlate the helium smoke to a fire smoke, a full-scale experiment with adequate measured data in the literature [8] is chosen to be reproduced by numerical model. The numerical model was first validated by comparing the predicted temperatures with measured data. After that, with scaling laws been applied, a sub-scale numerical model was also built to verify the scaling parameters.

There are limited data of helium smoke test for fire smoke filling in buildings. To provide such data and perform a credible analysis, it is necessary to conduct experiment on helium smoke test in physical models. A sub-scale acrylic building model was then built to provide measurement data and further verify the numerical models.

In helium smoke test, helium flow rate was determined from an analysis of atrium smoke filling based on the theory of ideal smoke plume. Smoke layer height results are compared to better understand the smoke filling process. Helium concentrations in helium smoke test were compared with thermocouple results in hot smoke test at the same measuring locations using non-dimensional values. Also visual inspection was realized by using laser optics and artificial smoke from commercial smoke machine. Video camera was used to record the images.

With the numerical model of helium smoke test developed and verified, we apply the method in other building environment to confirm its applicability, especially when physical experiments are not available. Applications of numerical model of helium smoke test are demonstrated in a full-scale fire testing facility and sub-scale road tunnel built in Institute for Research in Construction of National Research Council Canada (NRC-IRC).

9

1.3.1 Research Objectives

The research objectives of this thesis are:

- To develop a theoretical model from ideal smoke plume to simulate hot smoke from fire using pure helium as buoyant source.

  With this theoretical model, helium flow rate in helium smoke test could be directly calculated according to the heat release rate of fire.

- To develop a numerical (CFD) modeling approach simulating hot smoke test and helium smoke test.

  In the CFD models, a smoke generator was modeled to provide artificial smoke as the fire/helium source. This artificial smoke could not only clearly show the air movement inside the enclosure, but also help to record the smoke layer height through the simulation. Thus, qualitative and quantitative comparison between hot smoke test and helium smoke test could be performed. This method could also be applied in other studies of hot smoke test and helium smoke test.

- Validate the numerical model with real experiment measurements.

  Both full-scale and sub-scale experiment data are selected to validate the numerical model. Specific comparison of parameters of fire engineers' interest should be performed using appropriate method, e.g. non-dimensional values.

- Verify the developed method in various building configurations.

  Through verifications of helium smoke test model in other building configurations, helium smoke test is proved to be a useful commissioning method when hot smoke test is difficult to be conducted.

1.3.2 Thesis Outlines

Chapter 2 presents a literature review of using buoyant smoke by helium or helium-air mixture in study fire smoke in various applications. Field tests, sub-scale experiments and laboratory-scale tests were found to provide some confidence to use helium as buoyant source when simulating fire smoke, although some limitations are observed.

Chapter 3 presents a theoretical method to determine the helium flow rate when simulating specific fire size. Scaling laws for sub-scale tests is also discussed. Determination methods of smoke layer height from literatures are presented, and a new method in CFD model is developed by tracking the species concentrations.

Chapter 4 validates the numerical model and scaling law by full-scale test measurement from the literature. A grid sensitive study was conducted to obtain grid-independent results for CFD modeling. This chapter then introduced a sub-scale physical model built at Concordia University fire research lab. A helium supply system, gas sampling system and visual illustration system are described in details.

Chapter 5 analyzes the results of numerical simulations and sub-scale experiment. The comparison includes temperature, helium concentration, visual inspection and smoke optical density.

Chapter 6 demonstrates applications using helium smoke test in a full-scale test facility and a sub-scale road tunnel model. The goal of the application is to check if helium smoke test is practical for real cases.

Finally, conclusions are drawn and the future research work is suggested in Chapter 7.

2. LITERATURE REVIEW

This chapter presents several cases using helium or helium-air mixture in simulating buoyant smoke. A summary of calculation methods to determine the helium flow rate are also found in the literature, which is discussed in Chapter 3. Some key features of helium buoyant smoke are studied and compared to fire smoke. Principles of such buoyant smoke are examined by both numerical and experimental studies.

Some typical experimental set-ups as well as CFD models are presented in this chapter under specific sub-titles. The goal is to give a general idea on using helium smoke test in different environment. Note that here we call all tests using helium or helium-air mixture as helium smoke test and HeST in abbreviation.

2.1 Helium Smoke Test in Aircraft Test Applications

Maylor [16] from U.S. Federal Aviation Administration (FAA) evaluated the capability of environmental control system modifications to enhance the venting of neutral or buoyant smoke during a fire emergency in the passenger cabin. Artificially generated smoke with and without helium gas added were released at various locations in the cabin. Smoke movements were recorded by smoke meters, video cameras and observation notes during the series of tests.

In this study, helium smoke mixing chamber was developed at FAA to provide a smoke source of 200 cubic foot per minute equivalent to hot air at around 475 °F (Fig 2.1).
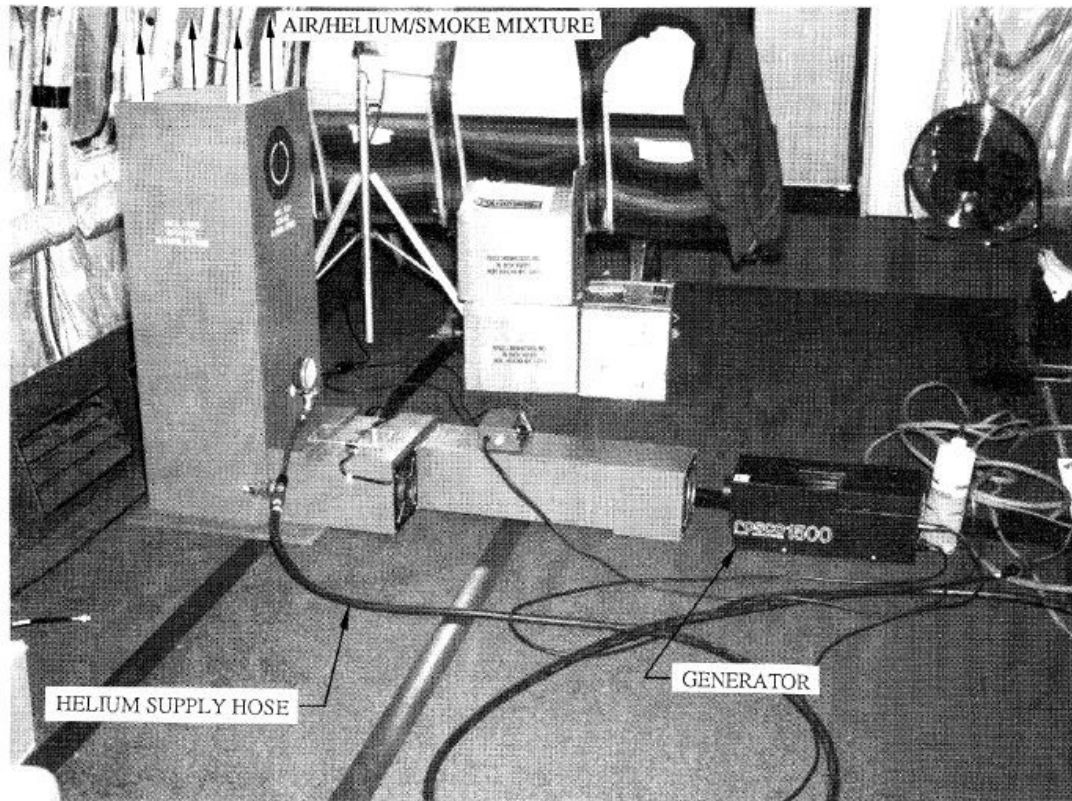
Figure 2.1 Helium smoke mixing chamber [16].

Special smoke density data acquisition system were developed and operated by FAA in the tests. Smoke meters were mounted at seat height and standing height above the floor, distributed evenly along the length of the aircraft cabin. Each smoke meter includes a photocell at one end inside a cylindrical light trap, and a light source on the other end. Smoke meters operate on a DC power supply. Details of the smoke meter are shown in Figure 2.2
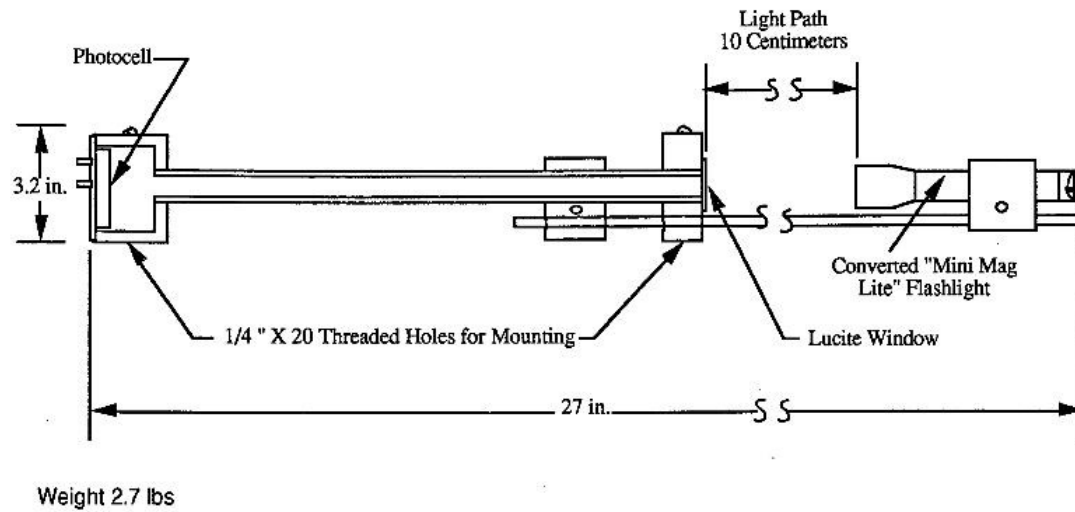
Figure 2.2 Smoke meter schematic [16].

In the tests using smoke with helium added, smoke density measurements were found to well represent the cabin conditions. But when using non-buoyant smoke without helium added, the smoke meters could not give a consistent measurement to the visual inspection.

Maylor [16] pointed out that when doing experiment with more artificial smoke generated, smoke density data recorded by smoke meters contains fewer errors than those with less smoke generated. The instrumentation "noise" which is in proportion to the signal should be kept below a certain level so the data analysis could be more accurate. This shows the great need to balance between the smoke yield best suited for video recording and that best suited for optimal smoke density measurement. Maylor also provided another potential solution, which was to increase the light path of smoke meter from current 10 centimeters to 0.5 meters.

14

Eklund [17] developed a buoyant artificial smoke generator in tests of aircraft cabin ventilation system. In this device, 200 cubic feet per minute flow of gas mixture of 50 % helium and 50 % air is used to simulate a hot gas from fire at 475 °F. The helium component not only provides the buoyant effect but also simulates the gaseous expansion of a fire smoke. Theatrical smoke was mixed with such gas mixture to help visual observation of smoke movement. The aerosol component could help in applications of smoke detection tests.

It was also found that the helium concentration tends to be constant downstream of a plume, which results in a stable buoyancy effect. This is inconsistent with an actual fire, where smoke temperature decreases downstream due to the loss of heat to the surrounding environment [18].

Besides the tests in passenger cabins, FAA [19] then developed a test procedure, which also mixes 50 % helium and 50 % air on a volumetric basis, to certify the smoke detection systems of aircraft cargo compartment. In such tests, a device called Helium Smoke Generator was patented by the engineering personnel at FAA Technical Center in 1991 [20]. This equipment could simulate a smoke plume at ambient temperatures with the same buoyant properties as those produced by real fire. The equipment was then used in smoke penetration and evacuation tests.

2.2 Helium Smoke Test in Sub-Scale Tunnel Model

Another typical longitudinal space, where fire could be a major risk, is road tunnel. In case of fire, combustion smoke will spread rapidly through the tunnel, causes reduced visibility for evacuation and deaths by asphyxiation. To study the control of smoke

propagation, Vauquelin et al. [21] developed an isothermal model based on continuous release of a mixture of air and helium gas in a 1:20 sub-scale tunnel (Fig 2.3, 2.4) to study longitudinal and transverse smoke control system. Mixing ratio of helium and air were determined by theoretical model of buoyant jet and ideal plume [22]. So by using the equations developed, a buoyant smoke source could be calculated to represent a fire smoke plume under specific conditions. Detailed discussion of calculation of helium and airflow rate and mixing ratio will be shown in Chapter 3. Also the theoretical model demonstrated that the air component in the mixture only increases total flow rate and decreases the density deficit to make sure the simulated smoke is coherent with the corresponding fire smoke [22].
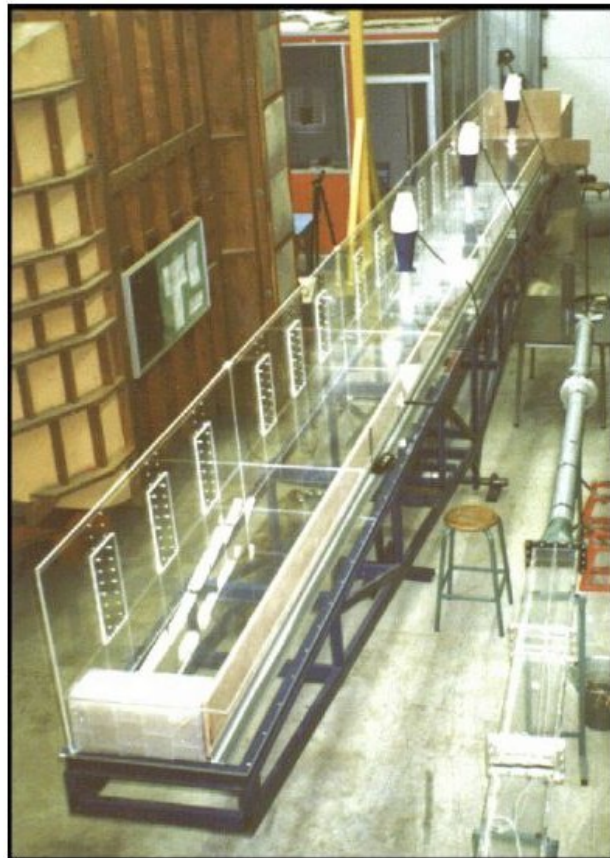
Figure 2.3 Sub-scale tunnel model [22].

(a)

(b)
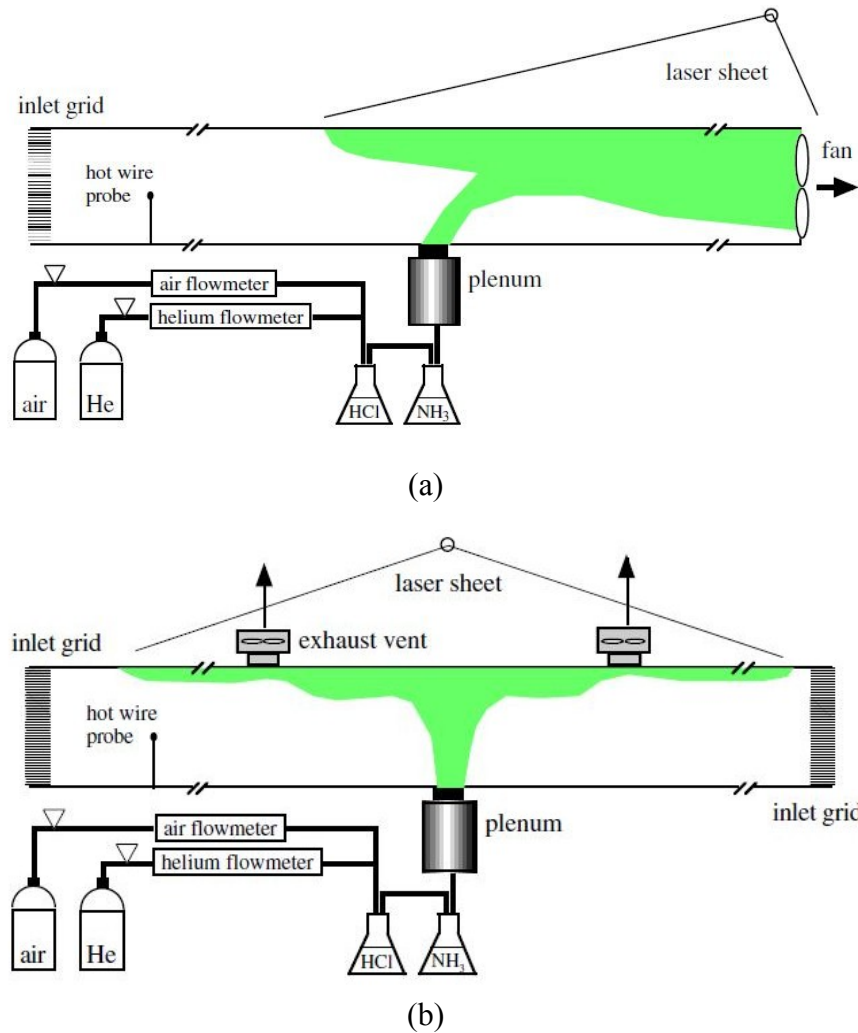
Figure 2.4 Experimental set-up for (a) longitudinal, (b) transverse smoke control tests [22].

Vauquelin [21] found this method to be a suitable tool to understand some flow phenomena, to get order of magnitude, and help to build simple but predictive models. Especially for tunnel smoke control system, such method could be an revolutionary help in design of ventilation and its automation systems.

Limitations are also found that such test could gather quantitative information, but in practical applications, the design which provides minimal extraction flow rate is not satisfactory to accurately design the ventilation system.

2.3 Helium Smoke Test in Sub-Scale Enclosure Experiment

Bryant [23] conducted sub-scale convective analog experiments using helium plume as the buoyant source to study its velocity through the doorway of an enclosure. The experiment was scaled to be 0.55 of the full-size experiment with fire. Particle Imaging Velocimetry (PIV) was also used in this sub-scale experiment. Detailed experimental set-ups are illustrated as follows,

- Sub-scale enclosure

Dimensions of the experiment enclosure were 1.53 m × 1.16 m × 1.53 m (width × height × length). Plexiglas was used to construct the walls of the enclosure to ensure visible light could pass through for PIV measurements. Locations and dimensions of doorway and helium flow inlet were shown in Figure 2.5 and Figure 2.6.
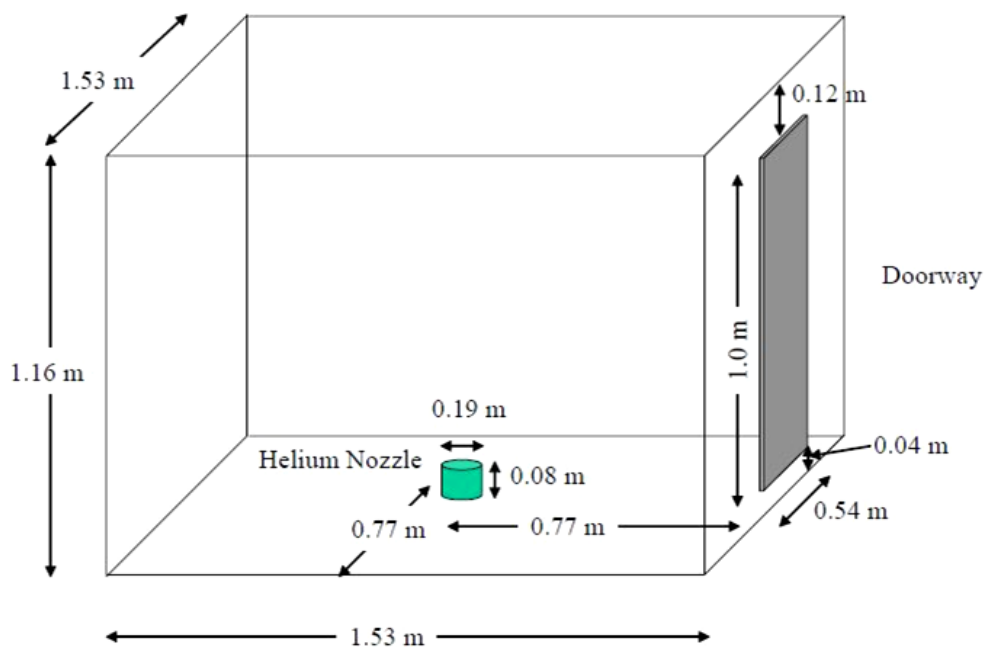
Figure 2.5 Schematic of sub-scale enclosure set-up with helium flow inlet at floor [23].

Figure 2.6 Photograph of sub-scale enclosure set-up [23].

- Helium flow system

Helium flow was provided by standard high pressure helium cylinders. Pressure gauges and flow meters were used to control the volumetric flow rate (Figure 2.7). A section of honeycombs were located at the flow exit to provide flow uniformity.
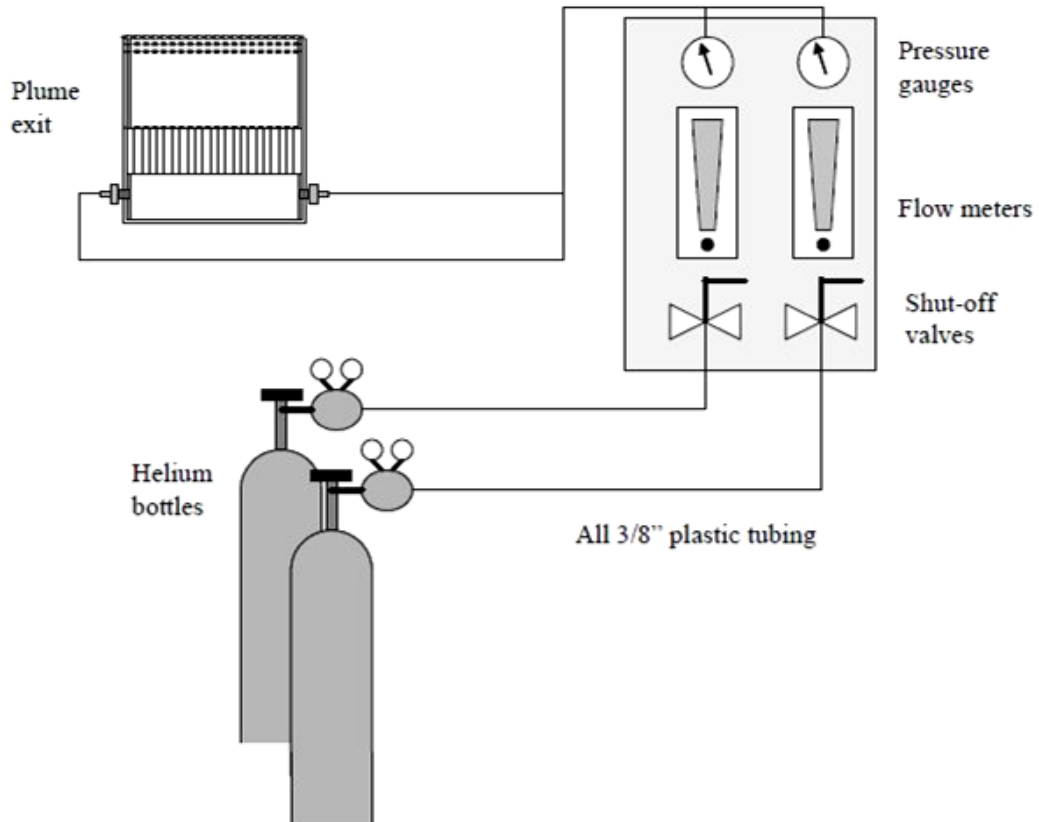
Figure 2.7 Schematic of helium flow system [23].

- Gas sampling system

A gas sampling system was designed to measure oxygen concentration so the mixture density could be calculated. A gas sampling pump provides the pressure different to pull

the sample gas from the flow and push it to a portable oxygen gas analyzer. A schematic of such gas sampling system is shown in Figure 2.8.
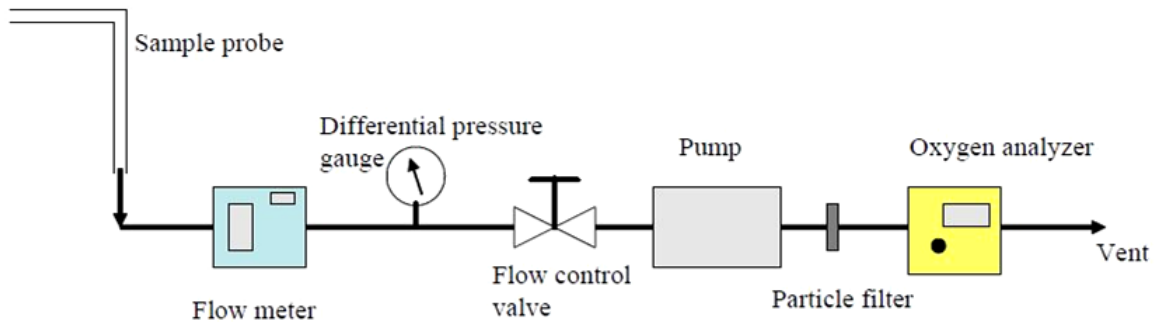
Figure 2.8 Gas sampling system to measure oxygen concentration [23].

In this study, fire scaling laws derived from the non-dimensional Navier-Stokes equations are developed and discussed. Furthermore, PIV provides reasonable and useful measurements in sub-scale experiments, which shows potential success in full-size applications. However, shortcomings of using PIV measurements for real fires should be quantified, especially for the thermally stratified outflows.

2.4 Helium Smoke in Laboratory-Scale Experiments

In typical pool fires, periodic pulsation has been observed by many researchers [24]. Hot smoke-laden gases from pool fires are characterized as a buoyant plume, which are of great interest in many engineering applications. To fully understand the behaviour of buoyant plume and its oscillations, Cetegen and Kasper [24] conducted experiments on the oscillatory behaviour of axisymmetric buoyant plumes of pure helium and helium-air mixtures, using a range of nozzle sizes (3.6 cm to 20 cm), source velocities and plume densities. Schematic of experimental set-up is shown in Figure 2.9 as below. In the series

21

of tests, Laser Doppler Velocimetry was used to measure the velocity as well as pulsation frequencies of buoyant plumes.
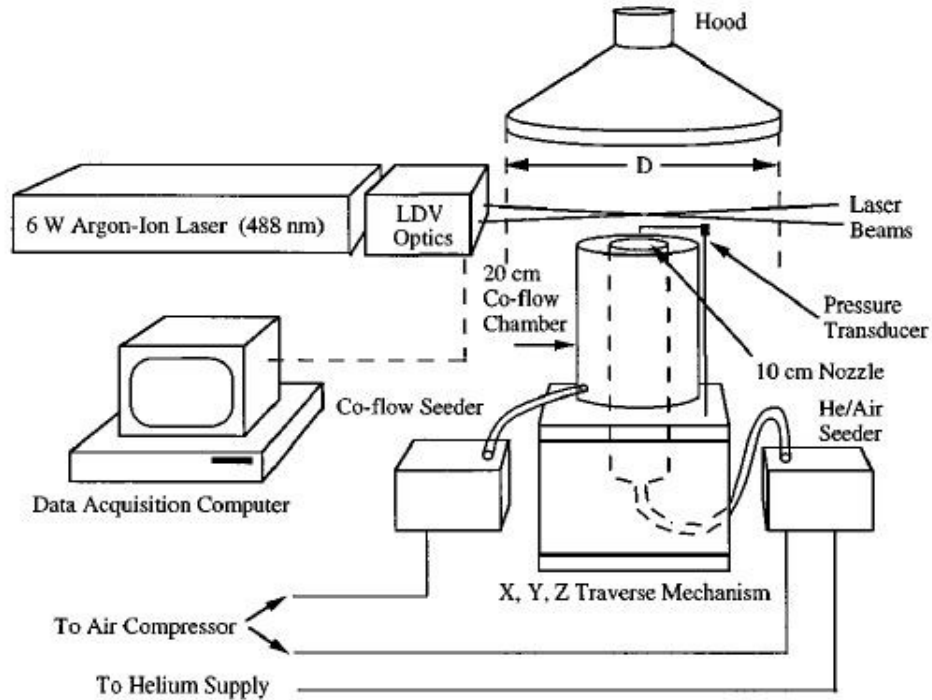
Figure 2.9 Schematic of experimental set-up [24].

They found these non-reacting buoyant plumes exhibit periodic oscillations of plume boundaries, followed with formation of toroidal vortices. Although the frequency scaling is not the same, these phenomena are found to be similar to those observed in pool fires.

O'Hern et al. [25] conducted an experiment to study the behaviour of large fully turbulent helium plume. Through the measurement of velocity and mass concentration, the measured data were then used to develop and validate sub-scale turbulence models [26, 27]. This helium plume experiment is of great convenience to study the turbulence

22

generated by buoyancy, compare to fire model, whose hot smoky plume contains complex combustion chemistry.

2.5 Helium Smoke Test in Residential Garage

Hydrogen-powered vehicle has been a trend all over the world. However, storage of vehicle with hydrogen cells in garages without specific ventilation system and fire detection system could be a potential risk. Due to its active chemistry properties, hydrogen could not be used or not preferred by researchers in field tests. As a result, helium has been chosen to do the job due to its chemical stability.

Swain et al. [28] conducted full-scale experiments to study the ventilation requirements for storage of hydrogen vehicles in a single car garage. The leaked hydrogen was simulated by helium at a flow rate of 7,200 liter/hour. While the field test focus on the modifications of garage ventilation system, a CFD simulation compared the concentration of hydrogen and helium at same locations. Results showed that no more than 15 % difference was observed between the concentration of hydrogen model and helium model.

Later Papanikolaou and Venetsanos [29] performed CFD simulations of Swain's experiment using standard k-ε turbulence model. Three different vent heights were modeled. In each case, the predicted concentrations were compared with the experiment measurement data while shown in Figure 2.10.
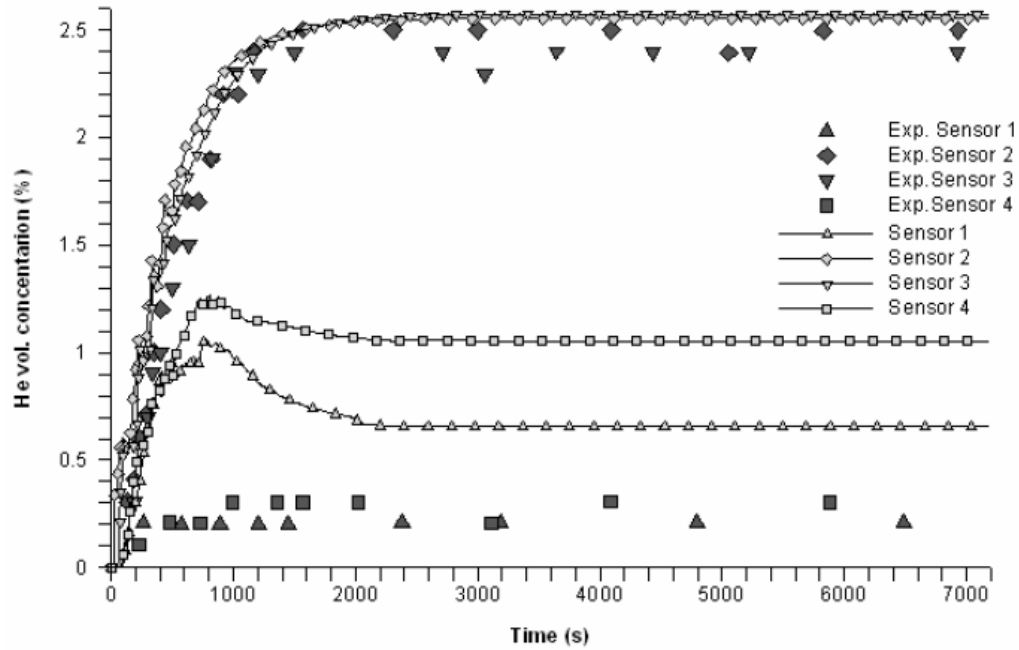
Figure 2.10 Predicted helium concentrations versus experiment measurements in (A) case 1 [29].

From Figure 2.10, predicted helium concentrations are in acceptable agreement with measurement data. In addition, predicted profile of helium concentration could be used to show the air flow pattern (Figure 2.11).
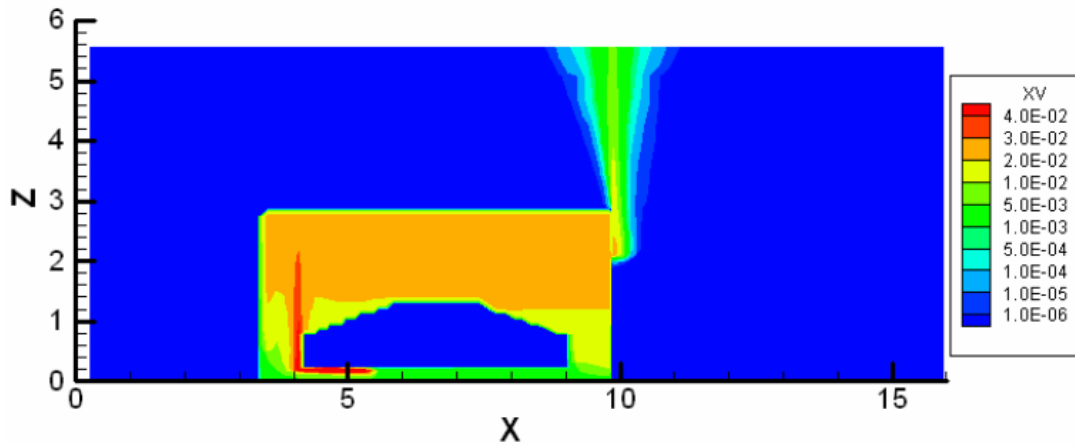
Figure 2.11 Contours of helium concentration at symmetry plane at 3,600s in case 1 [29].

Thus, it confirms that helium could provide a safer way to perform experiment inside hydrogen-powered vehicle garages. The authors considered the CFD methodology to be important to evaluate the hazards under complex conditions [29].

2.6 Summary

Literatures of using helium as buoyancy source in simulating hot fire smoke are presented above. In the FAA aircraft tests, helium smoke generator clearly showed the smoke movement inside aircraft compartment. Measurement methods are evaluated, visual inspections validated the principles. In sub-scale tunnel experiment, a method was provided by the author to determine the helium flow rate to simulate the corresponding fire smoke. However, the total flow rate was found to be too huge in real applications. In Chapter 3, a theoretical study of ideal plume and buoyancy flux will be conducted; a smaller required flow rate of helium is achieved. Ventilation system was examined by supplying helium-air mixture into the sub-scale tunnel model. Sub-scale experiments also showed the importance of application of scaling method. The literature review also shows the confidence to use helium gas in simulating pool fires. Furthermore, CFD modeling was used and provided acceptable results to investigate the airflow patterns and species concentrations.

In summary, helium smoke performs well when used to replace fire smoke in many previous studies. However, applications of using such method in buildings are found to be limited. Compared to tunnels or aircraft compartments, which are characterized by

longitudinal and/or horizontal spaces, buildings are comprised of multiple spaces with various sizes and complicated ventilation systems. In particular, large vertical spaces, e.g. atria, represent one of the many cases that distinguish building environment from aircrafts or tunnels. In an atrium, the size of smoke plume is much bigger than that in aircraft and tunnel environments. The application of HeST in these spaces is therefore more challenging and needs to be examined.

3. THEORY

As illustrated by the literature review, numerical and experimental approaches and/or combination of them were well accepted methods for a comprehensive study of HeST. So in this study, both approaches are applied to help fully understand the smoke filling process of HeST in building environment.

This chapter presents an overall theoretical background of HeST, including the determination of helium flow rate to achieve the same buoyant plume as fire plume, scaling laws for appropriate sub-scale modeling, CFD modeling principles and a new method to determine the smoke layer height in CFD model.

3.1 Helium Buoyant Plume

Vauquelin et al. [22] developed a HeST method by supplying a mixture of helium and air into a sub-scale tunnel to simulate tunnel fires. They suggested a relation of the buoyant plumes between HeST and HST based on buoyancy flux, in term of B. However, it was found that the required total supply flow rate is too huge to be practically used for full-scale facilities when helium and air mixture is used. Therefore, the method was limited to laboratory-scale tests.

In Vauquelin's method, air component in the helium-air mixture only provides the required total flow rate and reduces the density deficit. No air entrainment rate was considered in the helium-air plume while the total flow rate was calculated by using the ceiling temperature [22]. In this study, we propose using pure helium instead of helium and air mixture to simulate fire smoke with the same buoyancy effect. This section shows

how to determine the amount of helium necessary to create the same buoyancy as a fire smoke for a given heat release rate.

(a) Hot smoke test   (b) Helium smoke test
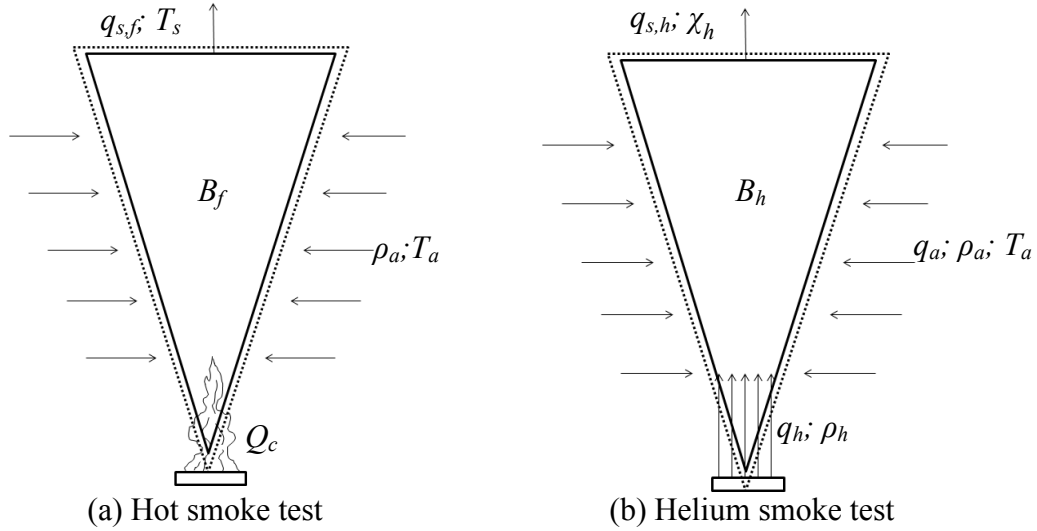
Figure 3.1 Schematics of the ideal plumes in (a) hot and (b) helium smoke tests.

Figure 3.1 shows the ideal plume models for the HST and the HeST. For a fire plume, the convective heat release rate (HRR), Q_c in kW, is calculated by

$$Q_c = \rho_s C_p q_{s,f} (T_s - T_a) \tag{3.1}$$

The buoyancy flux of a buoyant plume, B in m^4/s^3, is defined by:

$$B = g q_{s,f} \left(\frac{\rho_a - \rho_s}{\rho_a} \right) \tag{3.2}$$

Where ρ_s is the smoke density in kg/m^3, ρ_a is the surrounding air density in kg/m^3, g is the acceleration of gravity in m/s^2, C_p is the specific heat capacity in kJ/ (kg·K), $q_{s,f}$ is the volumetric flow rate of the fire plume in m^3/s, and T_s and T_a are the temperatures in

Kelvin of the smoke and the surrounding air, respectively. The buoyancy flux remains

constant at all heights of the plume [30].

Using the ideal gas law and combining Equations. (3.1) and (3.2),

$$Q_c = (\frac{\rho_a C_p T_a}{g})B \tag{3.3}$$

Eq. (3.3) shows a relation of convective heat release rate and buoyancy flux for a given

ambient condition.

In the HeST with pure helium, the same buoyant plume and smoke filling process as that

of the HST are considered to be created when:

$$B_h = B_f \tag{3.4a}$$

$$q_{s,h} = q_{s,f} \tag{3.4b}$$

where B_h is the buoyancy flux and $q_{s,h}$ is the volumetric flow rate of a helium smoke. B_f is

the buoyancy flux and $q_{s,f}$ is the volumetric flow rate of a fire smoke.

As shown in Figure 3.1(b), the pure helium is supplied at a rate of q_h, and mixed with the

entrained air at a rate of q_a. The resultant volumetric plume flow rate is therefore

$$q_{s,h} = q_h + q_a \tag{3.5}$$

The mixture density is then calculated by

$$\rho_s = \chi_a \rho_a + \chi_h \rho_h \tag{3.6}$$

where χ_a and χ_h is the volumetric fraction at a specific plume height of air and helium, respectively.

So the required volumetric flow rate of helium, q_h in m³/s, can be obtained from Equations (3.3), (3.4a) and (3.6)

$$q_h = \frac{Q_c}{C_p T_a (\rho_a - \rho_h)} \tag{3.7}$$

Eq. (3.7) shows that the amount of helium required is only a function of convective heat release rate for a given ambient condition. The total volumetric flow rate of the helium & air mixture at the same plume height, $q_{s,m}$ in m³/s, can be calculated from Equations (3.1) and (3.4b)

$$q_{s,h} = \frac{Q_c}{\rho_s C_p (T_s - T_a)} \tag{3.8}$$

3.2 Scaling Laws

To study the smoke movement in large spaces driven by fire, a sub-scale model is always a convenience and scientific strategy. Various scaling techniques are found in literatures that fits different modeling requirements [9, 10, 21, 22, 31, 32]. With the same theoretical basis, the scaling methods will be different when applied for different fire phenomena, since the ignored parameters are always in need of attention [33]. And appropriate assumptions should be made during the modeling.

In this section, an overall demonstration of governing equations and dimensionless groups for fire smoke research is presented; Froude modeling approach is presented and

30

discussed; certain assumptions for modeling HST and HeST are selected. Ultimately, advisable scaling laws are drawn in the last.

3.2.1 Froude Modeling

In the field of fire research, many scaling models have been used. Quintiere [33] proposed three modeling approaches effectively used in this field: Froude modeling, analog modeling and pressure modeling. Each strategy is incomplete since certain parameters are ignored, yet practical and functional for fire studies. With appropriate modeling approach been selected, scale test could be convenient and inexpensive.

Among these approaches, Froude modeling is considered to be the most common modeling approach used for fire smoke control studies. Froude modeling was recognized by NFPA 92B [34] as a method for studying smoke movement in large spaces.

Froude number can be defined as the ratio of inertial force to gravity force.

$$Fr = \frac{\rho_\infty u^2}{\Delta \rho g l} \tag{3.9}$$

Where ρ_∞ is the gas density of ambient, $\Delta\rho$ is the density difference between the plume and ambient, u is the plume gas velocity, g is the gravitational acceleration constant and l is the characteristic length scale (e.g. the diameter of a circular fire source).

When applied in large spaces, e.g. atria, Froude model is found to be adequate since the smoke flows are fully turbulent, viscous effects are less important. Also the smoke flows are governed by convection due to the buoyancy.

There are also other dimensionless numbers to characterize the smoke plume, e.g. Reynolds number. Steckler et al. [35] estimated that Reynolds number of the scale plume to be on the order of 10^4, compared to a full-scale turbulent plume with Reynolds number on the order of 10^5. Therefore, the Reynolds number could be ignored in the scaling analysis [23].

Some literatures using Froude modeling in smoke movement studies could be found. Chow and Lo [9, 10] studied natural smoke filling process in atria based on Froude modeling. Capote et al. [32] conducted scale tests of smoke filling in large atria. Vauquelin [21, 22] applied Froude modeling in simulating smoke extraction in sub-scale tunnel models. Bryant [23] used Froude number in modeling scaled PIV experiment on buoyant smoke moving through a doorway. The results gave a solid confidence for Froude modeling in scale tests.

3.2.2 Governing Equations

When scaling smoke movement driven by fire plume in buildings, the governing differential conservation equations are used. According to the studies of scaling applications in fire research by Quintiere [33], the governing equations are illustrated below with some phenomena been excluded due to their relatively less importance. Noting that to keep the generalization, equations are presented in one-dimensional form.

Conservation of mass:

$$\frac{\partial \rho}{\partial t} + \frac{\partial (\rho \cdot \alpha)}{\partial x} = 0 \qquad (3.10)$$

Conservation of momentum in vertical direction:

$$\rho(\frac{\partial \alpha}{\partial t}+\alpha\frac{\partial \alpha}{\partial x})=-\frac{\partial P'}{\partial x}+g(\rho_0-\rho)+\frac{4}{3}\mu\cdot\frac{\partial^2 \alpha}{\partial x^2} \qquad (3.11)$$

Conservation of enthalpy:

$$\rho\cdot C_\rho(\frac{\partial T}{\partial t}+\alpha\frac{\partial T}{\partial x})=k\frac{\partial^2 T}{\partial x^2}+\frac{\partial P}{\partial t}+Q''' \qquad (3.12)$$

In our study, only convective heat is considered in modeling HeST. So some governing equations are ignored, e.g. radiative transfer equation, heat conduction equation in solid, and energy boundary condition. One could use normalizing parameters to transfer the governing equations into dimensionless forms. The normalizing parameters are as follows:

- Geometric length scale: l
- Characteristics velocity: V
- Characteristics time: τ
- Initial ambient pressure: P_0
- Initial ambient density: ρ_0
- Initial ambient temperature: T_0
- Characteristics pressure: P^*

Then the dimensionless variables are defined as:

$$\hat{x}=\frac{x}{\ell} \qquad (3.13a)$$

33

$$\hat{t} = \frac{t}{\tau} \tag{3.13b}$$

$$\hat{\alpha} = \frac{\alpha}{V} \tag{3.13c}$$

$$\hat{\rho} = \frac{\rho}{\rho_0} \tag{3.13d}$$

By using these dimensionless variables in solving the governing equations, Scaling

relations for the Froude Modeling could be drawn. Detailed derivation is shown in

Appendix A while not to be repeated here. In Table 3.1, the scaling relations are

presented.

Table 3.1 Scaling relations for Froude modeling.

$x_m = x_f (\frac{l_m}{l_f})$	$U_m = U_f \sqrt{\frac{l_m}{l_f}}$	$t_m = t_f \sqrt{\frac{l_m}{l_f}}$
$T_m = T_f$	$\dot{V}_m = \dot{V}_f (\frac{l_m}{l_f})^{5/2}$	$\dot{Q}_m = \dot{Q}_f (\frac{l_m}{l_f})^{5/2}$
$\rho_m = \rho_f$	$\dot{m}_m = \dot{m}_f (\frac{l_m}{l_f})^{5/2}$	$\Delta\rho_m = \Delta\rho_f (\frac{l_m}{l_f})$

3.3 Computational Fluid Dynamics Modeling

CFD solves the fluid flow problems by using numerical methods and algorithms. It could

predict the fluid flow as well as heat transfer processes for a wide range of scientific and

practical applications. Many literatures on using CFD models for fire research could be

34

found in many studies. For studies on smoke movement in buildings, CFD models have been increasingly used as a useful tool over the last decade [36, 37].

Basic modeling procedure could be drawn from the principles of CFD. Before processing, a three-dimensional physical geometry is defined. Inside the geometry, the volume is divided into a number of cells known as control volumes. The number of cells could vary from thousands to millions, according to different calculation requirements. The boundary conditions, e.g. air supply rate, temperature, pressure etc. are then defined in the pre-process stage. After that, the simulation is started. In each numerical cell, conservation equations of mass, momentum, and energy are solved iteratively for a steady-state or transient analysis [15].

In this study, CFD was used to simulate HeST in both full-scale test facility and its sub-scale model. A conventional physical experiment could be costly and time-consuming due to the cumbersome process of construction and measurement. A CFD model could be a good alternative or a supplemental solution to examine more testing scenarios for a given time frame.

3.3.1 Fire Dynamics Simulator (FDS)

Fire Dynamics Simulator (FDS) models developed by McGrattan et al. [15] at National Institute of Standards and Technology (NIST) in USA are used in this study. FDS is a large eddy simulation (LES) computational fluid dynamics (CFD) model, which numerically solves the Navier-Stokes equations for heat transfer and smoke from fire. McGrattan et al. [15] gives a detailed description of FDS's fundamental equations and the numerical algorithms, which are not repeated in this section.

The results of simulations are visualized by Smokeview (version 5) developed by Forney

et al. [38]. Smokeview allows a three-dimensional viewing of FDS computation results in

snapshots or animations. Plane slices also allow viewer to track the contours of

temperatures, species concentrations, and velocity, etc.

3.4 Models on Smoke Filling

The study of smoke filling focuses on the time the fire smoke fills a space. The

descending time of hot smoke layer should be slow enough to allow people to evacuate

from when they are aware of the fire to finally exit the building through exits [13]. So it

is always important to study the smoke layer height in smoke filling process.

3.4.1 Analytical Calculation

There are many studies on determination of smoke layer height, h_n. Literatures could be

found for various methods to determine smoke layer height in case of fire [10].

a). USTC/PolyU Equation [10]:

Chow et al. developed an equation based on two-layer zone model to determine h_n at

USTC/PolyU (University of Science and Technology of China and The Hong Kong

Polytechnic University).

$$h_n = \begin{cases} \left[0.084(\dfrac{\alpha H^2 g}{\rho_0 c_p T_0 A^3})^{1/3} t^{5/3} + 1 \right]^{3/2} & \text{for } t < t_s \quad (3.14a) \\ \left[0.14(\dfrac{g Q_0 H^2}{\rho_0 c_p T_0 A^3})^{1/3} (t - t_s) + (\dfrac{H}{h_s})^{2/3} \right]^{3/2} & \text{for } t \geq t_s \quad (3.14b) \end{cases}$$

Where h_s is given by

$$h_s = \left[0.084 \left(\frac{\alpha g}{\rho_0 c_p T_0 A^3} \right)^{1/3} \left(\frac{Q_0}{\alpha} \right) + H^{2/3} \right]^{3/2}$$ (3.15)

b). Tanaka's Equation [39, 40]:

Tanaka et al. [39, 40] proposed a method to calculate h_n for a t^2-fire excludes the steady burning part:

$$h_n = \frac{1}{H \left(k_1 \frac{\alpha^{1/3}}{A} \frac{2}{5} t^{5/3} + \frac{1}{H^{2/3}} \right)^{3/2}}$$ (3.16)

c). NFPA Equation [34]:

Another equation for calculating h_n with no smoke exhaust operating is recommended by NFPA-92B [34]:

- For t^2-fire

$$h_n = 0.91 \left[\frac{t}{\left(\frac{1000}{\alpha} \right)^{1/5} H^{4/5} \left(\frac{A}{H^2} \right)^{3/5}} \right]^{1.45}$$ (3.17)

- For steady fire

$$h_n = 1.11 - 0.28 \ln \left[\left(\frac{t Q_0^{1/3}}{H^{4/3}} \right) \left(\frac{A}{H^2} \right) \right]$$ (3.18)

These equations apply for atria with geometries: $0.9 \leq A / H^2 \leq 14$ and $h_n \geq 0.2$

3.4.2 FDS Prediction

In FDS [15], the default smoke layer height calculation is based on the vertical temperature profile. When $z = 0$ indicates the floor of an atrium and $z = H$ is the ceiling, the smoke layer height z_s is defined

$$z_s = \frac{S_l(I_1 I_2 - H^2)}{I_1 + I_2 S_l^2 - 2S_l H} \tag{3.19}$$

The integrals, I_1 and I_2, are defined by

$$I_1 = \int_0^H S(z)dz \tag{3.20}$$

$$I_2 = \int_0^H \frac{1}{S(z)}dz \tag{3.21}$$

where the S is the temperature, $S_l = T_l$ is the temperature at the bottom height of the temperature profile, i.e. $z = 0$ m

The current version of FDS only predicts z_s based on gas temperatures. Because the current study uses helium mixed with air and artificial smoke as tracer, it is necessary to obtain the smoke layer height based on the species concentrations, e.g. those of helium or tracer smoke. Therefore, we define the $S(z)$ to be

$$S(z) = 1 - C_g \tag{3.22}$$

where C_g is the mass fraction of helium or the tracer smoke in kg/kg.

Note that the $S(z)$ is not set equal to C_g, which is often a very small decimal number so that round-off errors of I_1 and I_2 are often caused. Therefore, $S(z)$ is defined to be the

mass fraction of non-helium or non-tracer smoke in the mixture. This method is

programmed in FDS and compiled on a Linux cluster for later simulations.

4. METHODOLOGY

4.1 CFD Modeling Methodology

In this section, CFD modeling was used to simulate a hot smoke test and its corresponding helium smoke test in a full-scale atrium selected from literature [8]. Typical modeling procedure was followed in this study. Helium smoke test techniques were applied in CFD model, which was validated by field test measurement data in Chapter 5. As discussed in Chapter 3, proper scaling laws have been chosen to model HeST in sub-scale atrium for further verification by physical model experiment described in Section 4.2.

4.1.1 FDS Modeling Procedure

FDS, as a CFD model, was used in all numerical simulations. For the details of the FDS input files, please refer to Appendix B.

4.1.1.1 General Information of CFD Model

Chow et al. [8] conducted a series of hot smoke tests in a full-scale atrium to study the smoke filling process. A diesel pool fire with the heat release rate up to 1.6 MW was placed on the floor of the atrium with the size of 22.4 m (L) × 11.9 m (W) × 27 m (H) as shown in Figure 4.1. All the openings were closed except a vertical vent with the size of 11.9 m (W) × 0.2 m (H) was opened at the bottom. A vertical tree of 20 thermocouples was located at 2 m away from the walls. The data of thermocouples and smoke layer heights were very well documented therefore they are selected for this study. Figure 4.1 shows the full-size test facility and its instrumentation.
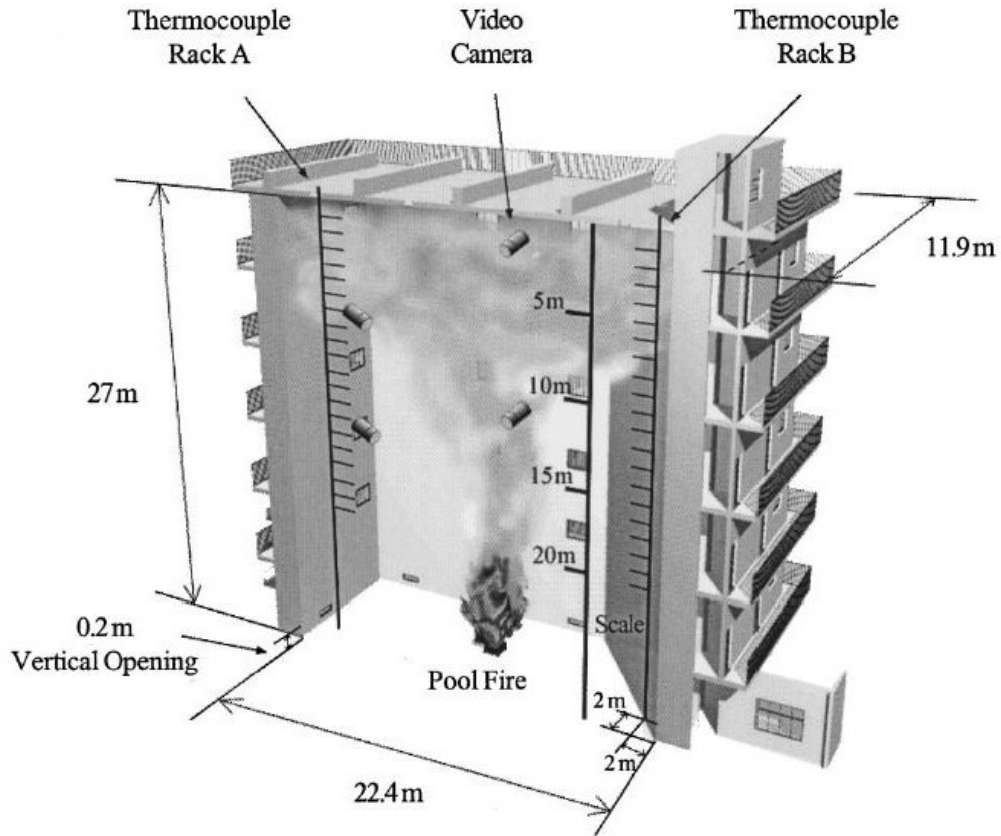
Figure 4.1 Hot smoke test in full-size atrium [8].

4.1.1.2 Geometry

The geometry of computational domain contains the inside space of the test atrium. Walls

properties are modeled as "Inert" since no radiative heat transfer is considered. The size

of atrium, pool fire and openings are strictly modeled as the same of the test atrium.

Figure 4.2 shows the FDS model of the full-scale test atrium. Details of each part of the

model will be discussed in the following paragraphs.
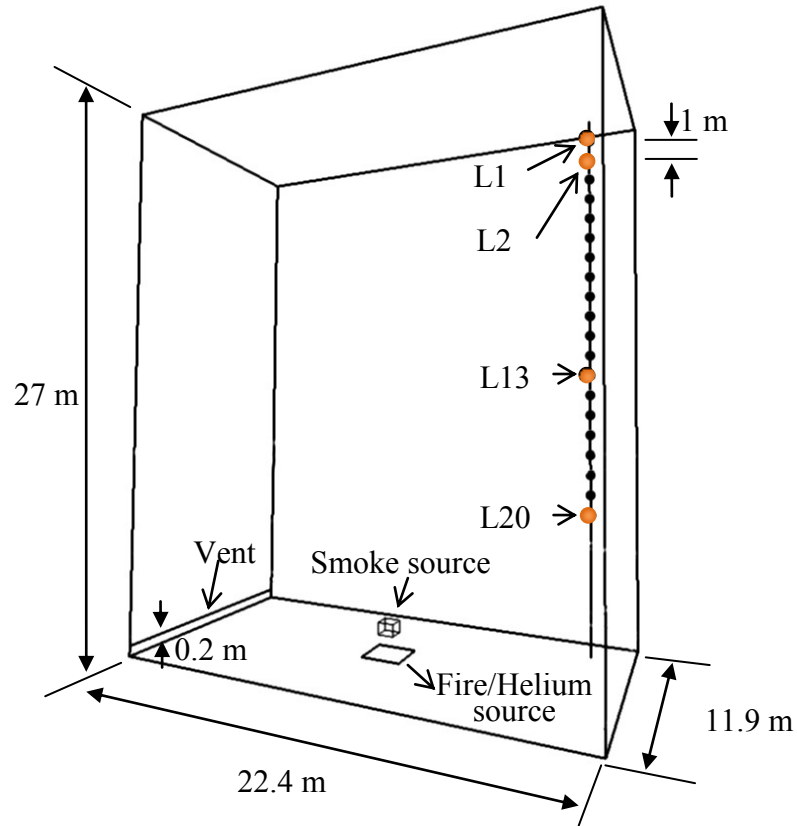
Figure 4.2 Numerical model of full-scale test atrium.

4.1.1.3 Grid Resolution

Grid (mesh) resolution is one of the most important parameters in CFD modeling. Higher grid resolution normally is believed to generate more accurate results while costing more computational time. It is often challenging to keep a balance between the required numerical accuracy and computational time for a CFD simulation. Thus, grid sensitive study should be examined carefully in preliminary runs [41].

In our study, a single uniform mesh is defined for the whole computational domain.

Numerical simulations with three grid resolutions were performed. Computational time

was recorded in FDS output files and it is presented in Table 4.1.

Table 4.1Parameters in the simulation of the atrium.

Atrium size	22.4 m (L) × 11.9 m (W) × 27 m (H)	
Pool size	0.6 m (L) × 0.6 m (W) for 300 kW; 1.0 m (L) × 1.0 m (W) for 500 kW; 2 m (L) × 2 m (W) for 1.6 MW.	
Lower vent size	11.9 m (W) × 0.2 m (H)	
Tracer smoke source size	0.3 m (L) × 0.3 m (W) × 0.3 m (H) for 300 and 500 kW; 0.5 m (L) × 0.5 m (W) × 0.5 m (H) for 1.6 MW.	
Device locations	Thermocouples	2 m away from walls
	Helium volumetric concentrations	
	Mass fractions and optical densities of tracer smoke	
Grid resolutions	Grid 1	114,300
	Grid 2	385,600
	Grid 3	914,000
Boundary conditions	Average total HRR	300 kW, 500 kW, 1.6 MW
	Lower opening	Free outflow
	Walls	Inert
	Tracer smoke source	Supply
Total simulation time	400 seconds	
Average total computational time	Grid 1	8 hrs
	Grid 2	24hrs
	Grid 3	72hrs

For grid sensitivity studies, comparison has been carried out between the predicted gas

temperatures and measured ones. In Chapter 6, results are shown and recommended grid

resolution is given.

4.1.1.4 Fire Source Design

In field test, heat release rates (HRR) of the pool fire was measured by the mass loss rate of burning fuel with known heat of combustion of 42,000 kJ/kg. The HRR curve has been given by Chow et al. [8], thus it is possible to model this curve in FDS simulations.

In FDS input file, pool fire has been modeled as "burner"; HRR has been modeled using "ramp" function. Figure 4.3 shows the transient HRR of pool fire from the experiment compared to that used in the simulation. The data shows that the fire lasted for about 400 seconds with the growth period of the first 100 seconds, the relatively steady fire from 100 to 300 seconds and the fluctuating period in the end. The average heat release rate in the steady period was measured to be about 1.6 MW.
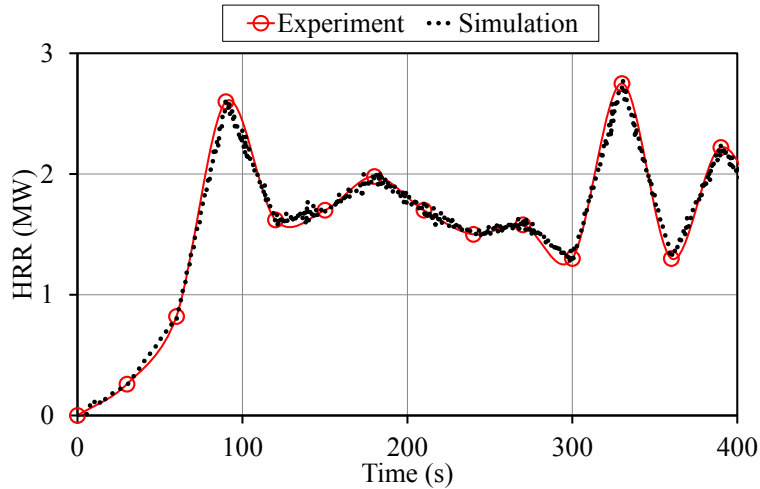
Figure 4.3 Comparison of HRR from the experiment and that used in the simulation for the fire of 1.6 MW.

4.1.1.5 Helium Source Design

As discussed in Chapter 3, helium flow rate to achieve the same buoyant effect in fire smoke is determined by the convective HRR of fire source. By the default setting of FDS,

the convective HRR of the liquid pool fire is defined to be 0.65 of the total HRR. However, Koseki et al. [42, 43] found that the radiative heat component was around 30% of total HRR for fires smaller than 1 m diameter and will decrease as the fire size increases. Vauquelin [21] used convective HRR valued as 0.7 of total HRR of fire in his study. We also use this value in our study to determine the helium flow rate.

Helium source in HeST was modeled at the same location with the same open size to the fire source in HST model. The surface property was set to "Supply" with designed helium supply rate. From Equation 3.7 in Chapter 3, designed helium supply rate (LPM) for 1.6 MW fire could be calculated.

When designing the helium supply flow, it is also necessary to model the growth of the fire using an appropriate approach. Compared to the HRR curve used in fire source design, same curve could not be used for helium source in practical applications. Chow [8] mentioned the growth of fire in his test was very close to unsteady t^2 - fire, also he measured the time to reach steady burning. Thus, in our helium source design, we use t^2 growth of helium supply rate for the first 100 seconds and constant flow for the last 300 seconds.

4.1.1.6 Smoke Generator Design

In order to simulate an artificial smoke used in hot smoke test for better visualization, a smoke generator was modeled and put above the fire/helium source. It constantly blows smoke with same density of ambient air from its four horizontal surfaces into the atrium space. With little momentum effect in the vertical direction, the tracer smoke from the

smoke generator was driven up by the buoyant plume. By using this modeling method, smoke flow patterns in hot smoke test and helium smoke test can be demonstrated.

Supply rate of tracer smoke should minimize its influence to the buoyant plume. As a result of that, mass flow rate of tracer smoke was set to be 0.001 kg/s.

4.1.1.7 Openings

In field tests carried out by Chow et al. [8], there were eight top vents and one vertical opening in the bottom of the atrium. The eight top vents were not modeled in the numerical model since they only work after each test to evacuate the smoke to the atmosphere. The vertical opening at bottom was modeled as a free outflow surface.

4.1.1.8 Predicted Parameters

In hot smoke test model, FDS predicts the temperatures from thermocouples located at two meters away from the walls. Four measuring locations at different height on the thermocouple tree were selected to compare the predictions to field test measurements.

Also at the same locations, smoke optical densities and concentrations predictions were recorded.

In helium smoke test model, FDS predicts helium concentrations instead of gas temperatures to show the buoyancy forces at that level. To compare the buoyancy effect and achieve the similarity, a non-dimensional comparison method is developed and discussed in Chapter 6.

4.1.1.9 Sub-Scale FDS Modeling

Chow et al. also built a 1/26.5 model of the full-size atrium to study the smoke filling

process. In this study, a 1/26.5 sub-scale atrium model was therefore constructed in FDS

to simulate HeST for further experimental studies. The sub-scale model has the same

instrumentation, boundary conditions to the full-scale atrium model. Since the modeling

followed the identical procedure, only applications of scaling laws is discussed here.

For the sub-scale model, the major parameters of interest are fire size, time and

temperatures. Use the given scaling relations shown in Table 3.1, these scaled parameters

could be calculated. Equations 4.1 – 4.3 illustrate the relations:

$$Q_m = Q_f \times 2.77 \times 10^{-4}$$

(4.1)

$$t_m = 0.194 \times t_f$$

(4.2)

$$T_m = T_f$$

(4.3)

4.1.2 Simulations

Numerical simulations were performed on the CIRRUS computer cluster at Concordia

University, with FDS software compiled to run on Linux operating system.

4.1.2.1 Design Helium Supply Rate

For all simulations, computational domain remains the same geometry size. Measuring

locations, vertical opening and smoke generator also keeps the same in all simulations.

HRR and size of the fire vary in the series of simulations, for which different helium

supply rate were calculated in Table 4.2. In addition, pure air was used to show the

different smoke flow pattern with non-buoyant plume. This is to provide a sufficient

proof for HeST to well represent a smoke plume in hot smoke test.

Table 4.2 Designed helium supply rate for 1.6 MW, 500 kW and 300 kW fires.

HRR (MW)	Convective HRR (MW)	Helium supply rate	
		Full-scale model (m^3/s)	Sub-scale model (LPM)
1.6	1.12	3.67	61.2
0.5	0.35	1.15	19.1
0.3	0.21	0.69	11.5

4.1.2.2 Parameters of Interest

As discussed in Chapter 3, smoke layer height, temperatures, helium concentrations etc.

are parameters affect the smoke filling process in the atrium model. Grid resolution,

boundary conditions and other settings also could influence the accuracy of FDS

simulation. Table 4.1 shows the important parameters in the simulations of hot smoke test

and helium smoke test in the test atrium.

4.1.2.3 Series of Simulations

Table 4.3 shows all simulations with different setting to achieve a comprehensive

demonstration of helium smoke test and hot smoke test in atrium model. With sufficient

simulation scenarios and their results, we could conduct reliable model validation and

application.

Table 4.3 Series of FDS simulations.

Simulation No.	Corresponding HRR of fire (MW)	Test approach		
		HST	HeST	Pure air
Full-scale				
1	1.6	✔		
2	1.6		✔	
3	1.6			✔
4	0.5	✔		
5	0.5		✔	
6	0.5			✔
7	0.3	✔		
8	0.3		✔	
9	0.3			✔
Sub-scale				
10	1.6		✔	
11	0.5		✔	
12	0.3		✔	

4.2 Sub-Scale Physical Experiment Methodology

A 1:26.5 sub-scale atrium model was constructed at the fire smoke research lab in

Concordia University to examine the smoke filling process by helium smoke test inside

the PolyU/USTC atrium [8, 9] under different simulated fire scenarios. Helium supply

system, gas sampling system and visualization system were carefully designed. Then the

results from experiments were used to validate CFD simulations. Details of tests were

described in the following sub-chapters, including experimental apparatus,

instrumentation, experimental methods and data analysis.

4.2.1 Sub-Scale Model

4.2.1.1 Geometry

The physical model used in our study is a 1:26.5 sub-scale atrium model of PolyU/USTC

atrium (Figure 4.4). Since the tests only apply to HeST, there is no fire or burner used.

The physical model was built strictly to the same geometry of sub-scale atrium model

used by Chow et al. [10]. Whole model was made of clear acrylic panels, 6 mm thick,

with heat resistance up to 160 ºC. The selected materials could provide clear visual

inspection through it and be easily assembled.

There were eight 5 mm × 5 mm vents on the top of the model. All of them were kept

closed during the experiments. After each test, the vents were open to ventilate the model.

One vertical gap of 10 mm was on the bottom of model's west wall for all-time

ventilation. Because the model was not built for study of smoke extraction, there was no

pressure measurement inside the model.

In the center of the bottom, one 8 mm × 8 mm opening was made as for helium source

supply. Also the left edge of the floor, one opening of 4 mm × 4 mm was used for

measurement instruments to go through. The model simulated a typical hot smoke test

within a single compartment atrium with various sizes of pool fire (2 m × 2 m, 1 m × 1 m

and 0.6 m × 0.6 m).
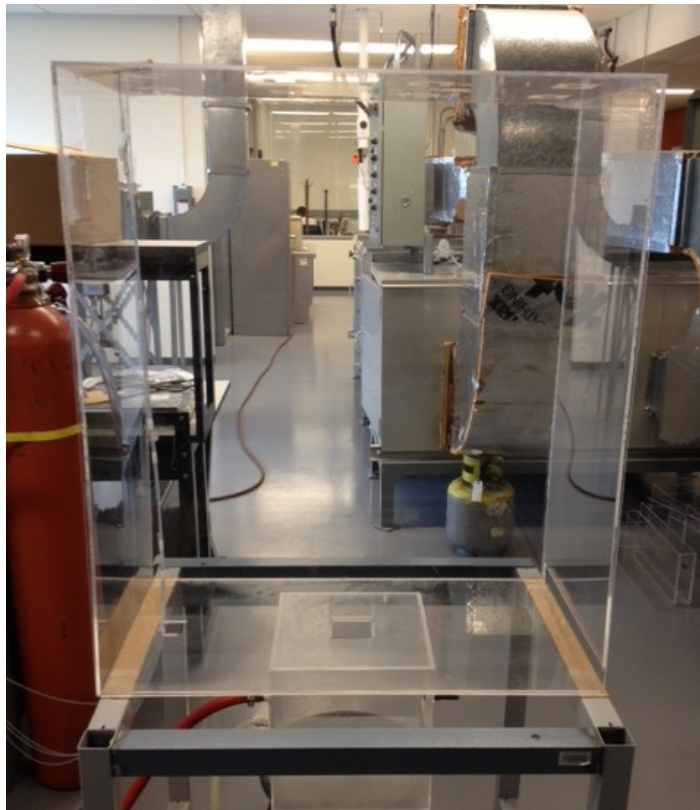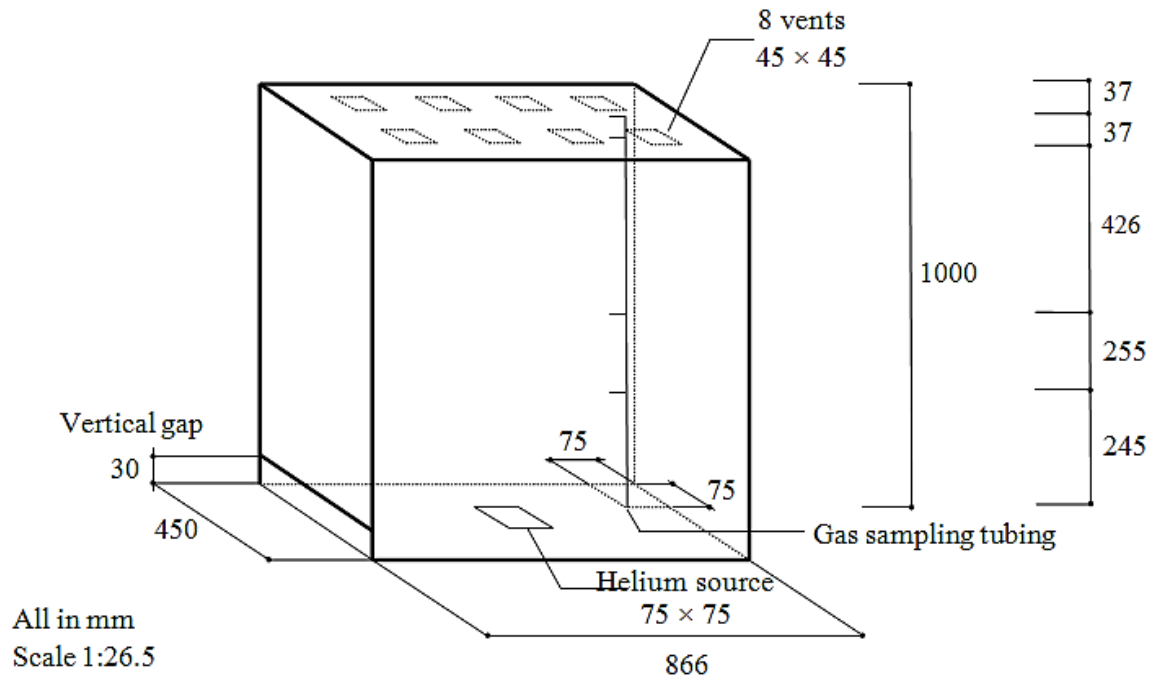
Figure 4.4 The sub-scale atrium model at Concordia University.

Table 4.4 Calculated flow rate of helium source supply.

Scenario	HRR of fire in HST (MW)	Pool size	Helium volumetric flow rate (LPM)
1	1.6	2 m × 2 m	3.67
2	0.5	1 m × 1 m	1.92
3	0.3	0.6 m × 0.6 m	1.19

4.2.1.2 Helium Supply

Pure helium was supplied into the model to simulate a buoyant plume in helium smoke test. Under different fire test scenarios, corresponding helium supply rate were calculated by using Equation 7 in Chapter 3. Table 4.4 shows the calculated volumetric flow rate of helium.

The helium was provided by a 40 liter compressed helium cylinder. A mass flow controller (Alicat MCR-250SLPM-D/5M) (Figure 4.5) was used to control the flow rate of helium. The mass flow controller was precisely calibrated according to NIST calibration standard. A commercial engineering software Flow Vision SC was used to control the mass flow controller.
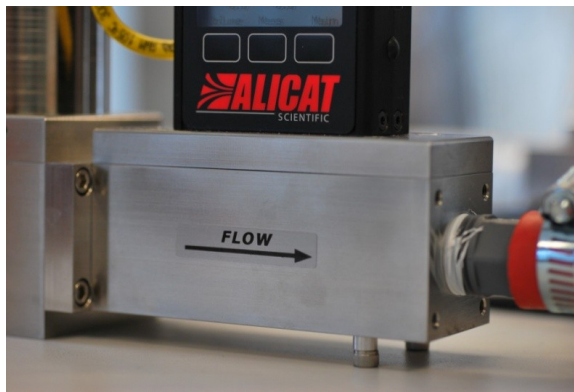
Figure 4.5 Mass flow controller.

4.2.1.3 Smoke Source

The buoyant smoke plume driven by pure helium was visualised by injecting artificial smoke from a smoke machine (Rosco fog machine 1500) into the model. Special fog fluid was heated into small particles which would give a clear visual inspection when illumined by a laser light sheet. The density of smoke particles are of the same to ambient air so the smoke does not create any extra buoyant effect.
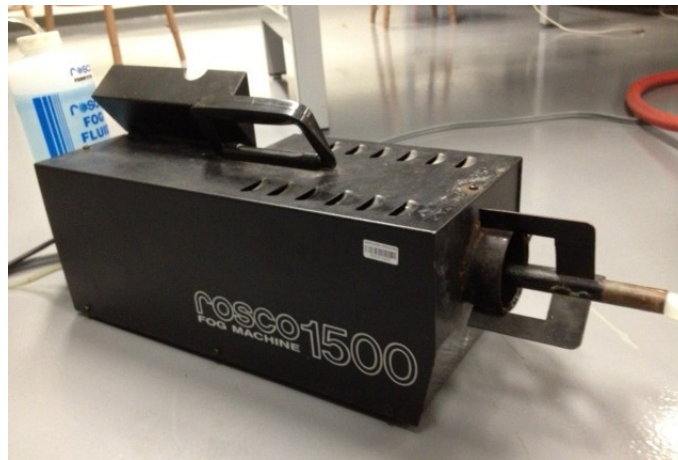
Figure 4.6 Smoke machine.

Smoke will pre-mix with helium supply in a "mixing box" (see Figure 4.7). Mixing box was made of 3 mm thick acrylic panels. The mixing box was constructed to take up to 30 psi pressure. The supply opening of the mixing box was the same sizes of the pool fires in hot smoke test (Table 4.4). Honeycomb was installed in the opening to create a uniform upward flow.
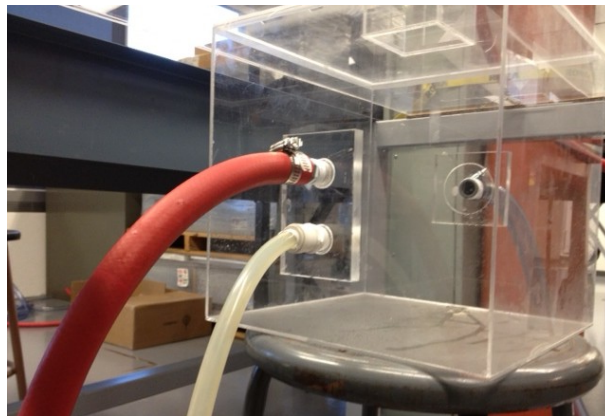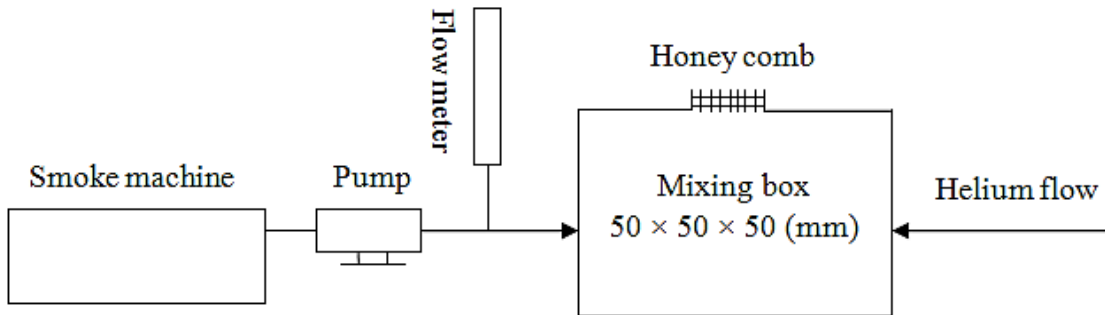
Figure 4.7 Smoke supply system.

After each test, compressed air was injected into the model to help better ventilating inside the model. Meanwhile, the indoor ventilation system with 1 % air change rate exhausts the smoke and helium gas from the testing room. For safety reason, a Standard Operating Procedure (SOP) was developed to meet the requirements of Environment Health & Safety office at Concordia University.

(a) (b)

Figure 4.8 Laser machine (a) and laser sheet optics module (b).

4.2.1.4 Laser Light Sheet

Nd:YAG Laser system (New Wave Research Solo 120) associated with light sheet optics

(DANTEC 80×80 series) provides a laser light sheet system for clear visual inspection of

smoke movement and layer height (see Figure 4.8).

4.2.2 Gas Sampling System

A gas sampling system with a helium analyzer (Divesoft helium analyzer), a selection

valve (Rheodyne 10 position selection valve) and a sampling pump (SKC twin-port

portable gas sampling pump) were used to measure the helium concentration at four

locations in the atrium model. Sampling gas was sucked through 1/8 inch PVC tubing

from the measuring locations to the helium analyzer. Figure 4.4 shows the measuring

locations which corresponded to the PolyU/STU atrium experiment [8]. HyperTerminal[®]

communication software was used to record the helium concentration data. A typical

recording file is shown in Appendix C.

According to the manufacturer, helium analyzer could measure the helium volumetric fraction within 250 ms. In Appendix C, * indicates the analyzer was measuring and could not give a reading. Sometimes the analyzer would be affected by the noise at the gas inlet. To better handle with this situation, sampling pump was set to a high flow and pause intermittently to allow the analyzer give readings of helium concentration.

Video recording was realised by using a commercial video camera located in front of the model. Then the photographs at certain time were obtained and reported in Section 5.3.2 in this thesis.

4.2.3 Experimental Method

This study was used to examine the smoke filling process in helium smoke test and how well a helium plume would represent the fire smoke plume in building with big interior space. Parameters of interest were discussed in the previous chapters. A summary of the parameters is shown below:

(a) HRR of simulated fire source

(b) Convective HRR of simulated fire source

(c) Dimensions of simulated fire source

(d) Supply rate of helium source

(e) Supply rate of tracer smoke source

The sub-scale physical experiment was used to validate the CFD models in the previous Chapter, only some numerical simulations were reproduced through physical experiment.

The HRR of simulated fire source used in this study varies from 1.6 MW to 300 kW (full-size), which corresponds to 0.44 kW to 0.08 kW (sub-scale size). The sizes of fire source also changed with its HRR. Convective HRR of simulated fire were considered to be 0.7 of the total HRR in all studies. Details of the fire source and helium source were discussed in Section 4.1.3, 4.1.4, 5.1.2.

4.2.3.1 Series of Tests

The series of test include helium concentration measurement and smoke layer height inspection for different fire sizes. Due to the limitation of instrumentation, helium concentration for the four measuring locations cannot be measured in the same test. As a result, tests are repeated with the same settings to measure enough data at the required measuring locations. Table 4.5 shows the series of tests indicating the object has been measured.

Table 4.5 Series of tests (✔ = measured).

Test No.	Helium flow rate (LPM)	Measuring location	Smoke for visualization
1	61	L1	N/A
2	61	L1	N/A
3	61	L1	N/A
4	61	L2	N/A
5	61	L2	N/A
6	61	L2	N/A
7	61	L13	N/A
8	61	L13	N/A
9	61	L13	N/A
10	61	L20	N/A
11	61	L20	N/A
12	61	L20	N/A
13	61	N/A	✔
14	19.2	L1	N/A
15	19.2	L2	N/A
16	19.2	L13	N/A
17	19.2	L20	N/A
18	19.2	N/A	✔
19	11.5	L1	N/A
20	11.5	L2	N/A
21	11.5	L13	N/A
22	11.5	L20	N/A
23	11.5	N/A	✔

4.2.3.2 Experimental Procedure

The experiment procedure of the series of test was developed based on lab safety requirements and laser safety requirements. Series of 1 to 12, 14 to 17 and 19 to 22 were conducted without smoke visualization; only helium concentration has been measured. The experiment procedures are as follows:

(1). Turn on the regulator of helium cylinder, check the mass flow controller;

(2). Locate the selection valve to the measured location;

(3). Turn on the helium gas analyzer, start its communication with Hyperterminal$^{®}$ software;

(4). Turn on the sampling pump, check helium analyzer's readings and pause it till the test starts;

(5). Set the mass flow controller at required flow rate, start the test;

(6). Measure the data through Hyperterminal$^{®}$ interface for 90 seconds and then stop the mass flow controller, sampling pump and helium analyzer;

(7). Save the data and turn off the helium cylinder and regulator.

(8). If necessary, ventilate the atrium model with compressed air at supply rate of 100 LPM for 2 minutes until the model has been completely cleaned;

Series of 13, 18 and 23 used laser sheet system to illuminate the smoke layer. Video were recorded during these tests. Accordingly, a different experiment procedure is as follows:

(1). Check all laser protections including laser barriers, laser signs and eye-glasses.

(2). Turn on the smoke generator and laser machine for warm up;

(3). When the smoke generator is ready to use, turn on the helium cylinder;

(4). Put video camera in position, start the recording;

(5). Turn off the lights, fill the mixing box with smoke and start the laser system;

(6). Set the required supply rate of helium, start the test;

(7). After 90 seconds, turn off the equipment in the following order: laser machine, smoke generator, mass flow controller, helium cylinder, video camera.

(8). Save the data and turn off the helium cylinder and regulator.

5. RESULTS AND DISCUSSION

5.1 Validation of CFD Model

5.1.1 Grid Sensitivity Study

As mentioned in Section 4.2.2, three grid resolutions are used in simulating hot smoke test / helium smoke test in the full-scale atrium model. In the FDS model, meshes, often refer to grids, should be chosen carefully to obtain grid-independent results, and achive a balance of accuracy and computational cost [41].

For simulations of smoke plumes, a non-dimensional expression $D^*/\delta x$ can be used as a measure of how well the flow field is resolved [44], where δx is the mesh size, D^* is the characteristic length scale of fire,

$$D^* = (\frac{Q}{\rho_\infty T_\infty C_p \sqrt{g}})^{2/5} \qquad (5.1)$$

In most studies, the non-dimensional expression $D^*/\delta x$ ranging from 1/5 to 1/10 were suggested [44, 45]. So in our study, we chose the mesh size of 0.4 m × 0.4 m as the coarsest and 0.2 m × 0.2 m as the finest. One medium mesh size of 0.26 m× 0.26 m was also used.

Table 5.1 Comparison of computing time of three mesh sizes in full-scale atrium model.

Group No.	Mesh size	Resolution	Computing time
1	0.4 m × 0.4 m	114,300	8 hrs
2	0.26 m× 0.26 m	385,600	24 hrs
3	0.2 m × 0.2 m	914,000	72 hrs

Table 5.1 shows an example of the mesh sizes, resolutions and their computing time in the study of full-scale atrium model. Computing time was determined on the basis of simulation time running on 2.2 GHz AMD Opteron 64-bit processor computer cluster system. From Table 5.1, we could see Group 1 costs only 1/3 computing time of Group 2 and 1/9 of Group3. In the following section 5.1.2, predicted temperatures with these three mesh sizes are shown and compared so a mesh refinement work will be achieved.

5.1.2 Temperature Comparison

In the modeling of hot smoke test in the full-size atrium, the predicted temperatures at four selected measuring locations: L1, L2, L13 and L20, of which the locations are shown in Figure 4.2, are plotted and compared to the field test measurement in Figure 5.1. In this study, the results of fire of 1.6 MW is used for comparison.

(a) L1

(b) L2
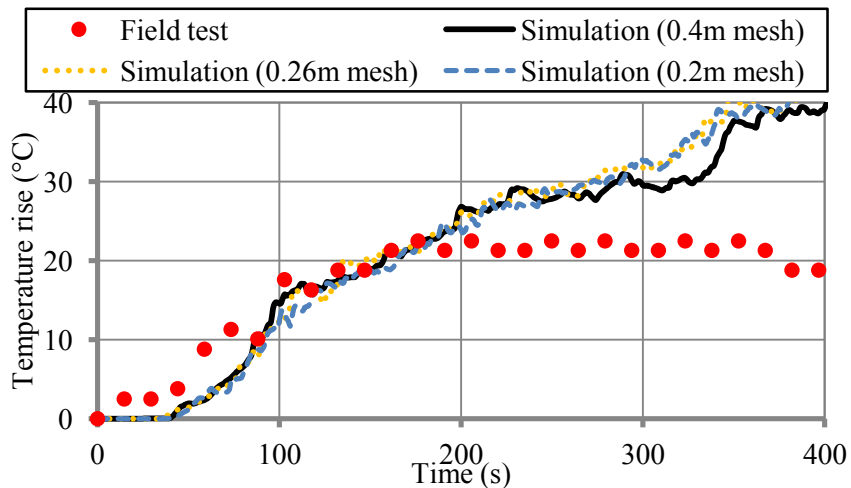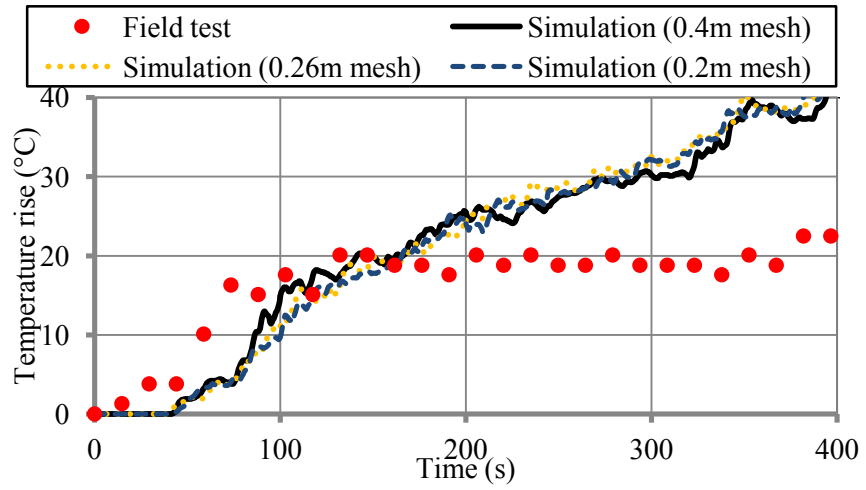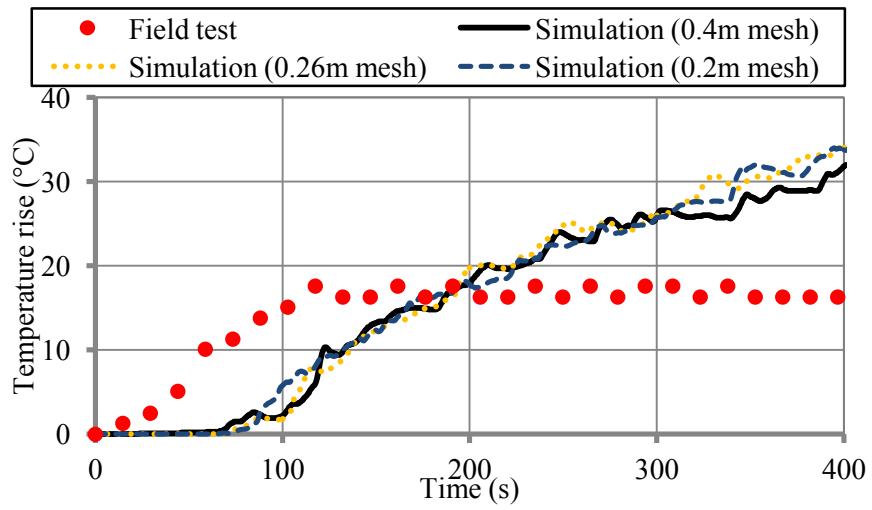
(c) L13

63
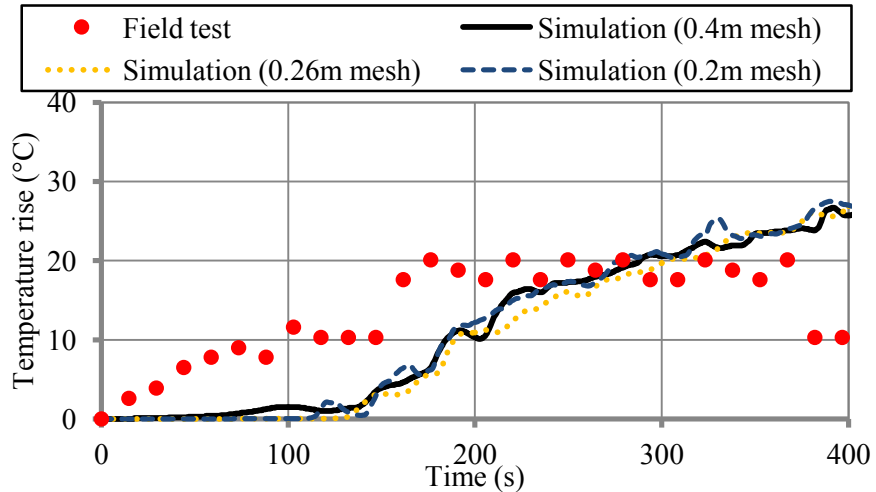
(d) L20

Figure 5.1 Comparison of predicted temperatures to the field test at (a) L1, (b) L2, (c) L13 and (d) L20 for the fire of 1.6 MW.

The predictions are reasonably good during the first 200 seconds and become significantly higher than the measured temperatures in the second half of the test. At L13 and L20, the simulation underestimates the temperatures in the beginning, and over-predicts the data when the measured temperatures reached a steady state after 200 seconds. For other locations of thermocouples (not shown here), similar trends are observed. The grid sensitivity study illustrates no major improvements of the predictions. The simulation results are independent of three grid resolutions as shown in Figure 5.1. One possible cause of the discrepancies is the FDS simulations in this study do not calculate the radiations but use directly the convective heat release rate, which is 65 % of the total HRR by default in FDS. The radiation solver is available in FDS but its calculation needs a fine grid in the order of at least one centimeter to correctly resolve the layers of fire flames and an accurate prediction of the chemical composites of the smoke.

For the current study, it is challenging to use the radiation solver due to limited

knowledge of the composites of the fire smoke and limited computing power. Another

reason could be that the initial condition of the air in the atrium and the wall temperatures

are unknown from the experiment so static air and constant wall temperature are assumed,

which could be different from the actual conditions. On the other hand, no uncertainties

of the measured heat release rates and the temperatures were provided from the original

study. It is hard to estimate the simulation errors due to many of these potential

uncertainties from the instruments and the surrounding conditions.

5.1.3 Smoke Layer Height Comparison

Figure 5.2 shows the comparison of the smoke layer height of the HST to the field test.

The visual inspection of the field test (the solid triangles) estimated a lower smoke layer

than that by using the measured temperatures (the solid circles). When the predicted TC

data are used, the calculated smoke layer height by Eq. (3.19) (the dashed line) is close to

the measured height. This reveals that the prediction of smoke layer height by

temperatures is not notably sensitive to the accuracy of the predicted temperatures. One

explanation is that Eq. (3.19) depends on the ratios of integrated temperatures rather than

absolute values. The predicted smoke layer height by using the concentrations of tracer

smoke (TS) (the dashed line) also generally agrees with the measured data.
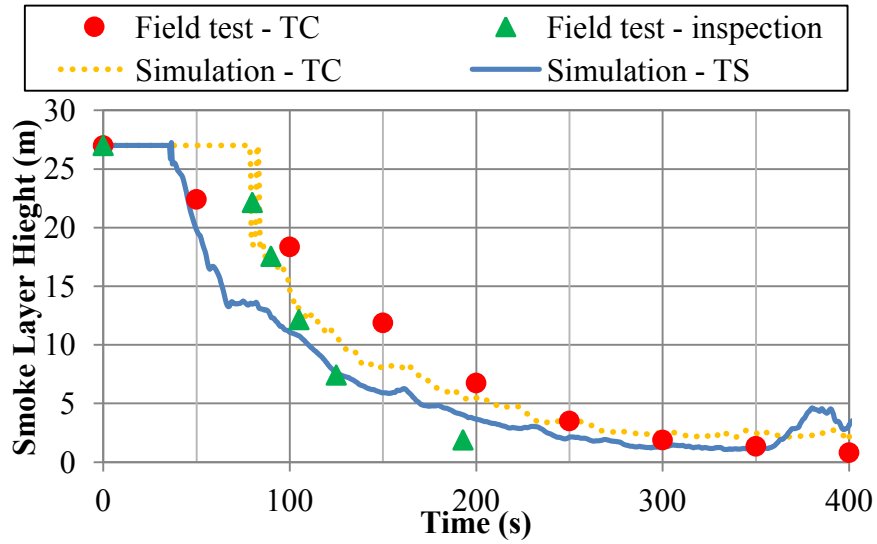
Figure 5.2 Comparison of predicted smoke layer heights by using thermocouple data and tracer smoke concentrations to the measured data in HST for the fire of 1.6 MW (TC = thermalcouple; TS = tracer smoke).

Note that the predicted smoke layer height in the case of simulation HST-TC is delayed for about 40 s when compared to the simulation HST-TS value. This is because FDS considers a smoke layer to start developing when there is a minimum temperature difference of 5 °C between the upper and lower layers. Therefore, the smoke layer is considered to be created at around 80 s in the simulation. When the concentrations of TS is used to calculate the smoke layer height, there is no minimum value of the concentration differences so the smoke layer height decreases earlier than that of the HST-TC case.

Generally, from the grid sensitive study, mesh size of 0.4 m × 0.4 m (group 1 in Table 5.1) is selected to conduct all the simulations in this study. Validation study shows that the FDS model predicts the field test results within a reasonable range. Therefore, HeST could be later modeled by applying the settings used in this section.

66

5.2 Simulations of Helium Smoke Test

5.2.1 Helium Concentration

The previous results reveal that the smoke plume driven by the density difference of helium and air is generally similar to that driven by the temperature difference of the hot smoke and the ambient in the atrium modeled. Based on Eq. (3.4a) and the ideal gas law, a relation exists between the helium concentrations of a helium smoke test and the temperatures of a hot smoke test, because the buoyancy effect is directly related to the helium concentrations or gas temperatures. If we define a non-dimensional temperature and concentration, respectively, by

$$T^* = \frac{T - T_{min}}{T_{max} - T_{min}} \tag{5.2a}$$

$$C^* = \frac{C - C_{min}}{C_{max} - C_{min}} \tag{5.2b}$$

Where T is the temperature, T_{min} is 20 °C, the minimum temperature for all thermocouples; T_{max} is 61.2 °C, the predicted maximum TC data; C is the helium volumetric fraction in mol/mol; C_{min} is zero, the minimum volumetric fraction, and C_{max} is 22 %, the maximum faction for all measured locations.
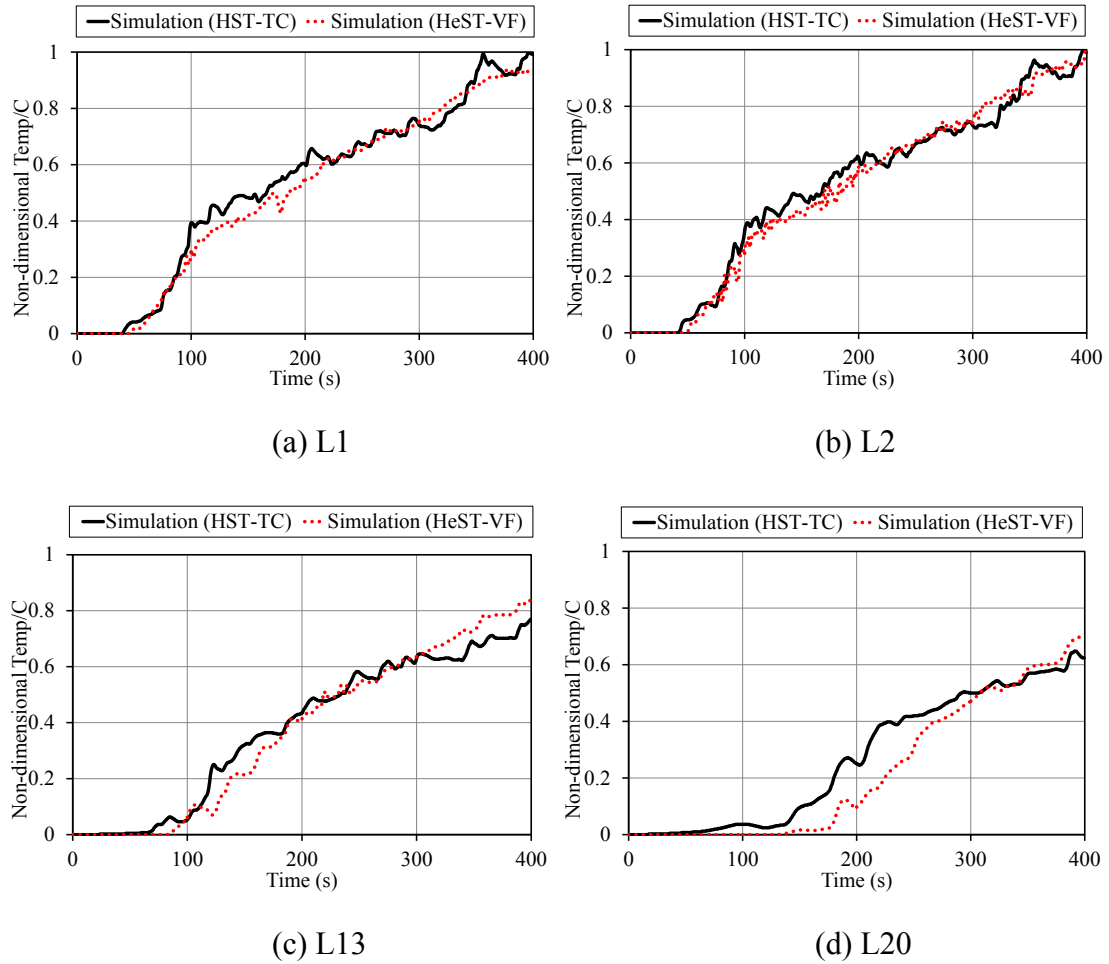
Figure 5.3 Comparison of non-dimensional temperatures and concentrations at (a) L1, (b) L2, (c) L13, and (d) L20 for the hot and the helium smoke tests for the fire of 1.6 MW.

Figure 5.3 compares the non-dimensional parameters at L1, L2, L13 and L20 in the atrium. It is shown that T^* is generally close to C^* for the atrium modeled. Therefore, it is possible to estimate the temperature of a fire smoke, given helium concentrations of a helium smoke in the atrium. We also compared the non-dimensional temperatures to the non-dimensional optical densities of the tracer smoke (not shown), defined in similar forms as Eq. (5.2b). Similar trends as Figure 5.3 are observed.

5.2.2 Smoke Layer Height

Figure 5.4 compares the predicted smoke layer height by Eq. (3.19) when using the mass

fractions of the tracer smoke (Eq. (3.22)) for the helium smoke test and the hot smoke test

for three different heat release rates. When the HRR is 1.6 MW, the predicted smoke

layer height in the HeST (the solid line, Figure 5.4) agrees well with the HST (the dot

line), while both predictions are close to the measurement (the solid circles). Furthermore,

a simulation of supplying pure air at the same flow rate as the HeST is conducted to study

the benefit of using helium. Figure 5.4 shows that the smoke layer height, based on the

tracer smoke mass fraction, is always higher in the pure air case (the multiplication signs)

than all the other cases, which indicates a much slower smoke filling process due to lack

of buoyancy in the pure air. The benefit of helium smoke test is therefore demonstrated.

Note that the predicted smoke layer height fluctuates from 100 s through 150 s in the pure

air case. This can be explained by that the momentum effect is somehow able to push up

the tracer smoke, which however cannot be stabilized without enough buoyancy. The

resultant smoke layer thus cannot develop steadily in the pure air case.
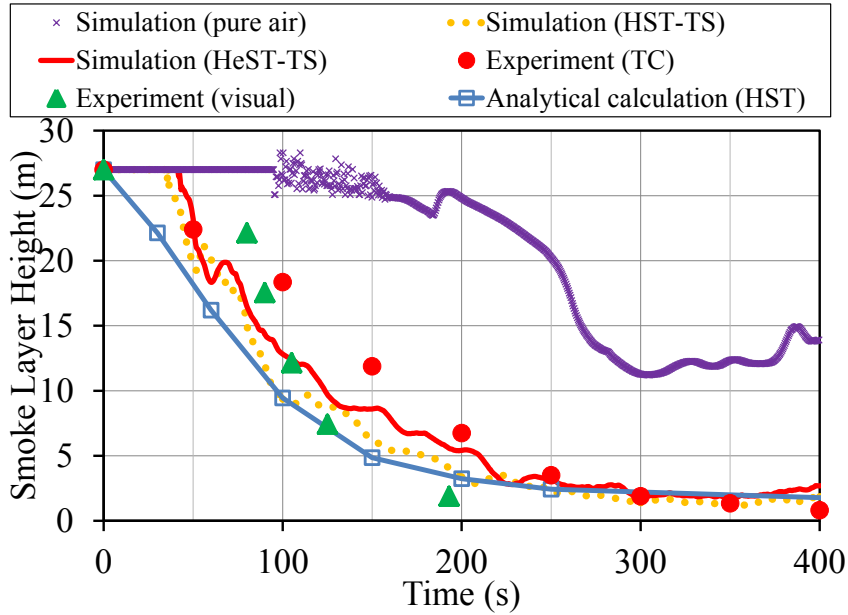
Figure 5.4 Comparison of predicted smoke layer height by different methods to the measured data for fire of 1.6 MW.

To obtain more proof, two more cases with HRR of fire 300 kW and 500 kW are simulated [46]. In both cases, the smoke layer heights in the HeST (the solid lines) agree well with those of the HST (the dot lines), which shows that the helium smoke test is able to model the similar smoke filling process as that of the hot smoke test.

Compared to the experiments, the predictions agree reasonably well with the measured data in Figure 5.5 (a) whereas overestimate the smoke layer height in Figure 5.5 (b). In field test, very low hot air temperatures were measured with no sharp change in vertical temperature profile. This might be a problem to determine the smoke layer in field tests. Thus, in these two cases, N-percentage rule was applied with the value of N taken to be 10 [46]. This explains the lower TC measurement lines than visual in Figure 5.5 while higher TC measurement line than visual line in Figure 5.4. Therefore, when comparing

smoke layer height in HST and HeST, special care should be taken and certain methods should be reexamined.

When plotting the analytical calculation based on the equation developed from the same paper [10], we find that all the predictions provide generally consistent results. Future studies, especially comparing to more other experimental data, are therefore needed.
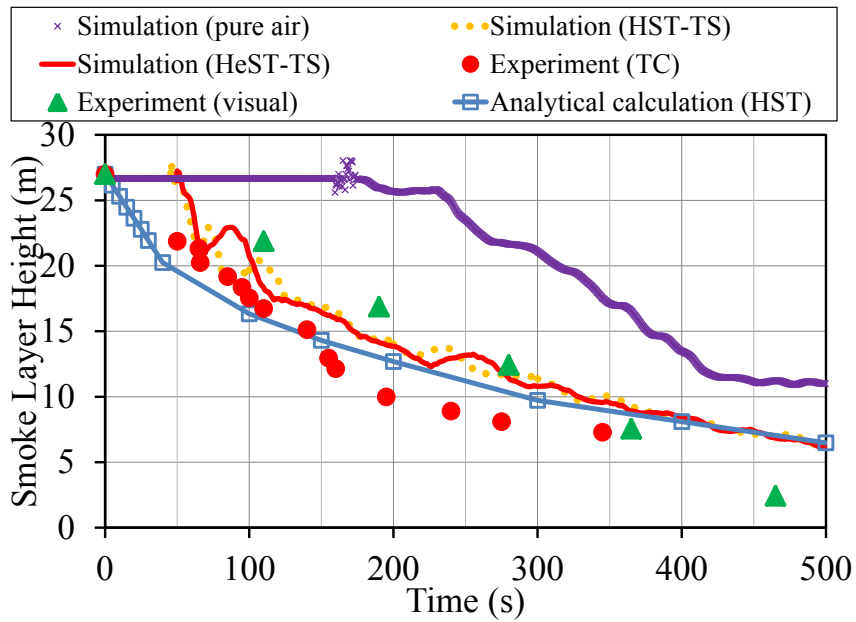
(a) 300 kW
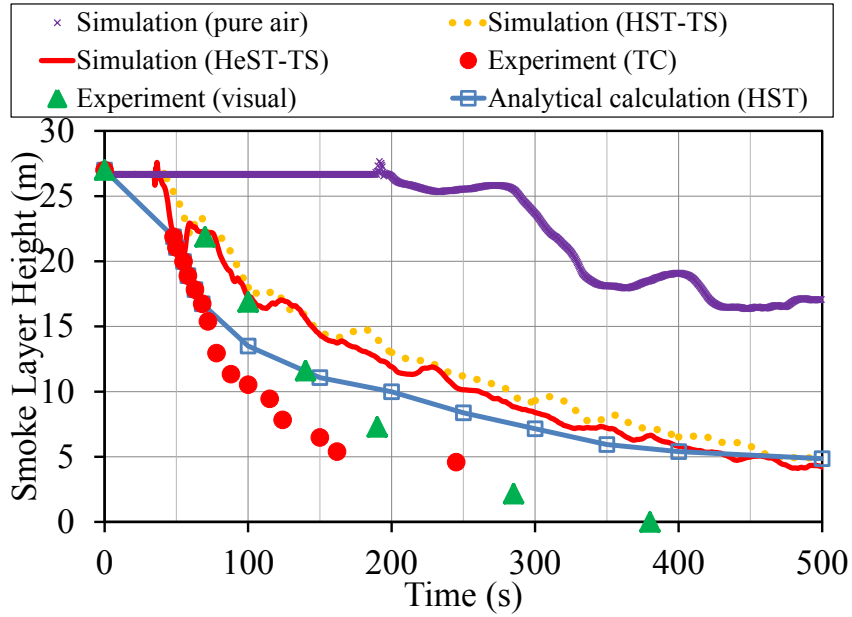
(b) 500 kW

Figure 5.5 Comparison of predicted smoke layer height by different methods to the measured data for fire of (a) 300 kW, (b) 500 kW.

5.2.3 Smoke Optical Density

A detailed comparison of the optical densities for the 1.6 MW fire in Figure 5.6 further confirms that the HeST is able to represent the HST for the atrium modeled. The predicted optical densities of the tracer smoke at L1, L2, L13 and L20 in the HeST are close to the HST. For L1 and L2, the HeST shows slightly higher optical densities yet lower values at L20 than the HST. However, the differences are not significant, which also explains why the smoke layer height based on the TS concentrations, in the HeST agrees well with that of the HST in Figure 5.6.

72
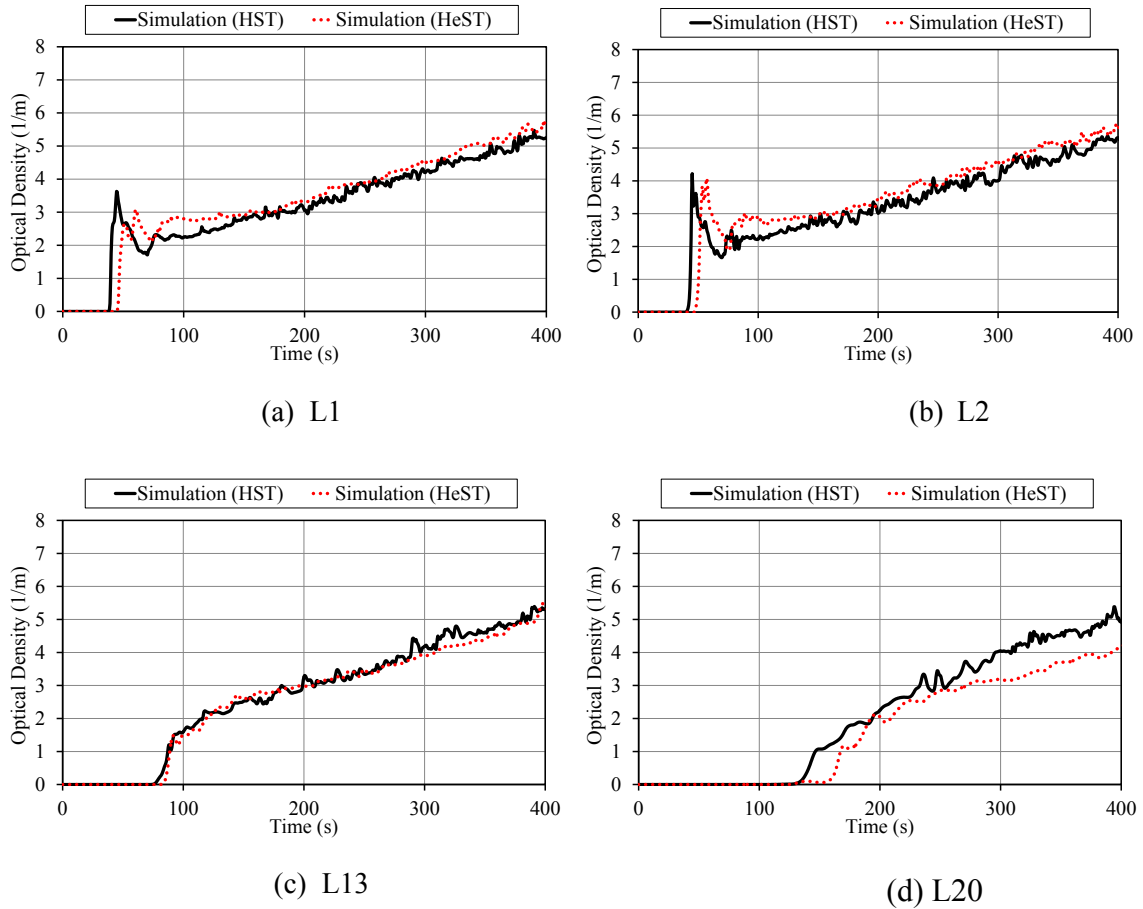
Figure 5.6 Comparison of the predicted optical densities at (a) L1, (b) L2, (c) L13 and (d) L20 for the hot and the helium smoke tests for the fire of 1.6 MW.

5.3 Validation of Helium Smoke Test

As mentioned above, numerical models always need to be validated and verified through experiment. In our study, sub-scale physical experiment provided measurement data on helium concentration and smoke filling process. Note that to keep the comparison consistent, all time scales in sub-scale physical experiment have been converted to full-scale time. In this section, only HeST with helium supply corresponding to fire of 1.6 MW are demonstrated. For the 300 kW and 500 kW cases, see Appendix D for detailed comparison.

5.3.1 Helium Concentration

Figure 5.7 compares the predicted helium volumetric fraction to those measured in experiment for fire of 1.6 MW. As can be seen from the figures, simulation results are close to measurement at all locations. At L2, simulation overestimates the helium concentration from 80s to the end, but the deviation still remains in acceptable range.
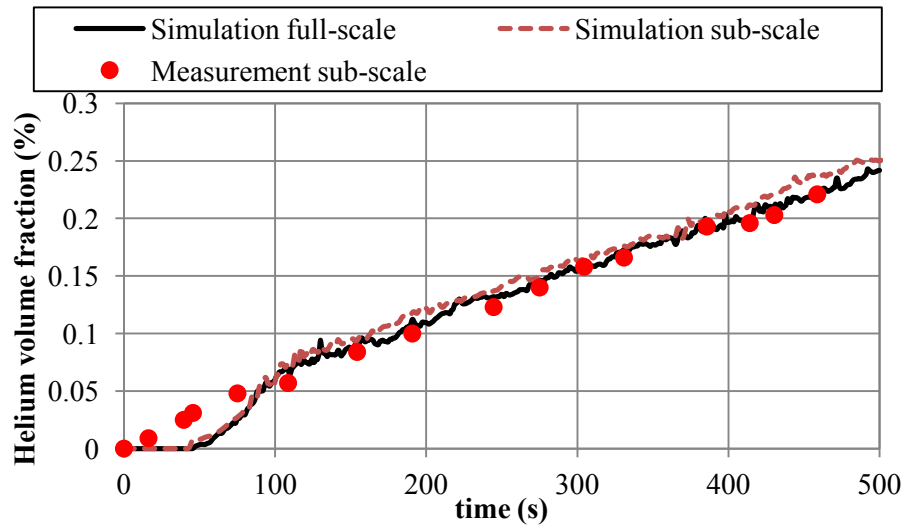
(a) L1
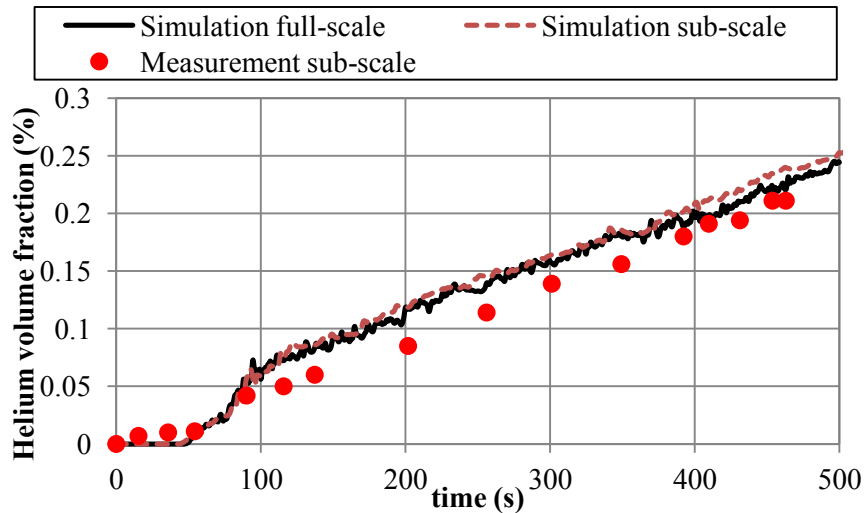
(b) L2
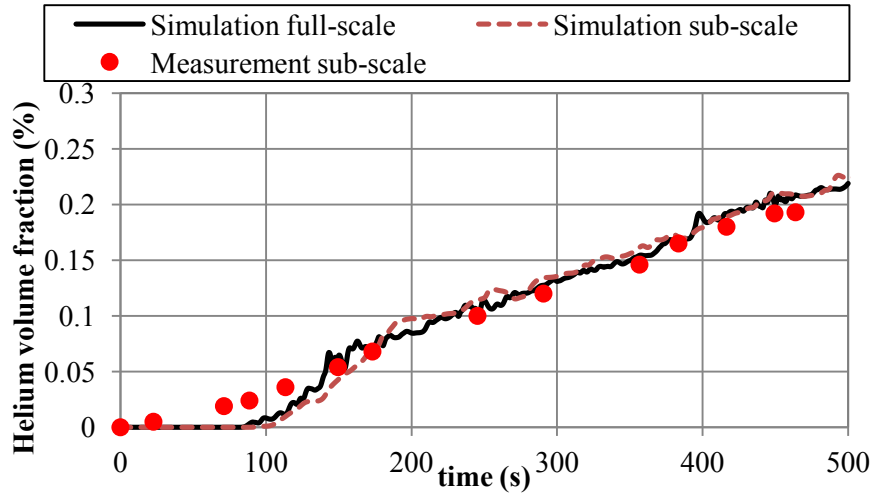
(c) L13
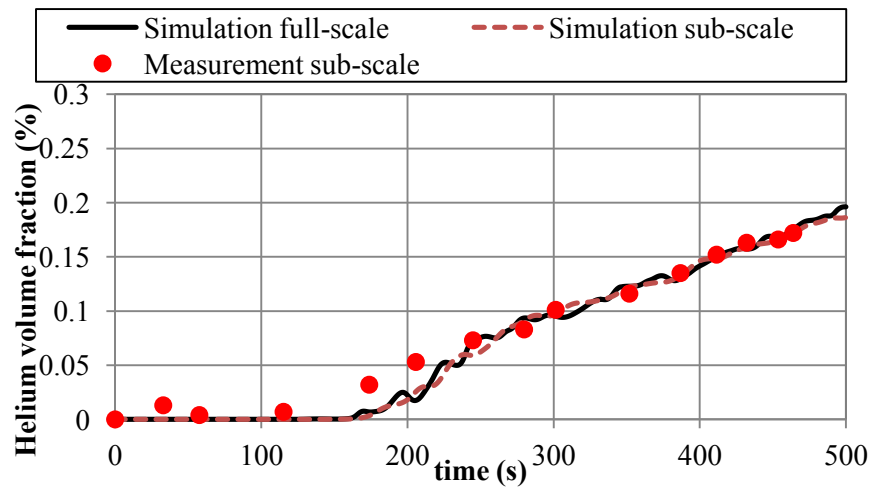
(d) L20

Figure 5.7 Comparison of helium volumetric fraction by simulation and experiment measurement at location (a) L1, (b) L2, (c) L13 and (d) L20.

5.3.2 Smoke Layer Height

Smoke layer height in sub-scale physical experiment was measured by illuminating the tracer smoke on the laser sheet, and recorded by video. Photographs of experiment recording at 50s, 100s, 150s and 200s are shown and compared with Smokeview files of

HST model in the following figure (Figure 5.8). Close similarity could be found between the helium smoke test experiment and hot smoke test simulation.
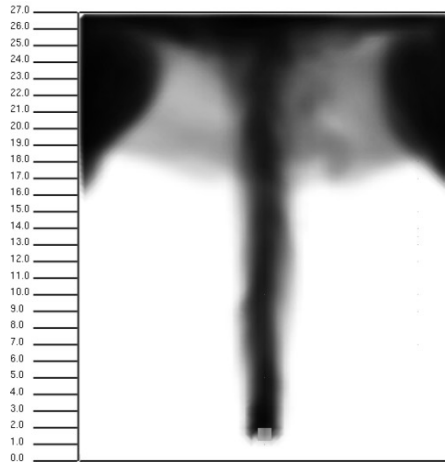
(1a) 50 s

(1b) 50s

(2a) 100 s

(1b) 100s

(3a) 150 s   (3b) 150s
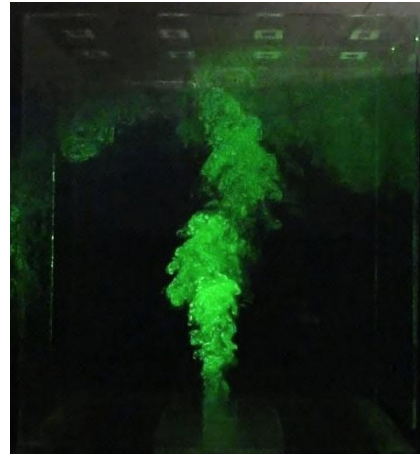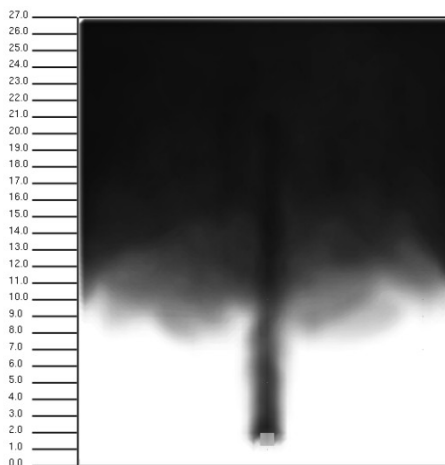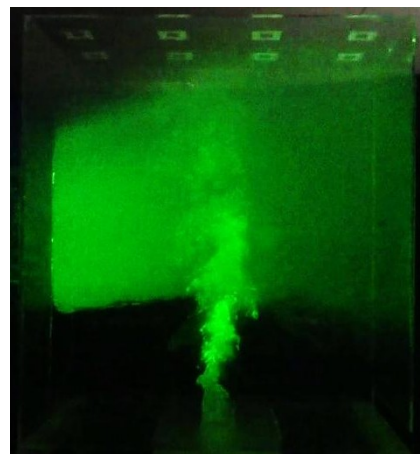
(4a) 200 s   (4b) 200s
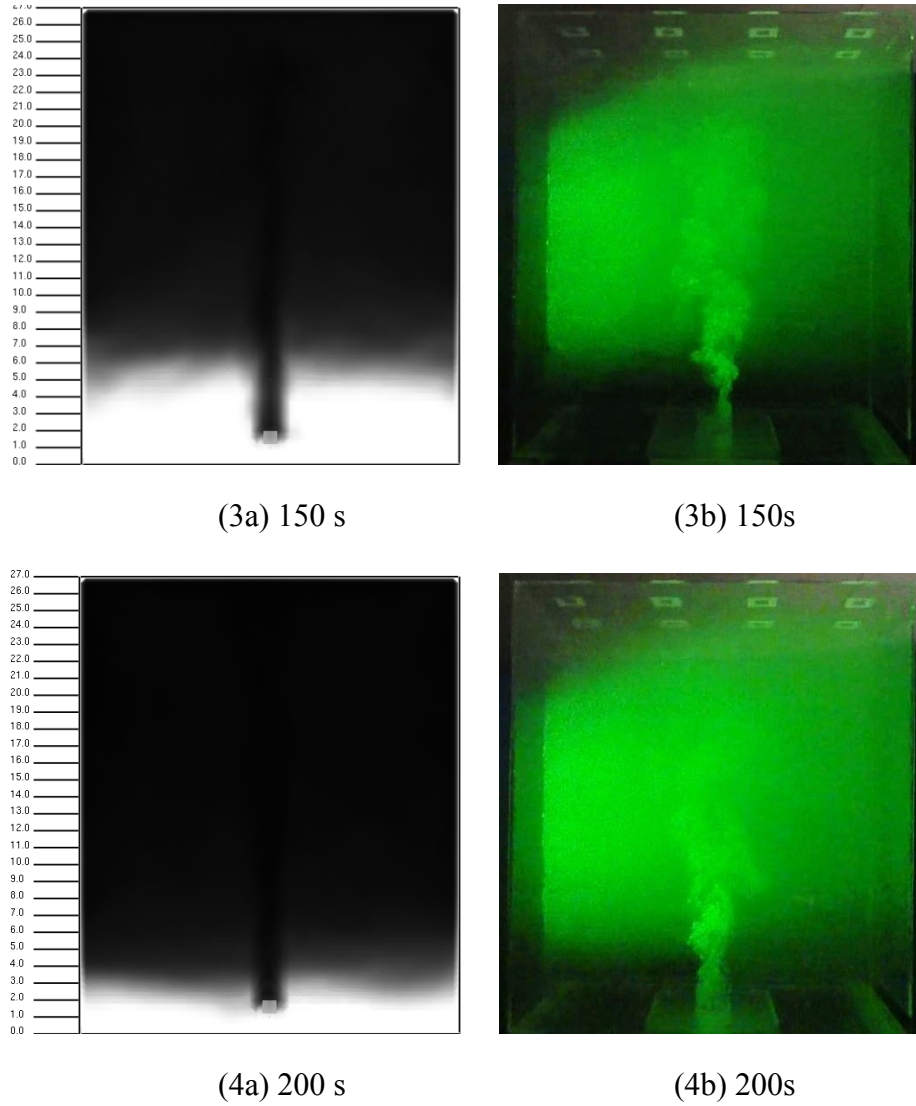
Figure 5.8 Comparison of smoke layer height at 50s, 100s, 150s and 200s in (a) HST simulation and (b) HeST experiment.

Experiment results are compared with sub-scale and full-scale HeST model, field test results and analytical calculation by Chow's Equation [10] in Figure 5.9.
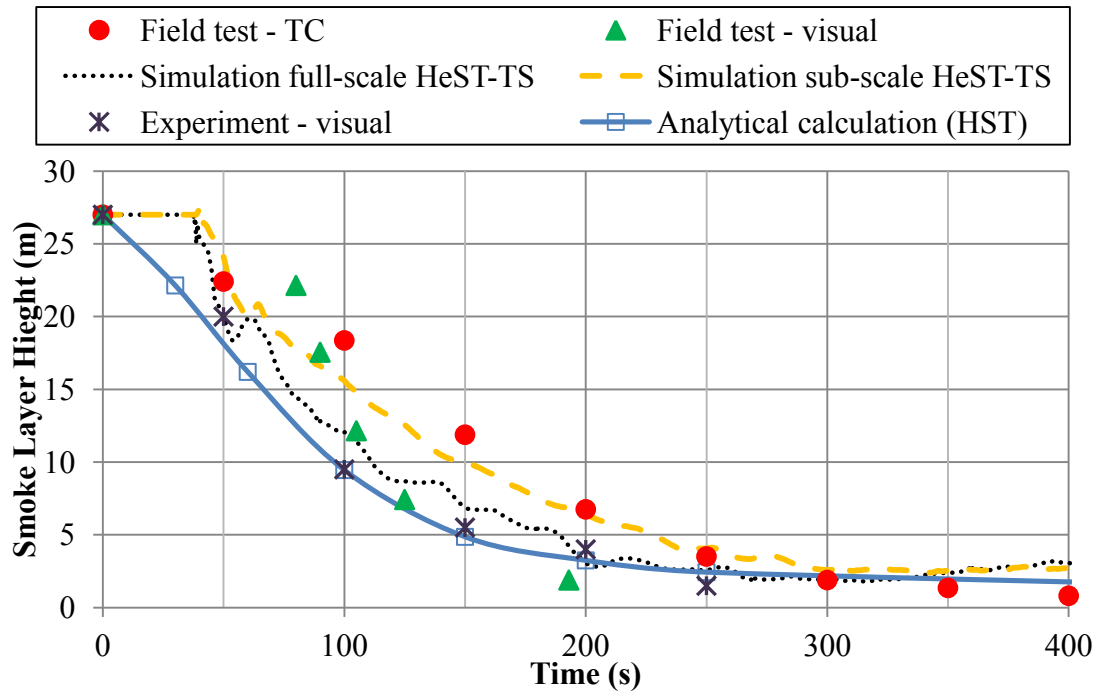
Figure 5.9 Comparison of smoke layer height in simulations and sub-scale physical experiment.

In Figure 5.9, visual inspection of smoke layer height in sub-scale experiment agrees well with full-scale HeST simulation and analytical calculation, but the sub-scale HeST simulation has higher smoke layer from 75s to 250s. Thus, the scaling laws for HeST model should be examined more in the future.

However, in field test, it is always hard to determine the clear smoke layer by visual inspection. Sub-scale experiment shows it advantages for observations, in addition, laser sheet helps to get clear photographs of smoke descending process.

In Figure 5.4 and 5.9, thermocouple measured smoke layer heights are higher than the visual inspection during the field tests. In the full-scale HST, the temperature profile is measured by thermocouple trees and hot air (not smoke) layer is then determined at the

position with sharp temperature change [47]. In visual inspections, smoke layer were directly observed, in which temperature changes might not be significant. The simulation underestimates the smoke layer height from 100 s to 200 s. The biggest difference of smoke layer height between field test and simulations occurred at $t = 150$ s, which was 5 m. This could be explained by the measured temperature results in the field test in Figure 5.1, the temperature rise at all measuring locations reached 20 °C at around 100 s, and then stay at that level till 350 s. The small temperature change in smoke plume might affect the prediction of the smoke layer height.

5.4 Summary

This chapter investigates the smoke filling process in a full-scale atrium by using a proposed method of helium smoke test. CFD model was first validated by comparing temperature and smoke layer height results to the field test data. A new method in numerical simulations of tracking the smoke layer height based on species concentrations is applied in the analysis. Reasonable mesh size was selected to conduct further simulations.

The helium smoke test model was then compared to hot smoke test model using the same comparison techniques. It was found that the smoke layer height based on the mass fractions of the tracer smoke in the helium smoke test is close to that in the hot smoke test. This similarity can be attributed to that the optical densities of the tracer smoke in the helium smoke test, which are found to agree well with that of the hot smoke test in the atrium. A relation is also found to exist between the non-dimensional temperatures in the hot smoke test and the non-dimensional helium concentrations in the helium smoke test.

79

It is therefore possible to estimate the hot smoke test gas temperature in the atrium from the helium concentrations in the helium smoke test.

Results from sub-scale physical model experiment were used to validate and verify the simulations. Helium smoke test in this sub-scale atrium model shows similar smoke filling process to hot smoke test in the full-size atrium. However, at some time point, the predicted smoke layer did not agree well to the field test. And even in field test, the clear smoke layer depth was hard to be determined. It is still a challenge to compare smoke layer height results from field test, numerical model and sub-scale experiment. Therefore, further study should focus on the methods to examine smoke layer height in hot smoke test and helium smoke test. More experimental validations and verifications of helium smoke test in other building configurations (e.g. multi-compartment buildings and tunnel section) are necessary to identify its potential limitations. The abovementioned potential problems will be discussed in the following chapter.

6. APPLICATIONS

In the previous chapter, the modeling of helium smoke test shows reasonable predictions of smoke filling process in a big single-space atrium. However, the smoke movement in various building configurations is always a challenge for fire safety engineers. Even in an atrium with irregular interior space, smoke layer are difficult to determine in hot smoke test [47]. In Section 1.2.2.2, hot smoke test has been used in tunnel smoke management commissioning for years. Therefore, to show the ability of helium smoke test representing hot smoke test, we applied helium smoke test model in a sub-scale road tunnel and a full-size building fire test facility at the Institute for Research in Construction of National Research Council Canada (NRC-IRC) in this chapter.

6.1 Helium Smoke Test in Sub-Scale Road Tunnel

6.1.1 Model Set-up

A 1/15 sub-scale road tunnel physical model with natural ventilation shafts was built at NRC-IRC [48]. The primary goal of using this model was to investigate the effect of some factors on smoke diffusion characteristics in tunnel fires with natural ventilation such as heat release rate, the tunnel section, shaft size and tunnel slope. The test data was well documented. Therefore, it was selected to conduct helium smoke test by FDS simulation.

6.1.1.1 Experiment Condition

The reduced-scale tunnel is cuboids, 17 m long, 0.7 m wide and 0.32 m high, designed according to Froude scaling. The wall of the tunnel was constructed with cement board. In experiment, four shafts are built in the middle of the width dimension of the model

tunnel. The distance between two shafts is four meters. The tunnel and shafts opening is open to the atmosphere so that all products of combustion are exhausted to the atmosphere. Figure 6.1 shows the layout of the model.
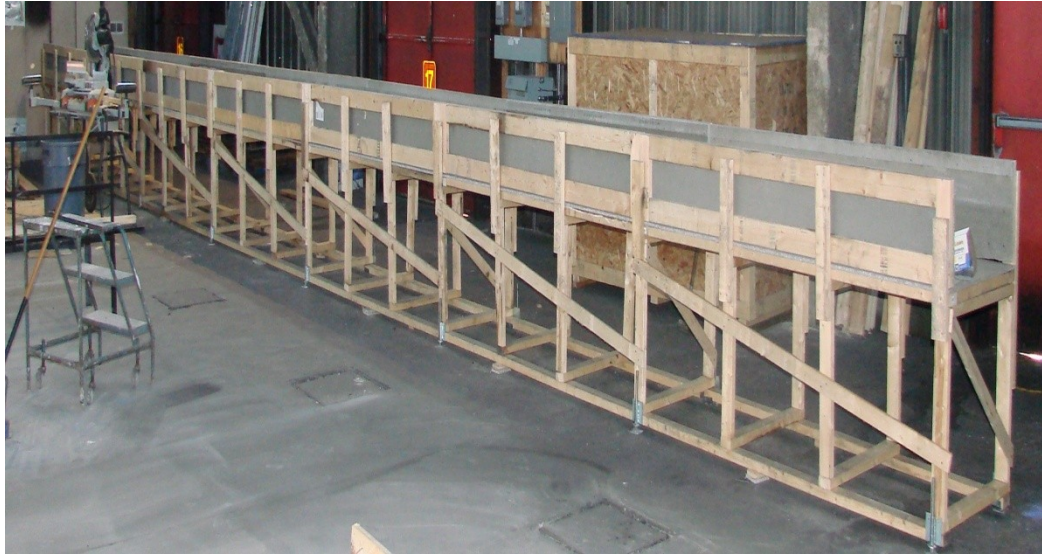
Figure 6.1 The NRC-IRC sub-scale road tunnel physical model.

In the experiments, smoke temperature and smoke exhaust volume flow rate through shafts were measured. The smoke temperature measurement was divided to three parts. The first part was located under the tunnel ceiling 10 mm. The space of two measurement points was 10 cm. The thermocouples were mainly put at one side of the tunnel center, due to the longitudinally symmetric distribution in the center of the fire source. The second part is located in the shaft to gain the smoke exhaust temperature. The third part includes four groups of thermocouple trees one meter away from the shafts that are closed to the fire to obtain the smoke layer in the tunnel. One TC tree was located above the fire source. Every group has five measurement points with a spacing of 50 mm. Detailed thermocouple distribution is shown in Figure 6.2.

82
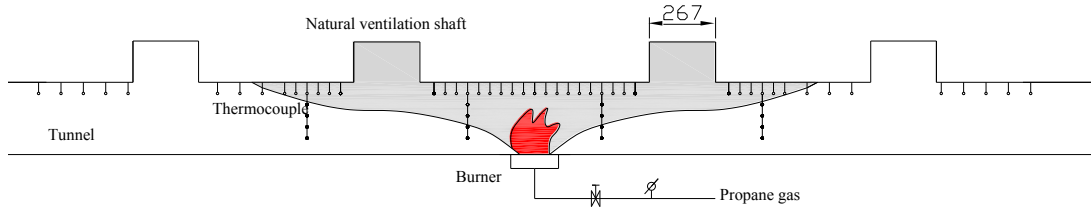
Figure 6.2 Distribution of thermocouples in tunnel model [48].

Four cases with different fire size were selected to conduct data analysis. A propane burner with 158 mm diameter was set up in the center of the tunnel as fire source (Figure 6.3). The detailed experimental conditions are listed below in Table 6.1.

Figure 6.3 Burner used in experiment (D = 158mm) [48].

Table 6.1 Experimental condition.

Case	Fire size (kW)	Shaft size (Length × height × width)	Slope (%)	Ambient temperature (°C)
1	11.89	0.667 × 0.267 × 0.167	0	19.1
2	14.07	0.667 × 0.267 × 0.167	2	23.3
3	11.70	0.667 × 0.400 × 0.167	0	26.4
4	13.68	0.800 × 0.267 × 0.167	0	26.5

6.1.1.2 CFD Modeling

In FDS model, the multi-mesh set-up was applied. Finer mesh was defined around the center of the tunnel where locates the burner/helium source. To achieve optimal calculation process, six meshes with averaged resolution were defined at each side of the tunnel section. In summary, the model contents 13 groups of mesh in total. Figure 6.4 shows the FDS model with mesh division.

Figure 6.4 FDS model set-up.

The fire/helium source was designed using the same modeling techniques mentioned in Section 4.1.1.4, 4.1.1.5 and 4.1.1.6. The calculated helium supply rates for the four cases respectively are 0.59 LPM, 0.69 LPM, 0.58 LPM and 0.67 LPM. Supply rate of tracer smoke is set to be 0.01 kg/m^2 s. Refer to Appendix E for detailed FDS input file information.

6.1.2 Results and Discussion

6.1.2.1 Validation

The FDS simulation was first validated by comparing the predicted longitudinal temperature to thermocouple measurements in the experiment (Figure 6.5). Thermocouples of part 1 in Section 6.1.1.1 were selected to do the validation. Noting that

only case 1 with 11.89 kW fire was shown in this section, for details of comparison of other cases, please refer to Appendix F. In the following figures, "-" means left tunnel section while "+" means right tunnel section.
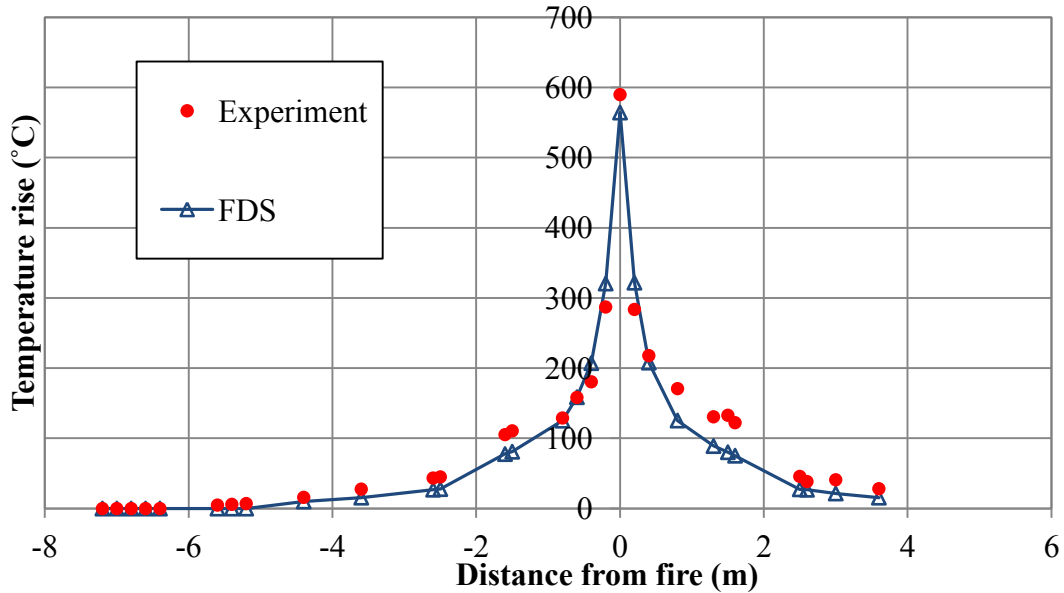
Figure 6.5 Longitudinal temperature rise distribution (case 1).

Figure 6.5 shows close comparison of predicted temperature with measured ones. The FDS model simulates reasonable temperature results near fire source. More deviation could be observed around -2 m to -1.5 m and 1 m to 2 m, where the ventilation shafts are located. Explanations could be that the mesh sizes around the shafts are bigger than those around the fire source; the uncontrollable ambient conditions also have some influence on the simulation results. In general, FDS model could provide acceptable predictions; the set-up of the model is reasonable and practical. Such set-up of the model can be used further to carry out helium smoke test discussed in the next section.

6.1.2.2 Simulation

By using the same tracer smoke source in hot smoke test model and helium smoke test model, the smoke optical density results could show the smoke movement pattern along the tunnel section and in the shafts. The longitudinal smoke optical densities are shown in Figure 6.6.
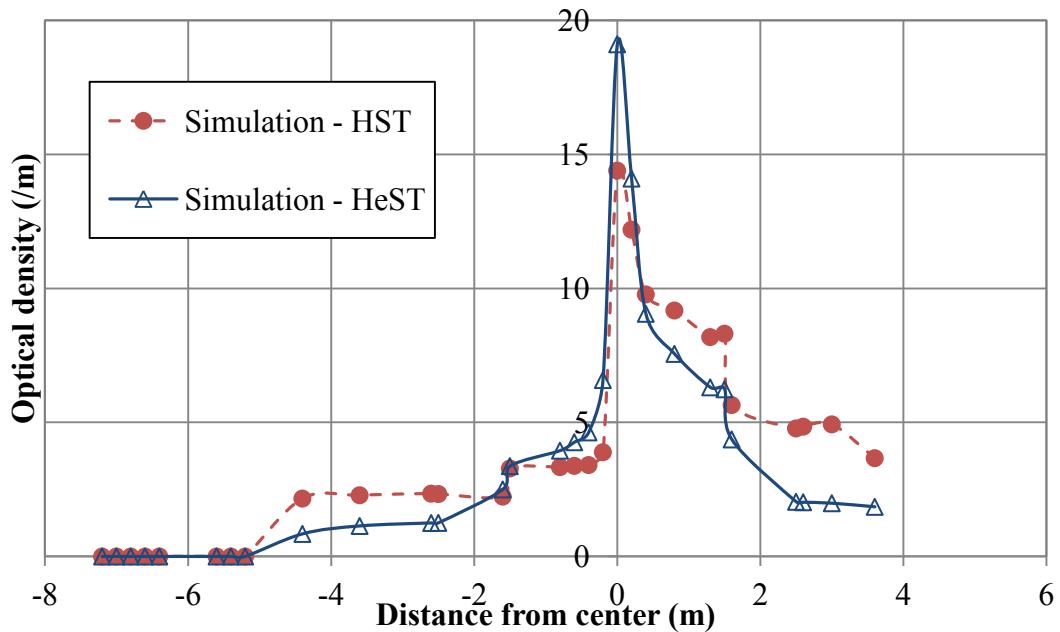
Figure 6.6 Longitudinal smoke optical density distributions (case 1).

The smoke flow pattern shows some differences in the two simulations. In hot smoke test model (solid circle with dashed line), smoke optical density is lower than that in helium smoke test model (hollow triangle with line) at -2 m to the center, while higher at other locations. Simulation results in both of the models shows poor symmetrical distribution even the ambient conditions are set to be the same. Same comparisons were observed in other cases. Thus the model need to be further examined.

To better understand the reason of the deviations, smoke layer measuring devices in FDS were put in the FDS model near the first ventilation shaft as shown in Figure 6.7.
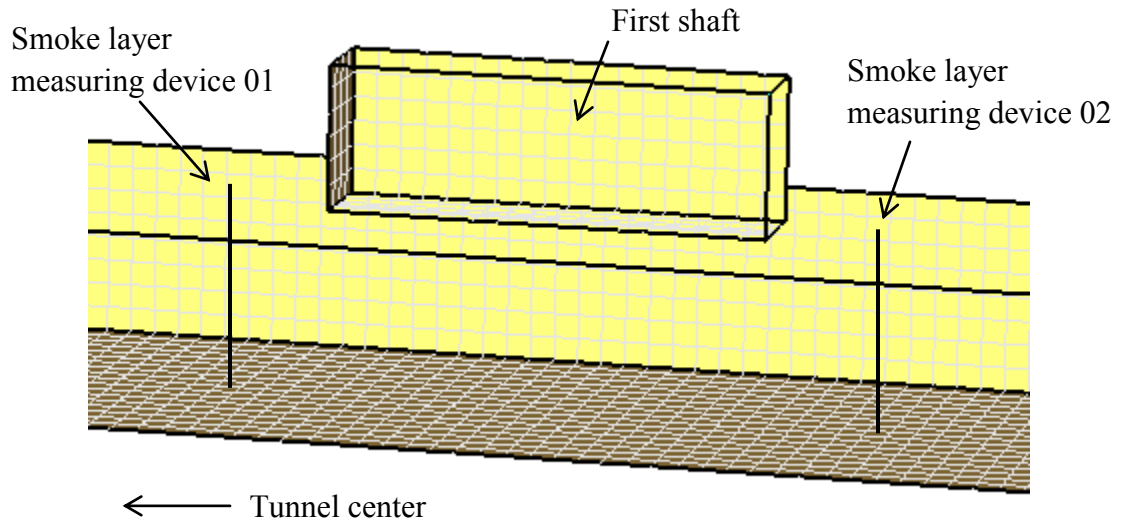
Figure 6.7 Smoke layer measurement locations
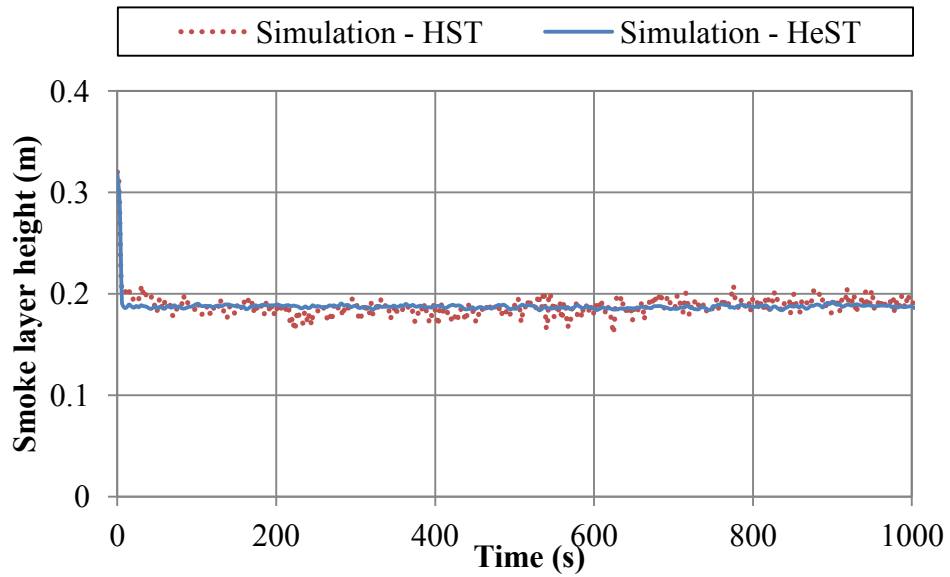
(a) Location 01
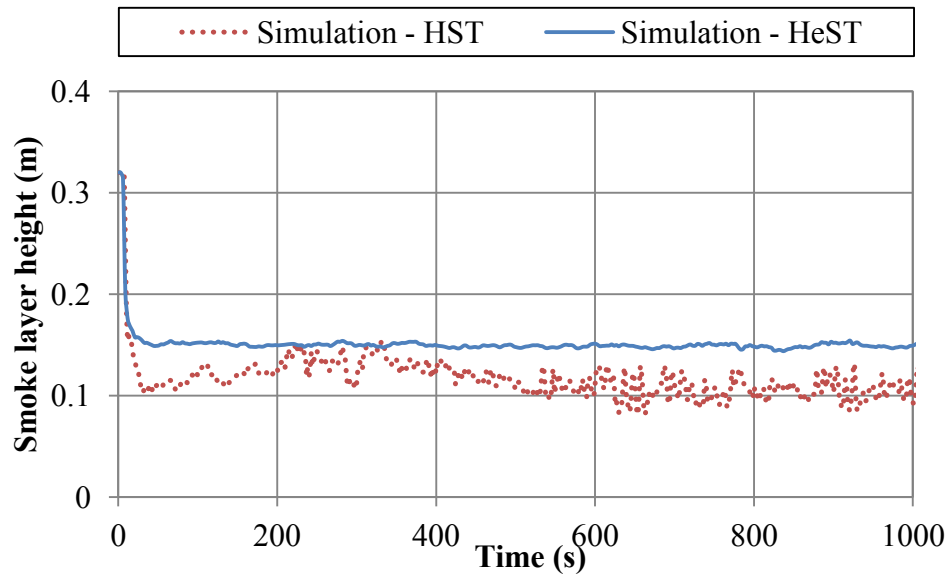
(b) Location 02

Figure 6.8 Smoke layer height results at (a) location 01 and (b) location 02.

In Figure 6.8(a), smoke layer in two models are almost at the same level, while in Figure 6.8(b), helium smoke plume remained higher than the fire smoke plume. This further explained the helium plume has a steady buoyancy than fire smoke plume, which losses its buoyancy when travelling through the tunnel section. More smoke in helium smoke test model went out through the first shaft than that of hot smoke test model. Same phenomenon could also be observed in other cases shown in Appendix F. Therefore, helium smoke test should be carefully used for studying the ventilation systems in tunnels.

6.2 Helium Smoke Test in a Full-Size Fire Test Facility

6.2.1 Model Set-up

Previously, we studied either an atrium with large vertical space or a tunnel with longitudinal space. No multi-compartment spaces have been studied for application of

88

helium smoke test. Therefore, a three-level fire test facility has been chosen to conduct

helium smoke test simulation [49, 50, 51]. The fire test facility was constructed at NRC-

IRC, primarily designed to study the impact of new building construction material and

systems on the safety of occupants in fire, it performed several tests with a designed fire

on the first (basement) level. Although the tests did not give exact information for

modeling the first and helium source in our study, it provided an example of the real

setups to study the smoke filling process in a multi-compartment building using helium

smoke test.

6.2.1.1 Layout and Dimensions

The layout of the basement is shown in Figure 6.9. A fire room with a 27.6 m^2 was

constructed inside the basement. An exterior opening was provided in the south wall of

the fire room and kept open in the simulation. It has the dimension of 2.0 m wide by 0.5

m high placed 1.8 m above the floor. A stairwell without stairs let the smoke to go

through from the basement to the upper floors.
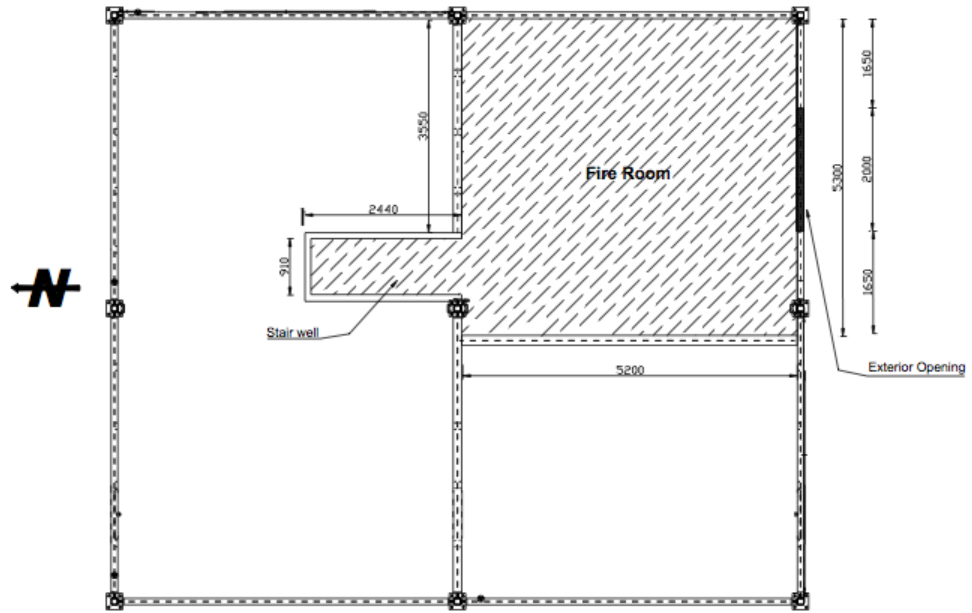
Figure 6.9 Basement plan view (all dimensions in mm) [49].
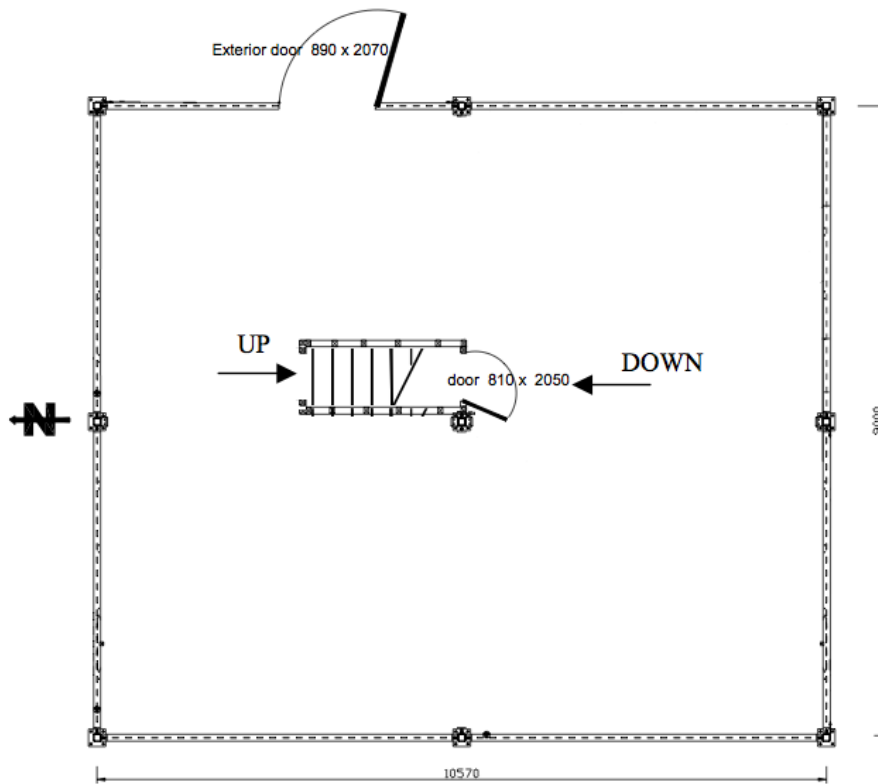
Figure 6.10 First floor plan view (all dimensions in mm) [49].

As shown in Figure 6.10，the first floor has an open-plan layout without inner walls. A doorway with 0.89 m wide by 2.07 m high led to the exterior. The stairwell to the second floor is open. There is no window opening on the first floor.
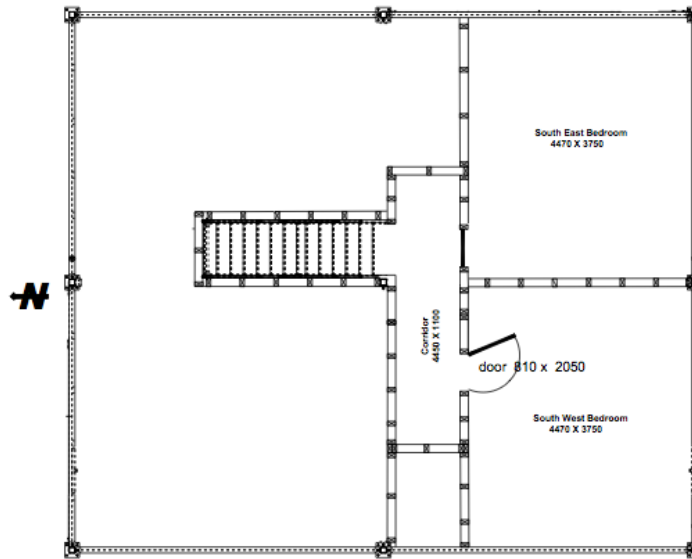
Figure 6.11 Second floor plan view (all dimensions in mm) [49].
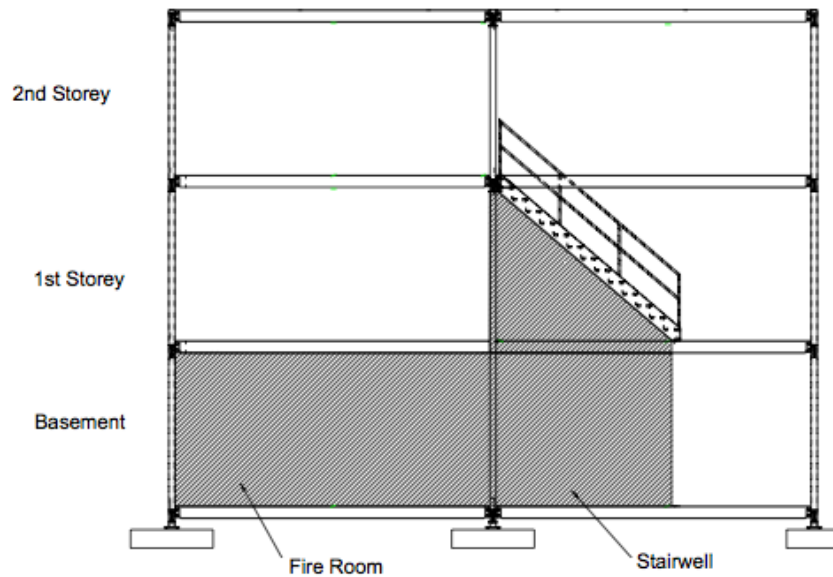
Figure 6.12 Vertical view [49].

The second floor plan is shown as Figure 6.11. A corridor at the top end of the stairs is connected with two identical bedrooms. Both the bedroom door openings are 0.81 m wide by 2.05 m high, and remained open for all simulations. The walls and floors are lined with cement boards. The ceilings are lined with 16 mm gypsum board. The ceiling height of all levels is 2.44 m. A sectional view of the house is shown in Figure 6.12.

6.2.1.2 CFD Modeling

A uniform single mesh of 0.25 m × 0.25 m × 0.25 m was applied to model the facility. Same modeling techniques of tracer smoke and instrumentation were used (Figure 6.13). Since the data of fire source in field tests were transient and hard to measure, for simplicity, we designed our own fire source for the simulations. In hot smoke test model, 300 kW fire was used, while in its corresponding helium smoke test model, helium supply rate was calculated to be 0.6875 m^3/s. A detailed FDS input file can be referred to Appendix G.
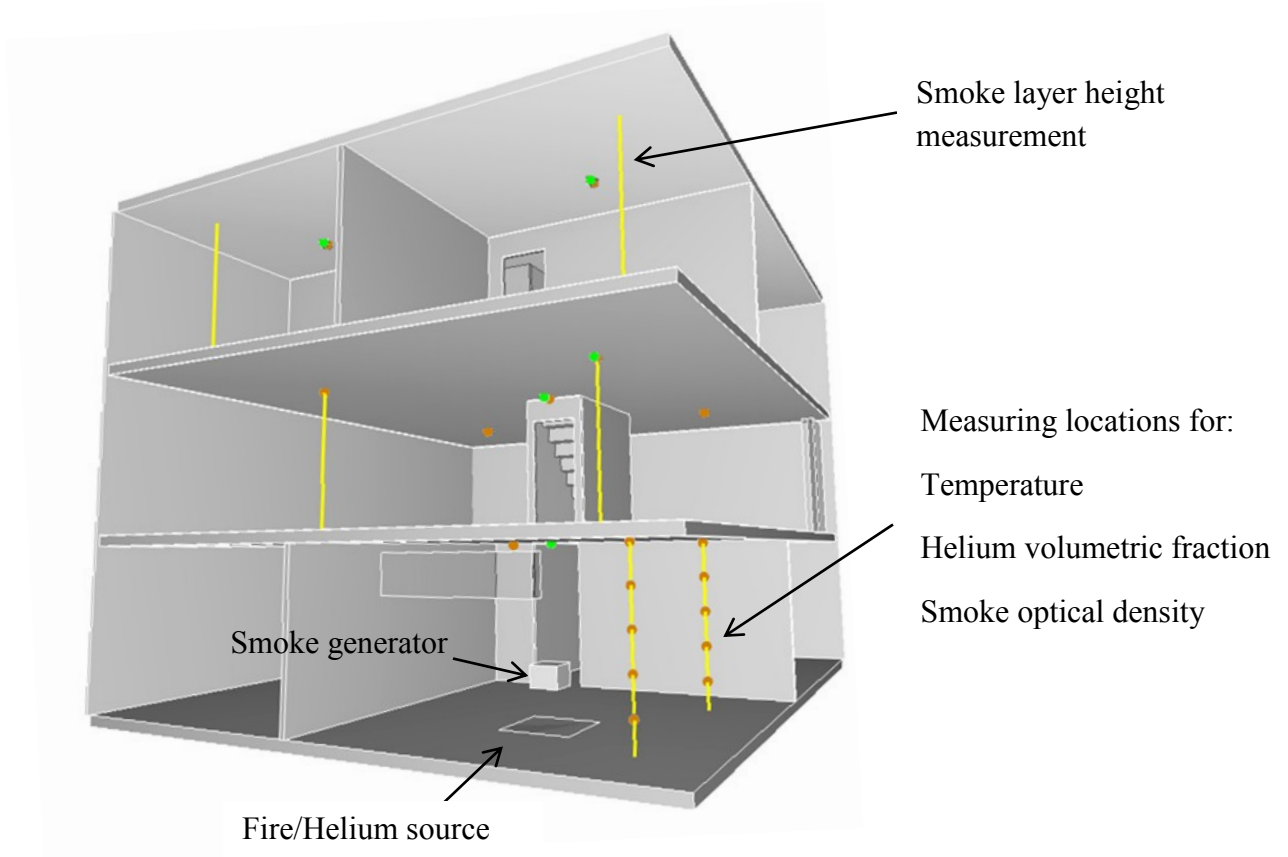
Figure 6.13 FDS model of the NRC-IRC fire test facility.

6.2.2 Results and Discussion

In this case, only a designed fire with heat release rate of 300 kW and its corresponding

helium supply were used in the simulations. No measurement data from field test were

available so helium smoke test model here is only to demonstrate its similarity to the hot

smoke test. Smoke layer heights at each level of building and non-dimensional

temperature/helium concentration are compared and discussed.

6.2.2.1 Smoke Layer Height

Figure 6.14 demonstrates the smoke layer height prediction at each floor of the building. Helium smoke test model represents similar smoke layer to the hot smoke test model. But some minor difference was observed. At the basement, helium smoke plume stay higher than hot smoke plume after 100 s. The same phenomenon could be found on the first floor, in which helium smoke plume remained higher than hot smoke plume after 150 s. Reversed situation occurred when smoke went to second floor where hot smoke plume was about 0.2 m higher than the helium smoke plume.

This again illustrates that in helium smoke test, smoke plume remained the same buoyancy at the same level while hot smoke plume losses its buoyancy, thus the helium smoke tends to travel faster to upper floors than the fire smoke does.
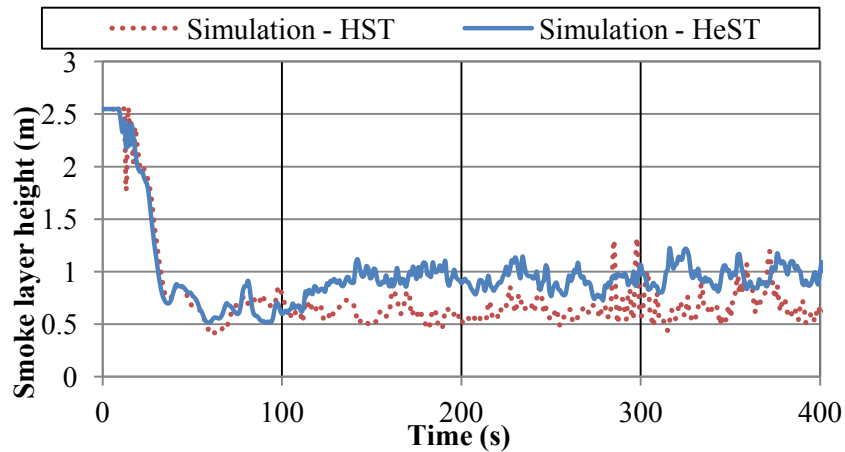
(a) Basement
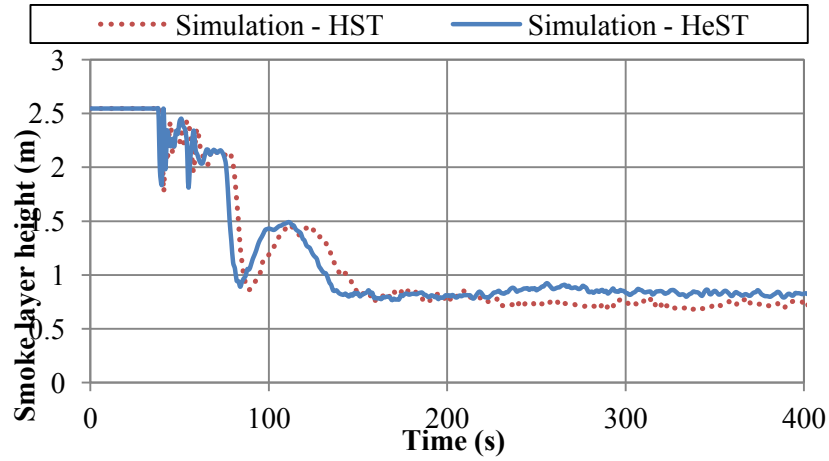
(b) First floor
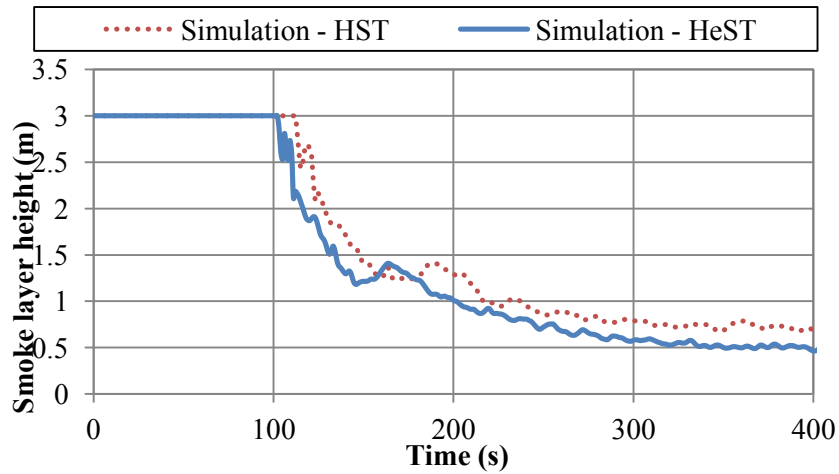
(c) Second floor

Figure 6.14 Smoke layer heights at (a) basement, (b) first floor and (c) second floor.

6.2.2.2 Non-dimensional Parameters

By using the same analysis techniques in Section 5.2.1, non-dimensional temperatures

were compared to non-dimensional helium concentrations. At each floor, T_{min}, T_{max}, C_{min}

and C_{max} from Eq. 5.2(a), (b) need to take the extreme value at each floor to make the

comparison consistent. Results are shown in Figure 6.15.

95
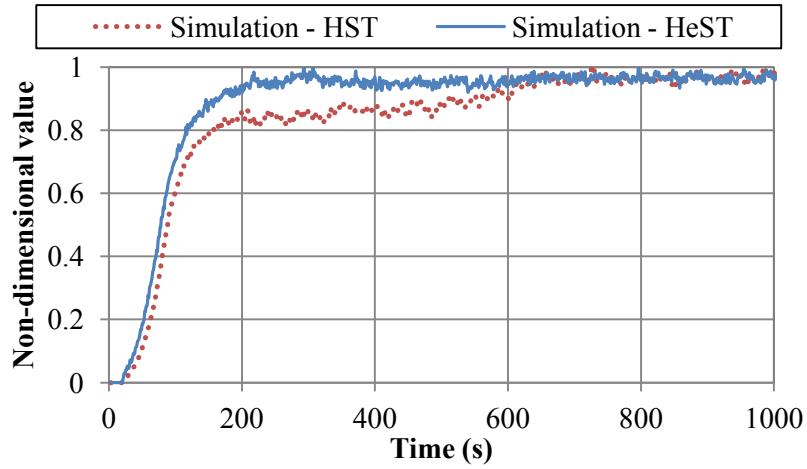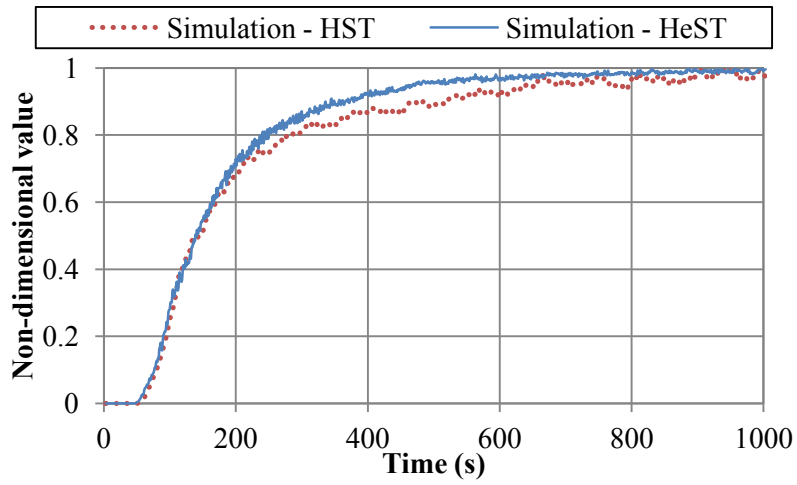
(a) Basement

(b) First floor
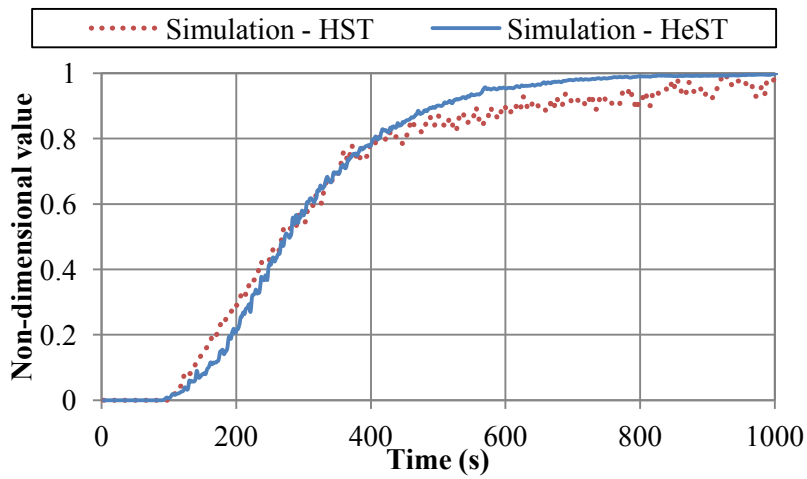
(c) Second floor

Figure 6.15 Non-dimensional comparisons at (a) basement, (b) first floor and (c) second floor.

6.2.2.3 Discussion

In this case, helium smoke test was evaluated for a multi-compartment building configuration. At each floor, smoke layer height and non-dimensional value were compared between helium smoke test model and hot smoke test model. Optical density results were not shown in this comparison to avoid repetition. Smoke layer height results showed the helium smoke test model predicts similar levels of smoke layer height as that of hot smoke test model, but helium smoke plume travels faster to upper floor. The same conclusion could be drawn from comparing the non-dimensional parameters. Thus, when dealing with experiment or field test conditions with multi-compartment interior spaces, helium smoke test should be carried out with more attention. Further studies with combination of numerical and experimental methodology should be performed for this type of interior spaces.

7. CONCLUSION AND FUTURE WORK

This thesis proposed an alternative commissioning method, helium smoke test, for fire smoke management system in buildings. The study included an overall literature review of applications of using helium as buoyant plume, a theoretical study of helium smoke, the key features and fundamentals on smoke filling process and scaling laws for sub-scale modeling. Then an atrium with large vertical interior space was selected for helium smoke tests by the means of numerical and experimental methodology. CFD predictions were then compared with the measured data from the field test. Conclusions could be drawn as follows.

7.1 Helium Plume

A method was developed theoretically to determine the helium flow rate necessary to simulate the fire source with certain buoyancy force. However, the smoke plume characteristics should be re-examined. Pure helium provides the buoyancy but the air entrainment was not considered in helium plume. Adding air or not in the helium plume still remains a question since the simulated smoke plume is subject to the gas temperature in pool fire tests. Because of the limitations, current studies are focusing on the modeling method and quantitative analysis. More theoretical studies are needed in the future on the plume temperature, air entrainment and momentum effects.

7.2 Smoke Filling Process

By studying the smoke layer height during hot smoke test and helium smoke test, positive results could be found that pure helium smoke represents the smoke filling process well as that in hot smoke test. However, the method to determine the clear smoke layer should

be re-examined. Traditionally, smoke layer in fire experiments was determined by the sharp change of temperature between two measuring locations. This method was found to have its own limitations when the temperature of smoke plume was not high enough, or the measuring locations are not sufficient. Visual inspection in full-size experiments was not practical, and produced unpredictable uncertainties.

Use of numerical simulations could provide fire safety researchers with visually smoke movement patterns. In our study, a modeling method was developed to supply tracer smoke not only to show the smoke movement, but also predict the smoke layer height by species concentration.

In sub-scale physical model experiment, helium smoke test reproduced the smoke filling process in hot smoke test. Through the laser sheet illumination, clear smoke layer of helium smoke test could be recorded. The experiment data validated the numerical models, and provided us with useful lessons and important experiences to conducted more experiments.

In addition, smoke optical density was regarded as a practical measurement of smoke obstruction. In our CFD simulations, smoke optical densities were plotted to show the smoke movement and clear smoke layer in visualization. But in real experiment, it is always hard to reproduce such tracer smoke as that used in the simulations. In another word, tracer smoke used in experiment is also hard to model in CFD simulations. Comparison of smoke layer height created by the artificial smoke in simulation and experiment still stays at the level of visual inspection, which was found to deviate from

other measurements. Future work should focus on the modeling of tracer smoke, as well as verification of the observed smoke layer with measured data.

In Chapter 6, two application of helium smoke test were studied but without experiment measurement data. The numerical models are in great need of validation and verification. The limitations of helium smoke test in these types of building should be discussed in the future with adequate experiment data. In future studies, sub-scale physical model of other building configurations should be developed to examine the performance of helium smoke test.

7.3 Economical Efficiency

As mentioned in introduction, hot smoke test has some limitations including the high cost of insurance and protection. Helium smoke test provides a safer way for commissioning the smoke management system. But the consumption and the total cost of helium smoke test cannot be neglected due to the expensive price of helium when conducting full-size tests. As a result, helium smoke test may be still limited to laboratory scale or medium scale. More work of developing new helium supply equipment and experimental methods are necessary in future studies, such as heated helium smoke test.

7.4 Contributions

This thesis proposed an alternative experimental and numerical method, helium smoke test, for building fire smoke control studies. The modeling process provides a realistic reproduction of field test. The set-ups of the numerical model sets an example for further modeling work. The sub-scale model experiment provides a convenient way to conduct

experiment when full-size tests are inaccessible. The limitations and potential problems of this method talked in the previous section shows a clear direction of the future studies.

7.5 Summary

Generally speaking, helium smoke test in this study provides a new thought to simulate a real pool fire test in a safer way. A combination of numerical and experimental methodology is found to be appropriate in fire safety studies. The CFD model of helium smoke test could be applied to simulate fire scenarios but always need to validate with adequate experiment data. Sub-scale physical model shows that in laboratory scale, helium smoke test could be an alternative experimental method when lab safety for fire research is concerned. More future work should focus on theoretical studies of helium smoke test and possibly full-scale applications.

REFERENCES

[1] A. Bounagui and N. Bénichou, "Fire Deaths, Injuries and Monetary Losses in Canada 1986-2000," 2007, IRC-RR-238

[2] Quebec SP. "Statistiques sur les indendies. In. Statistiques sur les indendies." Quebec, Quebec, Securite Publique Quebec, 2007.

[3] John R. Hall, Jr. "Burns, Toxic Gases, and Other Fire-like Hazards in Non-fire Situations," 2004

[4] J.M. Rubes, "Blowing Smoke: Commissioning Smoke Management Systems," 2000

[5] K.M. Elovitz, "Commissioning Smoke Control Systems," 2006

[6] H. Allan and M. Delichatsios, "Hot-Smoke Testing in Australian Tunnels"

[7] AS 4391-1999, Australian Standard, Smoke management systems – Hot smoke test, 1999

[8] W. K. Chow,Y.K. Li, E. Cui, R. Huo, "Natural Smoke Filling in Atrium with Liquid Pool Fires up to 1.6 MW," Building and Environment, vol 36, 2001, pp. 121-127

[9] W.K. Chow, and Anthony C.W. Lo, "Scale Modeling Studies on Atrium Smoke Movement and the Smoke Filling Process," Journal of Fire Protection Engineering 1995 7: 55

[10] W.K. Chow and Henry H.W. Lo, "Scale Modeling on Natural Smoke Filling in an Atrium," Heat Transfer Engineering, 29: 1, 2008, pp.76 — 84

[11] Makoto Tsujimoto, Testsuji Takenouchi, Shigeo Uehara, "A Scaling Law of Smoke Movement in Atrium," Fire Research and Safety, 11th Joint Panel Meeting, 1989

[12] Steve. Kerber and James A. Milke, "Using FDS to Simulate Smoke Layer Interface Height in a Simple Atrium," Fire Technology, 43, 2007, pp. 45-75

[13] W.K. Chow, C.L. Chow, and S.S. Li, "Simulating Smoke Filling in Big Halls by Computational Fluid Dynamics," Modelling and Simulation in Engineering, 2011

[14] A. Byström, X. Cheng, U. Wickström, and M. Veljkovic, "Full-scale Experiment and Numerical Studies on Compartment Fire under Low Ambient Temperature," Building and Environment, 51, 2012, pp. 255-262

[15] K. McGrattan, R. McDermott, S. Hostikka, J. Floyd, "Fire Dynamics Simulator (Version 5) User's Guide," NIST Special Publication 1019-5, Gaithersburg, National Institute of Standards and Technology 2010

[16] E.L. Maylor, "Airplane Tests of Enhanced Emergency Smoke Venting," FAA Technical Center, 1989

[17] T.I. Eklund "Generation of a Buoyant Plume of Artificial Smoke for Airplane Tests," FAA Technical Center, 1990

[18] M.R. Phipps, Y. Jaluria, and T. Eklund, "Helium-Based Simulation of Smoke Spread Due to Fire in Enclosed Spaces," Combustion Science and Technology, 128: 1, 1997, pp. 49-72

[19] FAA, Smoke Detection, Penetration and Evacuation Tests and Related Flight Manual Emergency Procedures, FAA Advisory Circlar, 1994

[20] R.J. Richard, C.J. Douglas, "Use of Inert Buoyant Gases for the Simulation of Real Fire Sources," U.S. Patent, 61/177, 041, 2009

[21] O.Vauquelin and O. Megret, "Smoke Extraction Experiment in Case of Fire in A Tunnel," Fire Safety Journal, 37, 2002, pp. 525-533

[22] O. Vauquelin, "Experimental Simulations of Fire-induced Smoke Control in Tunnels Using an "Air-helium Reduced Scale Model": Principle, Limitations, Results and Future," Tunnelling and Underground Space Technology, 23, 2008, pp. 171-178

[23] R.A. Bryant, "Particle Image Velocimetry Measurements of Buoyancy Induced Flow through a Doorway," NISTIR 7252, 2005

[24] B.M. Cetegen and K.D. Kasper, "Experiments on the Oscillatory Behavior of Buoyant Plumes of Helium and Helium-air Mixtures," Physics of Fluids, 8:11, 1996, pp. 2974-2984

[25] T. J. O'Hern, E .J. Weckman, A. L. Gerhart, S. R. Tieszen and R. W. Schefer, "Experimental Study of a Turbulent Buoyant Helium Plume," J. Fluid Mech. 544, 2005, pp. 143-171

[26] P.E. DesJardin, S.R. Tieszen, T.J. O'Hern, and A.L. Gerhart, "Numerical predictions and experimental measurements of the near-field of a large turbulent helium plume," ASME Intl Mech. Engng Conf. and Exposition, Symp. on Integrated Experimental and Simulation Investigations in Research and Design, Orlando, FL, November, 2000

[27] P.E. DesJardin, T.J. O'Hern, and S.R. Tieszen, "Large eddy simulation and experimental measurements of the near-field of a large turbulent helium plume," Phys. Fluids 16, 2004, pp. 1866–1883

 [28] M.R. Swain, E.S. Grilliot, & M.N.Swain, "Phase 2: Risks in indoor vehicle storage," Addendum to Hydrogen Vehicle Safety Report, 1998

[29] E. A. Papanikolaou and A. G.Venetsanos, "CFD modeling for helium releases in a private garage without forced ventilation" 2005

[30] SFPE, SFPE Handbook of Fire Protection Engineering - Third Edition - Chapter 1, Fire Plumes, Flame Height, and Air Entrainment, National Fire Protection Association, Massachusetts, 2002.

[31] O. Vauquelin, G. Michaux and C. Lucchesi, "Scaling laws for a buoyant release used to simulate fire-induced smoke in laboratory experiments," Fire Safety Journal, 44, 2009, pp. 665-667

[32] J.A. Capote, D. Alvear, O.V. Abreu, M. Lazaro and P. Espina, "Scale tests of smoke filling in large atria," Fire Technology, 45:2, 2009, pp. 201-220

[33] J.G. Quintiere, "Scaling Applications in Fire Research," Fire Safety Journal 15, 1989, pp. 3-29

[34] NFPA 92B: NFPA 92B: Smoke Management Systems in Malls, Atria, and Large Areas, National Fire Protection Association - Quincy, MA, USA, 2000

[35] K. Steckler, H.R. Baum, and J.G. Quintiere, Salt Water Modeling of Fire Induced Flows in Multicompartment Enclosures, Proceedings of the Combustion Institute 21 143-149 (1986).

[36] C. Gutierrez-Montes, E. Sanmiguel-Rojas, A. Viedma, G. Rein, "Experimental data and numerical modeling of 1.3 and 2.3 MW fires in a 20 m cubic atrium," Building and Environment, 44, 2009, pp. 1827-1839

[37] G. Hadjisophocleous and Q. Jia, "Comparison of FDS prediction of smoke movement in a 10-storey building with experimental data," Fire Technology, 45, 2009, pp. 163-177

[38] G.P. Forney, "Smokeview (Version 5) - A Tool for Visualizing Fire Dynamics Simulation Data Volume I: User's Guide," NIST special publication 1017-1, Gaithersburg, National Institute of Standards an d Technology 2010

[39] T. Tanaka and T. Yamana, "Smoke Control in Large Scale Spaces, Part 1," Fire Science and Technology, 5, 1985, pp. 31–40

[40] T. Yamana and T. Tanaka, "Smoke Control in Large Spaces—Part 2," Fire Science and Technology, 5:2, 1985, pp. 41–54

[41] G.V. Hadjisophocleous and C.J. McCartney, "Guidelines for the use of CFD simulations for fire and smoke modeling," ASHRAE Transactions, v. 111, no. 2,2005, pp. 583-594

[42] H. Koseki and H. Hayasaka, "Estimation of Thermal Balance in Heptane Pool Fire," Journal of Fire Sciences, 7:4, 1989, pp. 237-250

[43] H. Hayasaka, H. Koseki and Y. Tashiro, "Radiation measurements in large-scale kerosene pool flames using high-speed thermography," Fire Technology, 28:2, 1992, pp. 110-122

[44] K. McGrattan, "Fire dynamics simulator (version 4) technical reference guide," National Institute of Standards and Technology, NIST Special Publication 1018, 2004

[45] J. Dreisbach, K. McGrattan, "Verification and validation of selected fire models for nuclear power plant applications. In: Fire dynamics simulator (FDS)," NUREG-1824 final report, vol. 7. U.S. Nuclear Regulatory Commission, Office of Nuclear Regulatory Research; May 2007

[46] W.K. Chow, E. Cui, Y.Z. Li, R. Huo and J.J. Zhou, "Experimental Studies on Natural Smoke Filling in Atria," Journal of Fire Sciences, 2000, 18: 84

[47] W.K. Chow, "Determination of the Smoke Layer Interface Height for Hot Smoke Tests in Big Halls," Journal of Fire Sciences, 27:125, 2009

[48] A. Kashef, Z. Yuan and B. Lei, "Ceiling temperature distribution and smoke diffusion in tunnel fires with natural ventilation," unpublished

[49] B. Taber et al. "Fire Scenario Tests in Fire Performance of Houses Test Facility-Data Compilation," National Research Council Canada, Research Report: IRC-RR-208, 2006

[50] J.Z. Su et al. "Fire Performance of Houses, Phase 1, Study of Unprotected Floor Assemblies in Basement Fire Scenarios, Summary Report," National Research Council Canada, Research Report: RR-252, 2008

[51] N. Benichou, et al. "Fire Performance of Houses, Phase 1, Study of Unprotected Floor Assemblies in Basement Fire Scenarios, Part 3-Results of Test UF-04 (Light-Gaufe Steel C-Joists)," National Research Council Canada, Research Report: IRC-RR-248, 2009

APPENDIX A – SCALING LAWS

Equation A.1 – A.3 show the conservation of mass, momentum in vertical direction and energy respectively:

$$\frac{\partial \rho}{\partial t} + \frac{\partial (\rho \cdot \alpha)}{\partial x} = 0 \tag{A.1}$$

$$\rho(\frac{\partial \alpha}{\partial t} + \alpha \frac{\partial \alpha}{\partial x}) = -\frac{\partial P'}{\partial x} + g(\rho_0 - \rho) + \frac{4}{3}\mu \cdot \frac{\partial^2 \alpha}{\partial x^2} \tag{A.2}$$

$$\rho \cdot C_\rho (\frac{\partial T}{\partial t} + \alpha \frac{\partial T}{\partial x}) = k \frac{\partial^2 T}{\partial x^2} + \frac{\partial P}{\partial t} + Q''' \tag{A.3}$$

One could use normalizing parameters to transfer the governing equations into dimensionless forms. The normalizing parameters are as follows:

- Geometric length scale: l
- Characteristics velocity: V
- Characteristics time: τ
- Initial ambient pressure: P_0
- Initial ambient density: ρ_0
- Initial ambient temperature: T_0
- Characteristics pressure: P^*

Then the dimensionless variables are defined as:

$$\hat{x} = \frac{x}{\ell} \tag{A.4}$$

$$\hat{t} = \frac{t}{\tau} \tag{A.5}$$

$$\hat{\alpha} = \frac{\alpha}{V} \tag{A.6}$$

$$\hat{\rho} = \frac{\rho}{\rho_0} \tag{A.7}$$

By substituting equation (A.4 – A.7) into equation (A.1 –A.3), the conservation equations become:

$$\pi_1 \frac{\partial \hat{\rho}}{\partial \hat{t}} + \frac{\partial (\hat{\rho} \cdot \hat{\alpha})}{\partial \hat{x}} = 0 \tag{A.8}$$

$$\hat{\rho}(\pi_1 \frac{\partial \hat{\alpha}}{\partial \hat{t}} + \hat{\alpha} \frac{\partial \hat{\alpha}}{\partial \hat{x}}) = -\pi_2 \frac{\partial \hat{P}^l}{\partial \hat{x}} + \frac{4}{3}\pi_3 \frac{\partial^2 \hat{\alpha}}{\partial \hat{x}^2} + \pi_4(1-\hat{\rho}) \tag{A.9}$$

$$\hat{\rho}(\pi_1 \frac{\partial \hat{T}}{\partial \hat{t}} + \hat{\alpha} \frac{\partial \hat{T}}{\partial \hat{x}}) = \pi_3 \pi_5 \frac{\partial^2 \hat{T}}{\partial \hat{x}^2} + \pi_6 \frac{\partial \hat{P}}{\partial \hat{t}} + \hat{Q} \tag{A.10}$$

π_1, π_2, π_3, π_4, π_5 and π_6 in above equations are dimensionless groups:

$$\pi_1 = \frac{\ell}{V \cdot \tau} \tag{A.11}$$

$$\pi_2 = \frac{P^*}{\rho_0 \cdot V^2} = 1 \tag{A.12}$$

$$\pi_3 = \frac{\mu}{V \cdot \rho_0 \cdot \ell} = \frac{1}{Re} \tag{A.13}$$

$$\pi_4 = \frac{g \cdot \ell}{V^2} = \frac{1}{Fr^2} \tag{A.14}$$

$$\pi_5 = \frac{k}{\mu \cdot C_\rho} = \frac{1}{Pr} \tag{A.15}$$

$$\pi_6 = \frac{\ell \cdot P^*}{\rho_0 \cdot V \cdot C_p \cdot T_0 \cdot \tau} = \frac{\ell \cdot \rho_0 \cdot V^2}{\rho_0 \cdot V \cdot C_p \cdot T_0 \cdot \frac{\ell}{V}} = \frac{V^2}{C_p \cdot T_0} \tag{A.16}$$

For Froude modeling, experimental conditions for air are normal that π_4 preserved. For convection model, the solid boundary effects can be ignored (π_3 or Reynolds number). Set π_4 to 1 so the V can be given by $(gl)^{1/2}$.

Bousinnesq approximation can be written as:

$$\frac{\rho_0 - \rho}{\rho_0} = \frac{T - T_0}{T_0}$$

or

$$1 - \hat{p} = \hat{T} - 1 \tag{A.17}$$

The above equations apply for the areas far away from the fire's combustion zone. If we take the fire source as a point, a normalized temperature is:

$$\pi_4(1-\hat{\rho}) = (\pi_4 \cdot \zeta) \cdot (\frac{\hat{T}-1}{\zeta}) \tag{A.18}$$

Since π_4 is given by Equation (A.14), if we consider ζ as:

$$\zeta = \frac{V^2}{g \cdot \ell}$$

Then we can get:

$$\pi_4 \cdot \zeta = 1$$

or

$$\pi_4(1-\hat{\rho}) = \frac{\hat{T}-1}{\zeta} \tag{A.19}$$

Set

$$\frac{\hat{Q}}{\zeta} = 1 \tag{A.20}$$

Where Q is dimensionless variable given by

$$\hat{Q} = \frac{\ell \cdot (\frac{\dot{Q}}{\ell^3})}{\rho_0 \cdot V \cdot C_\rho \cdot T_0} \tag{A.21}$$

Substitute Equation (A.21) into Equation (A.20),

$$\frac{\hat{Q}}{\zeta} = \frac{\ell \cdot \frac{\dot{Q}}{\ell^3}}{\rho_0 \cdot V \cdot C_\rho \cdot T_0} \cdot \frac{g \cdot \ell}{V^2} = 1$$

or

$$\frac{\dot{Q} \cdot g}{\rho_0 \cdot V^3 \cdot C_\rho \cdot T_0 \cdot \ell} = 1$$

or

$$V = const. \cdot (\frac{\dot{Q}}{\ell})^{1/3} \tag{A.22}$$

In full-scale model and sub-scale model, π_4 is preserved,

$$(\pi_4)_m = (\pi_4)_f \tag{A.23}$$

so,

$$\frac{g \cdot \ell_m}{V_m^2} = \frac{g \cdot \ell_f}{V_f^2}$$

$$(\frac{\ell_m}{\ell_f})^{1/2} = \frac{V_m}{V_f} \tag{A.24}$$

And

$$t_f = \frac{\ell_f}{V_f} \quad , \quad t_m = \frac{\ell_m}{V_m}$$

Substitute into Equation (A.24),

$$\frac{t_m}{t_f} = \frac{\ell_m/V_m}{\ell_f/V_f} = \frac{\ell_m}{\ell_f} \cdot \frac{V_f}{V_m} = \frac{\ell_m}{\ell_f} \cdot (\frac{\ell_m}{\ell_f})^{-1/2}$$

Or

$$\frac{t_m}{t_f} = (\frac{\ell_m}{\ell_f})^{1/2} \tag{A.25}$$

Substitute into Equation (A.22),

$$\frac{V_m}{V_f} = (\frac{\dot{Q}_m}{\ell_m})^{1/3} (\frac{\ell_f}{\dot{Q}_f})^{1/3}$$

From Equation (A.24),

$$\frac{\dot{Q}_m}{\dot{Q}_f} = (\frac{\ell_m}{\ell_f})^{5/2} \tag{A.26}$$

110

APPENDIX B – FDS INPUT OF ATRIUM MODEL

Atrium_Fire.fds

&HEAD CHID='Atrium_Fire'/
&TIME T_END=500.00/
&DUMP RENDER_FILE='Atrium_Fire.ge1', DT_RESTART=300.00,
SMOKE3D_QUANTITY='MASS FRACTION', SMOKE3D_SPEC_ID='MySmoke'/

&MESH ID='Full Scale Model', IJK=56,30,68, XB=-11.20,11.20,-5.95,5.95,0.00,27.00/

&SPEC ID='MySmoke', MASS_EXTINCTION_COEFFICIENT=8.7000000E003/

&DEVC ID='massflow1', QUANTITY='MASS FLOW +', XB=-11.20,11.20,-
5.95,5.95,1.00,1.00/
&DEVC ID='massflow10', QUANTITY='MASS FLOW +', XB=-11.20,11.20,-
5.95,5.95,10.00,10.00/
&DEVC ID='massflow5', QUANTITY='MASS FLOW +', XB=-11.20,11.20,-
5.95,5.95,5.00,5.00/
&DEVC ID='massflowsmoke1', QUANTITY='MASS FLOW +', SPEC_ID='MySmoke',
XB=-11.20,11.20,-5.95,5.95,1.00,1.00/
&DEVC ID='massflowsmoke10', QUANTITY='MASS FLOW +', SPEC_ID='MySmoke',
XB=-11.20,11.20,-5.95,5.95,10.00,10.00/
&DEVC ID='massflowsmoke5', QUANTITY='MASS FLOW +', SPEC_ID='MySmoke',
XB=-11.20,11.20,-5.95,5.95,5.00,5.00/
&DEVC ID='MysmokeOpt01', QUANTITY='OPTICAL DENSITY',
SPEC_ID='MySmoke', XYZ=9.20,3.95,26.00/
&DEVC ID='MysmokeOpt02', QUANTITY='OPTICAL DENSITY',
SPEC_ID='MySmoke', XYZ=9.20,3.95,25.00/
&DEVC ID='MysmokeOpt13', QUANTITY='OPTICAL DENSITY',
SPEC_ID='MySmoke', XYZ=9.20,3.95,14.00/
&DEVC ID='MysmokeOpt20', QUANTITY='OPTICAL DENSITY',
SPEC_ID='MySmoke', XYZ=9.20,3.95,7.00/
&DEVC ID='Opt01', QUANTITY='OPTICAL DENSITY', XYZ=9.20,3.95,26.00/
&DEVC ID='Opt02', QUANTITY='OPTICAL DENSITY', XYZ=9.20,3.95,25.00/
&DEVC ID='Opt13', QUANTITY='OPTICAL DENSITY', XYZ=9.20,3.95,14.00/
&DEVC ID='Opt20', QUANTITY='OPTICAL DENSITY', XYZ=9.20,3.95,7.00/
&DEVC ID='Smoke layer', QUANTITY='LAYER HEIGHT',
XB=9.20,9.20,3.95,3.95,0.00,27.00/
&DEVC ID='THCP01', QUANTITY='THERMOCOUPLE', XYZ=9.20,3.95,26.00/
&DEVC ID='THCP02', QUANTITY='THERMOCOUPLE', XYZ=9.20,3.95,25.00/
&DEVC ID='THCP03', QUANTITY='THERMOCOUPLE', XYZ=9.20,3.95,24.00/
&DEVC ID='THCP04', QUANTITY='THERMOCOUPLE', XYZ=9.20,3.95,23.00/
&DEVC ID='THCP05', QUANTITY='THERMOCOUPLE', XYZ=9.20,3.95,22.00/
&DEVC ID='THCP06', QUANTITY='THERMOCOUPLE', XYZ=9.20,3.95,21.00/

111

&DEVC ID='THCP07', QUANTITY='THERMOCOUPLE', XYZ=9.20,3.95,20.00/
&DEVC ID='THCP08', QUANTITY='THERMOCOUPLE', XYZ=9.20,3.95,19.00/
&DEVC ID='THCP09', QUANTITY='THERMOCOUPLE', XYZ=9.20,3.95,18.00/
&DEVC ID='THCP10', QUANTITY='THERMOCOUPLE', XYZ=9.20,3.95,17.00/
&DEVC ID='THCP11', QUANTITY='THERMOCOUPLE', XYZ=9.20,3.95,16.00/
&DEVC ID='THCP12', QUANTITY='THERMOCOUPLE', XYZ=9.20,3.95,15.00/
&DEVC ID='THCP13', QUANTITY='THERMOCOUPLE', XYZ=9.20,3.95,14.00/
&DEVC ID='THCP14', QUANTITY='THERMOCOUPLE', XYZ=9.20,3.95,13.00/
&DEVC ID='THCP15', QUANTITY='THERMOCOUPLE', XYZ=9.20,3.95,12.00/
&DEVC ID='THCP16', QUANTITY='THERMOCOUPLE', XYZ=9.20,3.95,11.00/
&DEVC ID='THCP17', QUANTITY='THERMOCOUPLE', XYZ=9.20,3.95,10.00/
&DEVC ID='THCP18', QUANTITY='THERMOCOUPLE', XYZ=9.20,3.95,9.00/
&DEVC ID='THCP19', QUANTITY='THERMOCOUPLE', XYZ=9.20,3.95,8.00/
&DEVC ID='THCP20', QUANTITY='THERMOCOUPLE', XYZ=9.20,3.95,7.00/
&DEVC ID='Vis01', QUANTITY='VISIBILITY', SPEC_ID='carbon dioxide',
XYZ=9.20,3.95,26.00/
&DEVC ID='Vis10', QUANTITY='VISIBILITY', SPEC_ID='carbon dioxide',
XYZ=9.20,3.95,17.00/
&DEVC ID='Vis20', QUANTITY='VISIBILITY', SPEC_ID='carbon dioxide',
XYZ=9.20,3.95,7.00/
&DEVC ID='Volumeflow1', QUANTITY='VOLUME FLOW +', XB=-11.20,11.20,-
5.95,5.95,1.00,1.00/
&DEVC ID='Volumeflow10', QUANTITY='VOLUME FLOW +', XB=-11.20,11.20,-
5.95,5.95,10.00,10.00/
&DEVC ID='Volumeflow5', QUANTITY='VOLUME FLOW +', XB=-11.20,11.20,-
5.95,5.95,5.00,5.00/
&DEVC ID='Volumeflowsmoke1', QUANTITY='VOLUME FLOW +',
SPEC_ID='MySmoke', XB=-11.20,11.20,-5.95,5.95,1.00,1.00/
&DEVC ID='Volumeflowsmoke10', QUANTITY='VOLUME FLOW +',
SPEC_ID='MySmoke', XB=-11.20,11.20,-5.95,5.95,10.00,10.00/
&DEVC ID='Volumeflowsmoke5', QUANTITY='VOLUME FLOW +',
SPEC_ID='MySmoke', XB=-11.20,11.20,-5.95,5.95,5.00,5.00/
&SURF ID='pool fire',
    COLOR='RED',
    HRRPUA=400.00,
    RAMP_Q='pool fire_RAMP_Q'/
&RAMP ID='pool fire_RAMP_Q', T=0.00, F=0.00/
&RAMP ID='pool fire_RAMP_Q', T=30.00, F=0.1625/
&RAMP ID='pool fire_RAMP_Q', T=60.00, F=0.51/
&RAMP ID='pool fire_RAMP_Q', T=90.00, F=1.62/
&RAMP ID='pool fire_RAMP_Q', T=120.00, F=1.01/
&RAMP ID='pool fire_RAMP_Q', T=150.00, F=1.06/
&RAMP ID='pool fire_RAMP_Q', T=180.00, F=1.24/
&RAMP ID='pool fire_RAMP_Q', T=210.00, F=1.06/
&RAMP ID='pool fire_RAMP_Q', T=240.00, F=0.94/

&RAMP ID='pool fire_RAMP_Q', T=270.00, F=0.99/
&RAMP ID='pool fire_RAMP_Q', T=300.00, F=0.81/
&RAMP ID='pool fire_RAMP_Q', T=330.00, F=1.72/
&RAMP ID='pool fire_RAMP_Q', T=360.00, F=0.81/
&RAMP ID='pool fire_RAMP_Q', T=390.00, F=1.39/
&RAMP ID='pool fire_RAMP_Q', T=420.00, F=0.99/
&RAMP ID='pool fire_RAMP_Q', T=450.00, F=0.82/
&SURF ID='smoke ',
    RGB=26,204,26,
    MASS_FLUX(1)=1.0000000E-003,
    TAU_MF(1)=1.00/

&OBST XB=-0.2650,0.2650,-0.2650,0.2650,1.32,1.86, SURF_IDS='INERT','smoke
','INERT'/ smoke generator

&VENT SURF_ID='pool fire', XB=-1.00,1.00,-1.00,1.00,0.00,0.00, COLOR='RED'/ Fire
Pool
&VENT SURF_ID='OPEN', XB=-11.20,-11.20,-5.95,5.95,0.00,0.2000/ Vent

&SLCF QUANTITY='MASS FRACTION', SPEC_ID='MySmoke', VECTOR=.TRUE.,
PBY=0.00/
&SLCF QUANTITY='VOLUME FRACTION', SPEC_ID='MySmoke',
VECTOR=.TRUE., PBY=0.00/
&SLCF QUANTITY='DENSITY', VECTOR=.TRUE., PBY=0.00/
&SLCF QUANTITY='TEMPERATURE', VECTOR=.TRUE., PBY=0.00/
&SLCF QUANTITY='VELOCITY', VECTOR=.TRUE., PBY=0.00/

&TAIL /

Atrium_Helium.fds

&HEAD CHID='Atrium_Helium'/
&TIME T_END=500.00/
&DUMP RENDER_FILE='Atrium_Helium.ge1', DT_RESTART=300.00,
SMOKE3D_QUANTITY='MASS FRACTION', SMOKE3D_SPEC_ID='MySmoke'/
&MISC ISOTHERMAL=.TRUE./

&MESH ID='Full Scale Model', IJK=56,30,68, XB=-11.20,11.20,-5.95,5.95,0.00,27.00/

&SPEC ID='MySmoke', MASS_EXTINCTION_COEFFICIENT=8.7000000E003/
&SPEC ID='HELIUM'/

&DEVC ID='Helium V fraction 01', QUANTITY='VOLUME FRACTION',
SPEC_ID='HELIUM', XYZ=9.20,3.95,26.00/
&DEVC ID='Helium V fraction 02', QUANTITY='VOLUME FRACTION',
SPEC_ID='HELIUM', XYZ=9.20,3.95,25.00/
&DEVC ID='Helium V fraction 03', QUANTITY='VOLUME FRACTION',
SPEC_ID='HELIUM', XYZ=9.20,3.95,24.00/
&DEVC ID='Helium V fraction 04', QUANTITY='VOLUME FRACTION',
SPEC_ID='HELIUM', XYZ=9.20,3.95,23.00/
&DEVC ID='Helium V fraction 05', QUANTITY='VOLUME FRACTION',
SPEC_ID='HELIUM', XYZ=9.20,3.95,22.00/
&DEVC ID='Helium V fraction 06', QUANTITY='VOLUME FRACTION',
SPEC_ID='HELIUM', XYZ=9.20,3.95,21.00/
&DEVC ID='Helium V fraction 07', QUANTITY='VOLUME FRACTION',
SPEC_ID='HELIUM', XYZ=9.20,3.95,20.00/
&DEVC ID='Helium V fraction 08', QUANTITY='VOLUME FRACTION',
SPEC_ID='HELIUM', XYZ=9.20,3.95,19.00/
&DEVC ID='Helium V fraction 09', QUANTITY='VOLUME FRACTION',
SPEC_ID='HELIUM', XYZ=9.20,3.95,18.00/
&DEVC ID='Helium V fraction 10', QUANTITY='VOLUME FRACTION',
SPEC_ID='HELIUM', XYZ=9.20,3.95,17.00/
&DEVC ID='Helium V fraction 11', QUANTITY='VOLUME FRACTION',
SPEC_ID='HELIUM', XYZ=9.20,3.95,16.00/
&DEVC ID='Helium V fraction 12', QUANTITY='VOLUME FRACTION',
SPEC_ID='HELIUM', XYZ=9.20,3.95,15.00/
&DEVC ID='Helium V fraction 13', QUANTITY='VOLUME FRACTION',
SPEC_ID='HELIUM', XYZ=9.20,3.95,14.00/
&DEVC ID='Helium V fraction 14', QUANTITY='VOLUME FRACTION',
SPEC_ID='HELIUM', XYZ=9.20,3.95,13.00/
&DEVC ID='Helium V fraction 15', QUANTITY='VOLUME FRACTION',
SPEC_ID='HELIUM', XYZ=9.20,3.95,12.00/
&DEVC ID='Helium V fraction 16', QUANTITY='VOLUME FRACTION',
SPEC_ID='HELIUM', XYZ=9.20,3.95,11.00/

&DEVC ID='Helium V fraction 17', QUANTITY='VOLUME FRACTION', SPEC_ID='HELIUM', XYZ=9.20,3.95,10.00/
&DEVC ID='Helium V fraction 18', QUANTITY='VOLUME FRACTION', SPEC_ID='HELIUM', XYZ=9.20,3.95,9.00/
&DEVC ID='Helium V fraction 19', QUANTITY='VOLUME FRACTION', SPEC_ID='HELIUM', XYZ=9.20,3.95,8.00/
&DEVC ID='Helium V fraction 20', QUANTITY='VOLUME FRACTION', SPEC_ID='HELIUM', XYZ=9.20,3.95,7.00/
&DEVC ID='massflow1', QUANTITY='MASS FLOW +', XB=-11.20,11.20,-5.95,5.95,1.00,1.00/
&DEVC ID='massflow10', QUANTITY='MASS FLOW +', XB=-11.20,11.20,-5.95,5.95,10.00,10.00/
&DEVC ID='massflow5', QUANTITY='MASS FLOW +', XB=-11.20,11.20,-5.95,5.95,1.00,1.00/
&DEVC ID='massflowsmoke1', QUANTITY='MASS FLOW +', SPEC_ID='MySmoke', XB=-11.20,11.20,-5.95,5.95,1.00,1.00/
&DEVC ID='massflowsmoke10', QUANTITY='MASS FLOW +', SPEC_ID='MySmoke', XB=-11.20,11.20,-5.95,5.95,10.00,10.00/
&DEVC ID='massflowsmoke5', QUANTITY='MASS FLOW +', SPEC_ID='MySmoke', XB=-11.20,11.20,-5.95,5.95,1.00,1.00/
&DEVC ID='Opt01', QUANTITY='OPTICAL DENSITY', SPEC_ID='MySmoke', XYZ=9.20,3.95,26.00/
&DEVC ID='Opt02', QUANTITY='OPTICAL DENSITY', SPEC_ID='MySmoke', XYZ=9.20,3.95,25.00/
&DEVC ID='Opt03', QUANTITY='OPTICAL DENSITY', SPEC_ID='MySmoke', XYZ=9.20,3.95,24.00/
&DEVC ID='Opt04', QUANTITY='OPTICAL DENSITY', SPEC_ID='MySmoke', XYZ=9.20,3.95,23.00/
&DEVC ID='Opt05', QUANTITY='OPTICAL DENSITY', SPEC_ID='MySmoke', XYZ=9.20,3.95,22.00/
&DEVC ID='Opt06', QUANTITY='OPTICAL DENSITY', SPEC_ID='MySmoke', XYZ=9.20,3.95,21.00/
&DEVC ID='Opt07', QUANTITY='OPTICAL DENSITY', SPEC_ID='MySmoke', XYZ=9.20,3.95,20.00/
&DEVC ID='Opt08', QUANTITY='OPTICAL DENSITY', SPEC_ID='MySmoke', XYZ=9.20,3.95,19.00/
&DEVC ID='Opt09', QUANTITY='OPTICAL DENSITY', SPEC_ID='MySmoke', XYZ=9.20,3.95,18.00/
&DEVC ID='Opt10', QUANTITY='OPTICAL DENSITY', SPEC_ID='MySmoke', XYZ=9.20,3.95,17.00/
&DEVC ID='Opt11', QUANTITY='OPTICAL DENSITY', SPEC_ID='MySmoke', XYZ=9.20,3.95,16.00/
&DEVC ID='Opt12', QUANTITY='OPTICAL DENSITY', SPEC_ID='MySmoke', XYZ=9.20,3.95,15.00/

&DEVC ID='Opt13', QUANTITY='OPTICAL DENSITY', SPEC_ID='MySmoke',
XYZ=9.20,3.95,14.00/
&DEVC ID='Opt14', QUANTITY='OPTICAL DENSITY', SPEC_ID='MySmoke',
XYZ=9.20,3.95,13.00/
&DEVC ID='Opt15', QUANTITY='OPTICAL DENSITY', SPEC_ID='MySmoke',
XYZ=9.20,3.95,12.00/
&DEVC ID='Opt16', QUANTITY='OPTICAL DENSITY', SPEC_ID='MySmoke',
XYZ=9.20,3.95,11.00/
&DEVC ID='Opt17', QUANTITY='OPTICAL DENSITY', SPEC_ID='MySmoke',
XYZ=9.20,3.95,10.00/
&DEVC ID='Opt18', QUANTITY='OPTICAL DENSITY', SPEC_ID='MySmoke',
XYZ=9.20,3.95,9.00/
&DEVC ID='Opt19', QUANTITY='OPTICAL DENSITY', SPEC_ID='MySmoke',
XYZ=9.20,3.95,8.00/
&DEVC ID='Opt20', QUANTITY='OPTICAL DENSITY', SPEC_ID='MySmoke',
XYZ=9.20,3.95,7.00/
&DEVC ID='Smoke layer', QUANTITY='LAYER HEIGHT',
XB=9.20,9.20,3.95,3.95,0.00,27.00/
&DEVC ID='Volumeflow1', QUANTITY='VOLUME FLOW +', XB=-11.20,11.20,-
5.95,5.95,1.00,1.00/
&DEVC ID='Volumeflow10', QUANTITY='VOLUME FLOW +', XB=-11.20,11.20,-
5.95,5.95,10.00,10.00/
&DEVC ID='Volumeflow5', QUANTITY='VOLUME FLOW +', XB=-11.20,11.20,-
5.95,5.95,5.00,5.00/
&DEVC ID='Volumeflowsmoke1', QUANTITY='VOLUME FLOW +',
SPEC_ID='MySmoke', XB=-11.20,11.20,-5.95,5.95,1.00,1.00/
&DEVC ID='Volumeflowsmoke10', QUANTITY='VOLUME FLOW +',
SPEC_ID='MySmoke', XB=-11.20,11.20,-5.95,5.95,10.00,10.00/
&DEVC ID='Volumeflowsmoke5', QUANTITY='VOLUME FLOW +',
SPEC_ID='MySmoke', XB=-11.20,11.20,-5.95,5.95,5.00,5.00/
&SURF ID='Helium',
    RGB=26,204,26,
    EMISSIVITY=0.00,
    MASS_FLUX(2)=0.1468,
    TAU_MF(2)=-90.00/
&SURF ID='smoke ',
    RGB=26,204,26,
    MASS_FLUX(1)=1.0000000E-003,
    TAU_MF(1)=1.00/

&OBST XB=-0.2650,0.2650,-0.2650,0.2650,1.32,1.86, SURF_IDS='INERT','smoke
','INERT'/ smoke generator

&VENT SURF_ID='Helium', XB=-1.00,1.00,-1.00,1.00,0.00,0.00, COLOR='RED'/
Helium

```
&VENT SURF_ID='OPEN', XB=-11.20,-11.20,-5.95,5.95,0.00,0.2000/ Vent

&SLCF QUANTITY='MASS FRACTION', SPEC_ID='HELIUM', PBY=0.00/
&SLCF QUANTITY='VOLUME FRACTION', SPEC_ID='HELIUM', PBY=0.00/
&SLCF QUANTITY='MASS FRACTION', SPEC_ID='MySmoke', PBY=0.00/
&SLCF QUANTITY='VOLUME FRACTION', SPEC_ID='MySmoke', PBY=0.00/
&SLCF QUANTITY='DENSITY', VECTOR=.TRUE., PBY=0.00/
&SLCF QUANTITY='TEMPERATURE', VECTOR=.TRUE., PBY=0.00/
&SLCF QUANTITY='VELOCITY', VECTOR=.TRUE., PBY=0.00/
&SLCF QUANTITY='TEMPERATURE', PBZ=0.2000/


&TAIL /
```

APPENDIX C – HELIUM ANALYZER RECORDING DATA

A typical recorded data on HyperTerminal® software:

He	***.*	O2	20.5
He	***.*	O2	20.5
He	***.*	O2	20.6
He	6.3	O2	20.5
He	***.*	O2	20.5
He	1.3	O2	20.6
He	***.*	O2	20.5
He	***.*	O2	20.5
He	0.2	O2	20.5
He	***.*	O2	20.5
He	***.*	O2	20.6
He	***.*	O2	20.6
He	***.*	O2	20.5
He	***.*	O2	20.5
He	***.*	O2	20.5
He	***.*	O2	20.6
He	0	O2	20.6
He	0	O2	20.5
He	0	O2	20.5
He	0	O2	20.5
He	***.*	O2	20.5
He	1.7	O2	20.5
He	***.*	O2	20.6
He	***.*	O2	20.5
He	***.*	O2	20.6
He	0.4	O2	20.5
He	***.*	O2	20.5
He	***.*	O2	20.6
He	***.*	O2	20.5
He	***.*	O2	20.5
He	0.6	O2	20.5
He	***.*	O2	20.5
He	***.*	O2	20.5
He	***.*	O2	20.6
He	***.*	O2	20.6
He	***.*	O2	20.5
He	***.*	O2	20.5
He	***.*	O2	20.6

APPENDIX D – HELIUM CONCENTRATION RESULTS
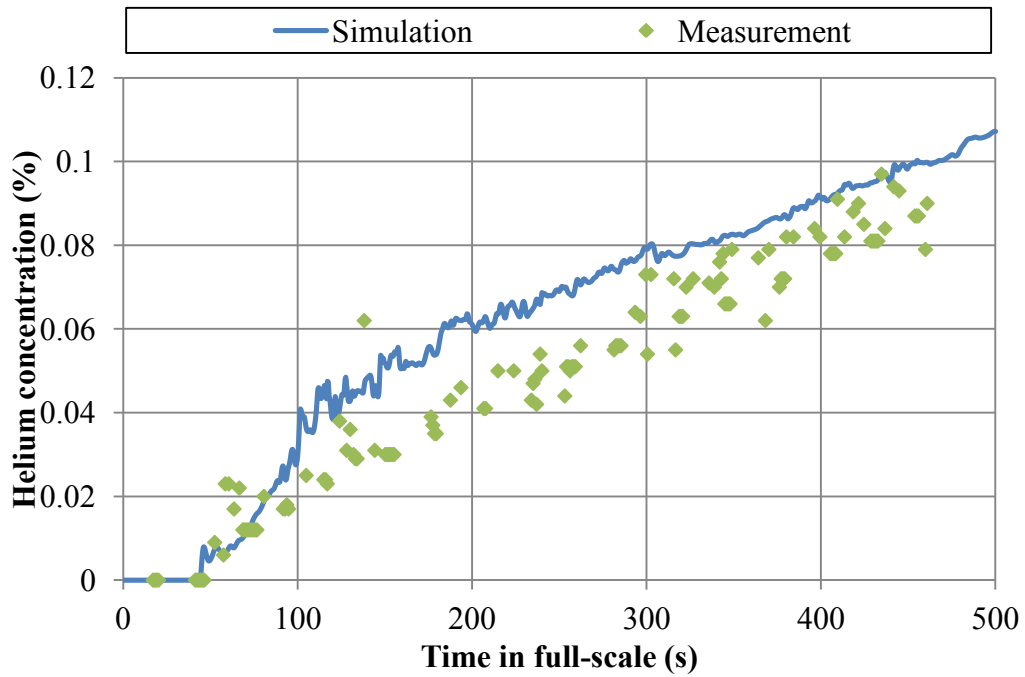
Comparison of measured and predicted helium concentration for 500 kW fire case at L1.
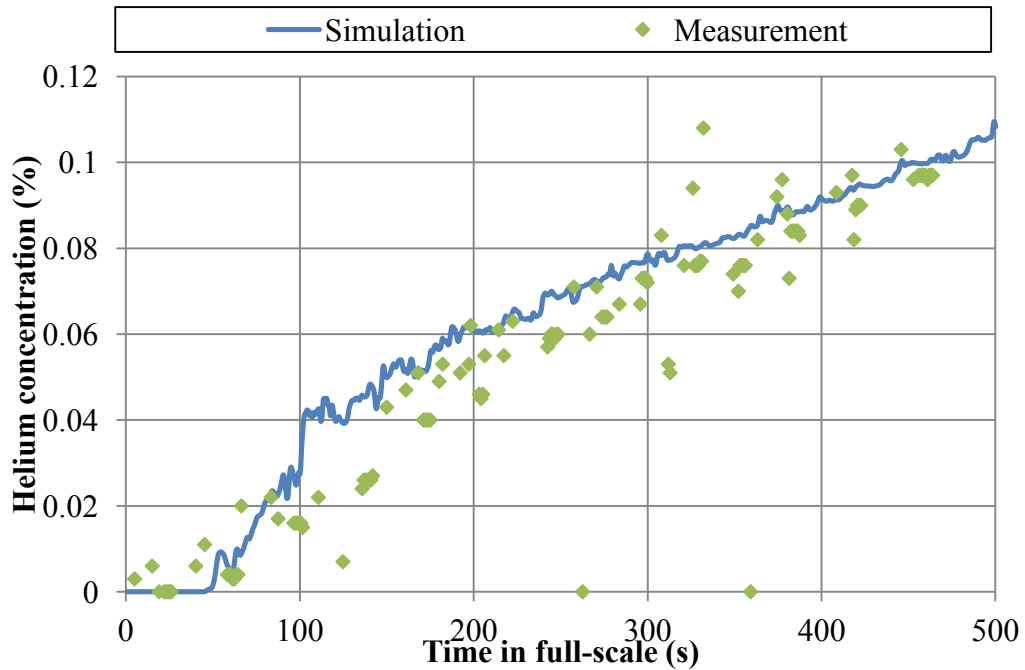
Comparison of measured and predicted helium concentration for 500 kW fire case at L2.
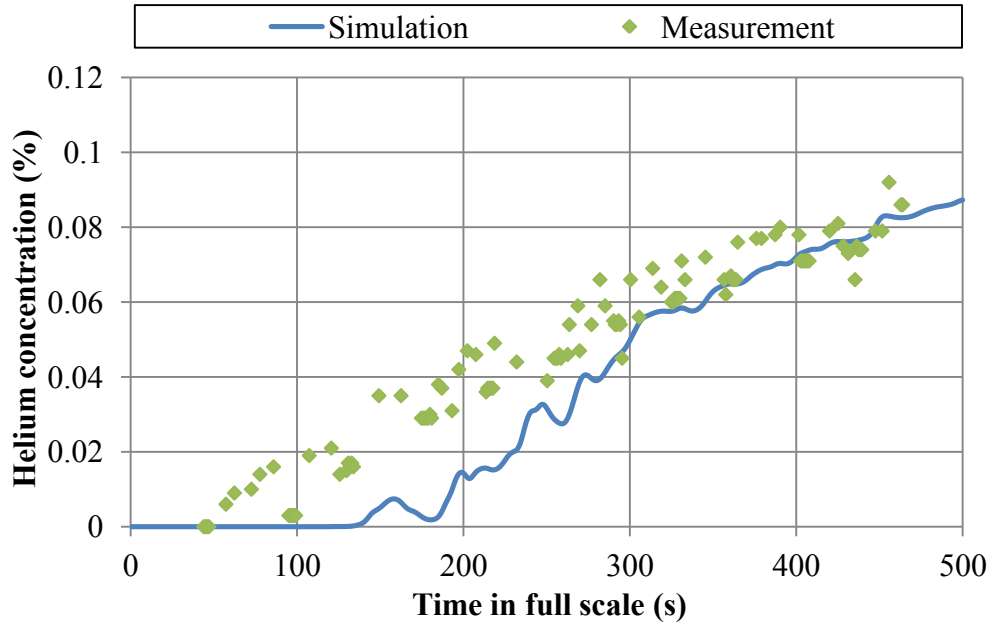
Comparison of measured and predicted helium concentration for 500 kW fire case at L13.
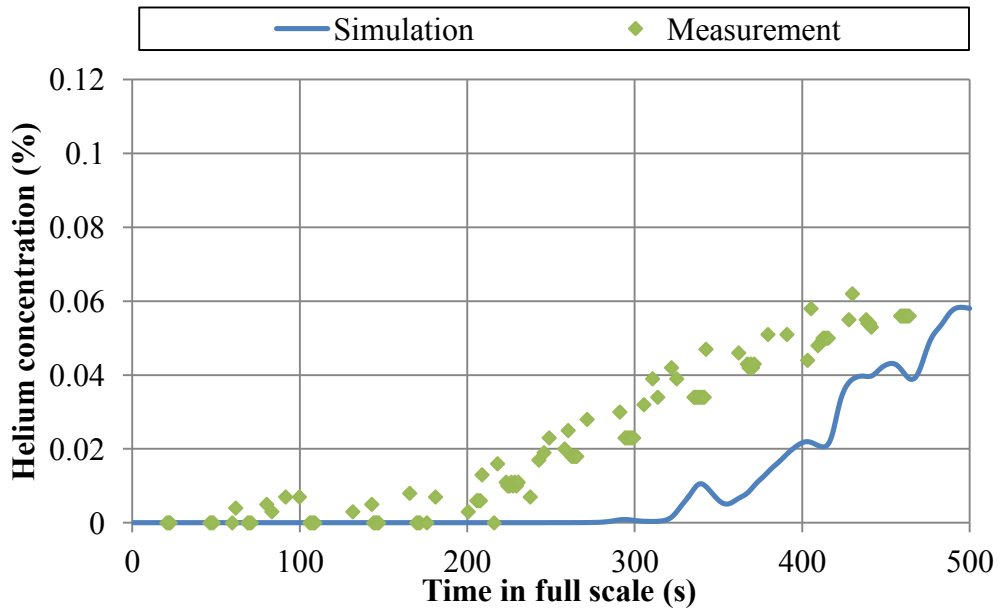
Comparison of measured and predicted helium concentration for 500 kW fire case at L20.
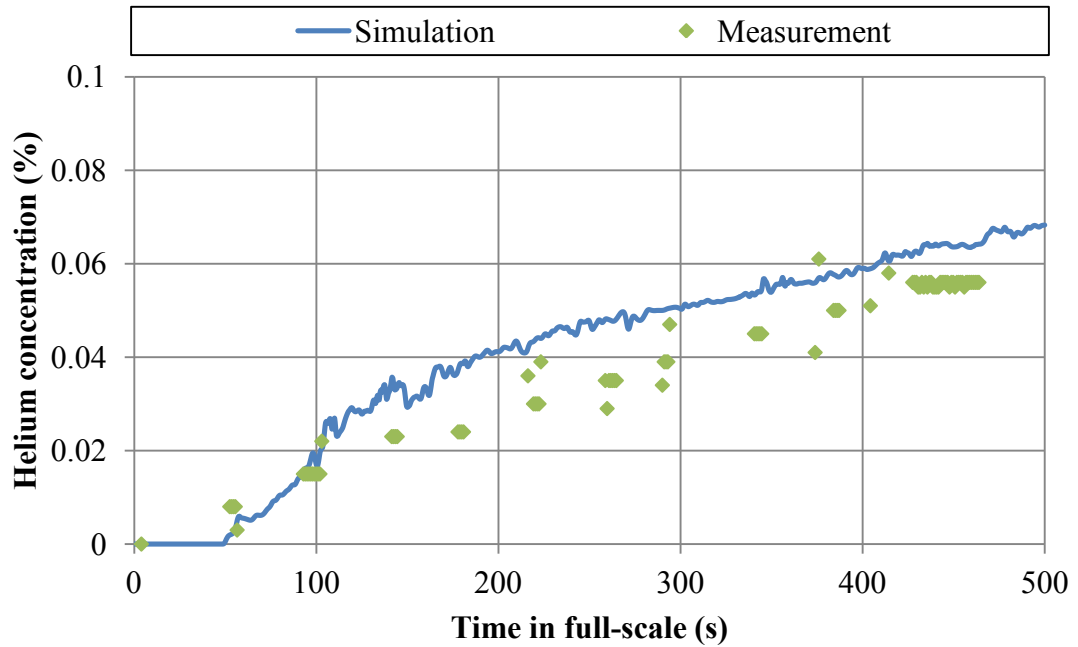
Comparison of measured and predicted helium concentration for 300 kW fire case at L1.
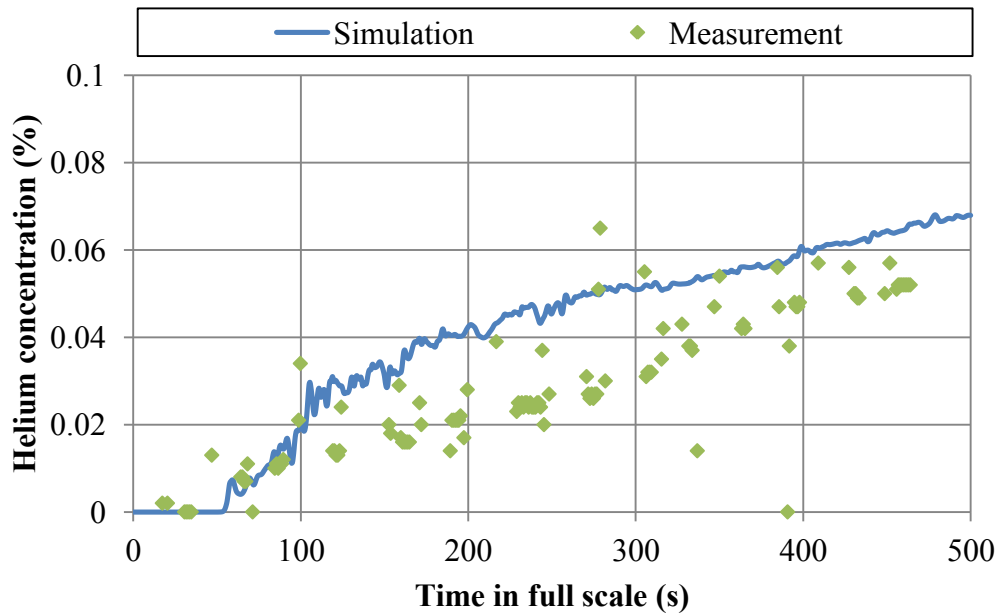
Comparison of measured and predicted helium concentration for 300 kW fire case at L2.
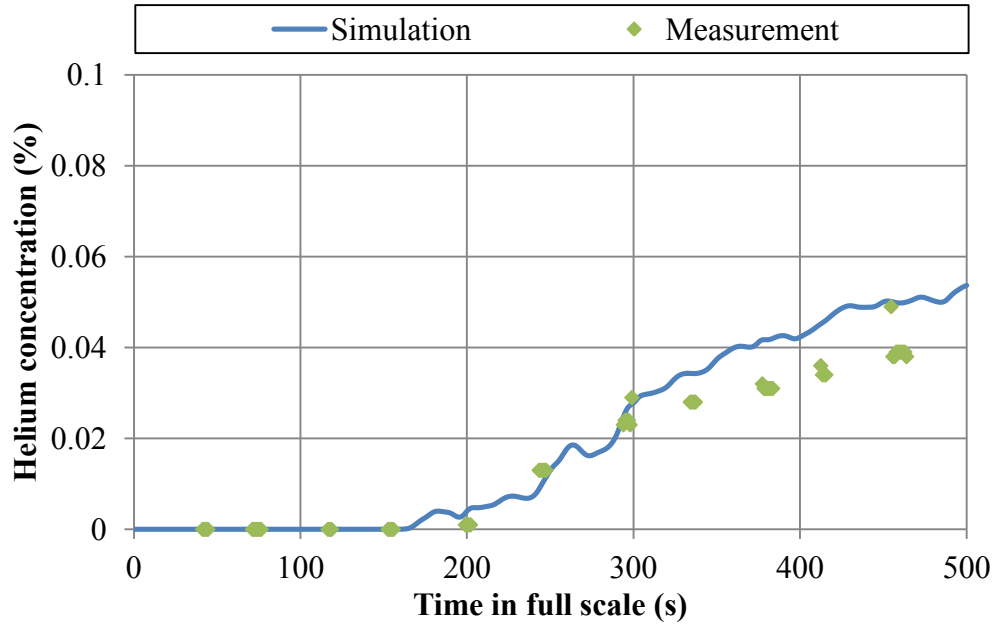
Comparison of measured and predicted helium concentration for 300 kW fire case at L13.
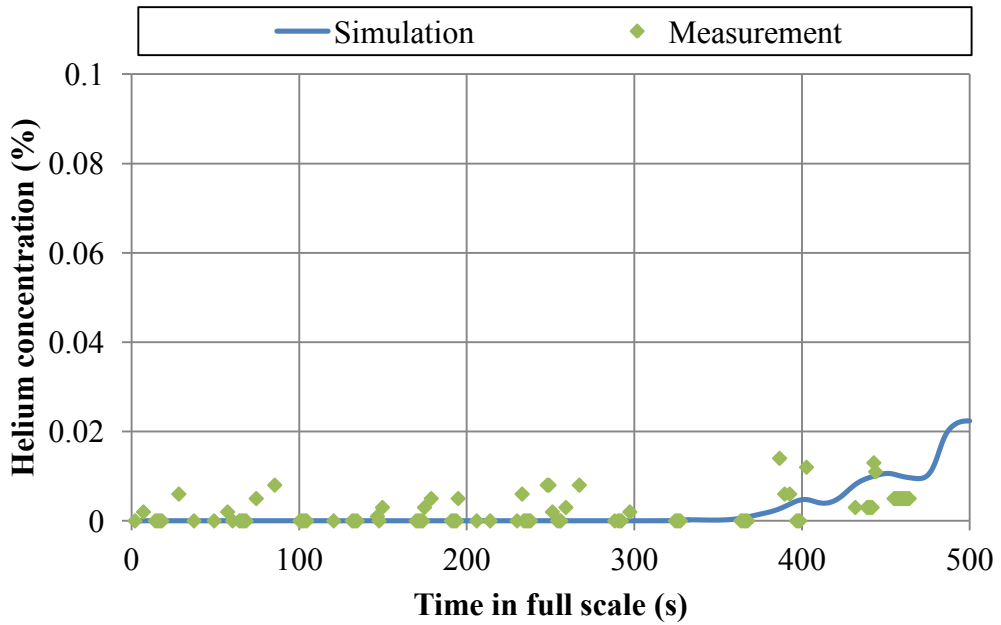
Comparison of measured and predicted helium concentration for 300 kW fire case at L20.

APPENDIX E – FDS INPUT OF TUNNEL MODEL

Tunnel_Fire_1.fds

&HEAD CHID='Tunnel_Fire_1'/
&TIME T_END=1500.0/
&DUMP RENDER_FILE='Tunnel_Fire_1.ge1', DT_RESTART=300.0,
SMOKE3D_QUANTITY='MASS FRACTION', SMOKE3D_SPEC_ID='Smoke'/
&MISC TMPA=19.1/

&MESH ID='Tunnel_center', FYI='Near burner', IJK=28,36,16, XB=-0.28,0.28,-
0.36,0.36,0.0,0.32/
&MESH ID='Shaft_1', FYI='Shaft_1', IJK=18,4,6, XB=1.64,2.36,-0.08,0.08,0.32,0.56/
&MESH ID='Shaft_2', FYI='Shaft_2', IJK=18,4,6, XB=5.64,6.36,-0.08,0.08,0.32,0.56/
&MESH ID='Tunnel_+1', FYI='Between burner and shaft_1', IJK=50,18,8,
XB=0.28,2.28,-0.36,0.36,0.0,0.32/
&MESH ID='Shaft_-1', FYI='Shaft_-1', IJK=18,4,6, XB=-2.36,-1.64,-
0.08,0.08,0.32,0.56/
&MESH ID='Shaft_-2', FYI='Shaft_-2', IJK=18,4,6, XB=-6.36,-5.64,-
0.08,0.08,0.32,0.56/
&MESH ID='Tunnel_-1', FYI='Between burner and shaft_-1', IJK=50,18,8, XB=-2.28,-
0.28,-0.36,0.36,0.0,0.32/
&MESH ID='+2', IJK=50,18,8, XB=2.28,4.28,-0.36,0.36,0.0,0.32/
&MESH ID='+3', IJK=50,18,8, XB=4.28,6.28,-0.36,0.36,0.0,0.32/
&MESH ID='+4', IJK=55,18,8, XB=6.28,8.48,-0.36,0.36,0.0,0.32/
&MESH ID='-2', IJK=50,18,8, XB=-4.28,-2.28,-0.36,0.36,0.0,0.32/
&MESH ID='-3', IJK=50,18,8, XB=-6.28,-4.28,-0.36,0.36,0.0,0.32/
&MESH ID='-4', IJK=55,18,8, XB=-8.48,-6.28,-0.36,0.36,0.0,0.32/

&SPEC ID='Smoke', FYI='artificial smoke',
MASS_EXTINCTION_COEFFICIENT=8700.0/

&DEVC ID='LAYER', QUANTITY='LAYER HEIGHT', XB=1.6,1.6,0.0,0.0,0.0,0.31/
&DEVC ID='LAYER02', QUANTITY='LAYER HEIGHT', XB=5.6,5.6,0.0,0.0,0.0,0.31/
&DEVC ID='LAYER03', QUANTITY='LAYER HEIGHT', XB=2.5,2.5,0.0,0.0,0.0,0.31/
&DEVC ID='LAYER04', QUANTITY='LAYER HEIGHT', XB=1.3,1.3,0.0,0.0,0.0,0.31/
&DEVC ID='LAYER05', QUANTITY='LAYER HEIGHT', XB=2.8,2.8,0.0,0.0,0.0,0.31/
&DEVC ID='LAYER06', QUANTITY='LAYER HEIGHT', XB=5.3,5.3,0.0,0.0,0.0,0.31/
&DEVC ID='Optical Density_1', QUANTITY='OPTICAL DENSITY',
SPEC_ID='Smoke', XYZ=1.6,0.0,0.31/
&DEVC ID='Optical Density_10', QUANTITY='OPTICAL DENSITY',
SPEC_ID='Smoke', XYZ=-1.3,0.0,0.31/
&DEVC ID='Optical Density_11', QUANTITY='OPTICAL DENSITY',
SPEC_ID='Smoke', XYZ=-1.5,0.0,0.31/

&DEVC ID='Optical Density_12', QUANTITY='OPTICAL DENSITY', SPEC_ID='Smoke', XYZ=-1.6,0.0,0.31/
&DEVC ID='Optical Density_13', QUANTITY='OPTICAL DENSITY', SPEC_ID='Smoke', XYZ=-2.5,0.0,0.31/
&DEVC ID='Optical Density_14', QUANTITY='OPTICAL DENSITY', SPEC_ID='Smoke', XYZ=-2.6,0.0,0.31/
&DEVC ID='Optical Density_15', QUANTITY='OPTICAL DENSITY', SPEC_ID='Smoke', XYZ=-3.0,0.0,0.31/
&DEVC ID='Optical Density_16', QUANTITY='OPTICAL DENSITY', SPEC_ID='Smoke', XYZ=-3.6,0.0,0.31/
&DEVC ID='Optical Density_2', QUANTITY='OPTICAL DENSITY', SPEC_ID='Smoke', XYZ=1.5,0.0,0.31/
&DEVC ID='Optical density_21', QUANTITY='OPTICAL DENSITY', SPEC_ID='Smoke', XYZ=2.5,0.0,0.31, ORIENTATION=0.0,-1.0,0.0/
&DEVC ID='Optical Density_22', QUANTITY='OPTICAL DENSITY', SPEC_ID='Smoke', XYZ=2.6,0.0,0.31/
&DEVC ID='Optical Density_23', QUANTITY='OPTICAL DENSITY', SPEC_ID='Smoke', XYZ=2.8,0.0,0.31/
&DEVC ID='Optical Density_24', QUANTITY='OPTICAL DENSITY', SPEC_ID='Smoke', XYZ=3.6,0.0,0.31/
&DEVC ID='Optical Density_25', QUANTITY='OPTICAL DENSITY', SPEC_ID='Smoke', XYZ=4.4,0.0,0.31/
&DEVC ID='Optical Density_26', QUANTITY='OPTICAL DENSITY', SPEC_ID='Smoke', XYZ=5.2,0.0,0.31/
&DEVC ID='Optical Density_27', QUANTITY='OPTICAL DENSITY', SPEC_ID='Smoke', XYZ=5.4,0.0,0.31/
&DEVC ID='Optical density_28', QUANTITY='OPTICAL DENSITY', SPEC_ID='Smoke', XYZ=5.6,0.0,0.31, ORIENTATION=0.0,-1.0,0.0/
&DEVC ID='Optical density_29', QUANTITY='OPTICAL DENSITY', SPEC_ID='Smoke', XYZ=6.4,0.0,0.31, ORIENTATION=0.0,-1.0,0.0/
&DEVC ID='Optical density_3', QUANTITY='OPTICAL DENSITY', SPEC_ID='Smoke', XYZ=1.3,0.0,0.31, ORIENTATION=0.0,-1.0,0.0/
&DEVC ID='Optical density_30', QUANTITY='OPTICAL DENSITY', SPEC_ID='Smoke', XYZ=6.6,0.0,0.31, ORIENTATION=0.0,-1.0,0.0/
&DEVC ID='Optical density_31', QUANTITY='OPTICAL DENSITY', SPEC_ID='Smoke', XYZ=6.8,0.0,0.31, ORIENTATION=0.0,-1.0,0.0/
&DEVC ID='Optical density_32', QUANTITY='OPTICAL DENSITY', SPEC_ID='Smoke', XYZ=7.0,0.0,0.31, ORIENTATION=0.0,-1.0,0.0/
&DEVC ID='Optical density_33', QUANTITY='OPTICAL DENSITY', SPEC_ID='Smoke', XYZ=7.2,0.0,0.31, ORIENTATION=0.0,-1.0,0.0/
&DEVC ID='Optical density_35', QUANTITY='OPTICAL DENSITY', SPEC_ID='Smoke', XYZ=2.0,0.0,0.45, ORIENTATION=0.0,-1.0,0.0/
&DEVC ID='Optical density_36', QUANTITY='OPTICAL DENSITY', SPEC_ID='Smoke', XYZ=1.65,0.0,0.45, ORIENTATION=0.0,-1.0,0.0/

&DEVC ID='Optical density_38', QUANTITY='OPTICAL DENSITY',
SPEC_ID='Smoke', XYZ=6.0,0.0,0.45, ORIENTATION=0.0,-1.0,0.0/
&DEVC ID='Optical density_39', QUANTITY='OPTICAL DENSITY',
SPEC_ID='Smoke', XYZ=5.65,0.0,0.45, ORIENTATION=0.0,-1.0,0.0/
&DEVC ID='Optical Density_4', QUANTITY='OPTICAL DENSITY',
SPEC_ID='Smoke', XYZ=0.8,0.0,0.31/
&DEVC ID='Optical Density_40', QUANTITY='OPTICAL DENSITY',
SPEC_ID='Smoke', XYZ=0.4,0.0,0.31/
&DEVC ID='Optical Density_41', QUANTITY='OPTICAL DENSITY',
SPEC_ID='Smoke', XYZ=0.0,0.0,0.26/
&DEVC ID='Optical Density_42', QUANTITY='OPTICAL DENSITY',
SPEC_ID='Smoke', XYZ=0.0,0.0,0.21/
&DEVC ID='Optical Density_43', QUANTITY='OPTICAL DENSITY',
SPEC_ID='Smoke', XYZ=0.0,0.0,0.16/
&DEVC ID='Optical Density_44', QUANTITY='OPTICAL DENSITY',
SPEC_ID='Smoke', XYZ=0.0,0.0,0.11/
&DEVC ID='Optical density_45', QUANTITY='OPTICAL DENSITY',
SPEC_ID='Smoke', XYZ=1.3,0.0,0.26, ORIENTATION=0.0,-1.0,0.0/
&DEVC ID='Optical density_46', QUANTITY='OPTICAL DENSITY',
SPEC_ID='Smoke', XYZ=1.3,0.0,0.21, ORIENTATION=0.0,-1.0,0.0/
&DEVC ID='Optical density_47', QUANTITY='OPTICAL DENSITY',
SPEC_ID='Smoke', XYZ=1.3,0.0,0.16, ORIENTATION=0.0,-1.0,0.0/
&DEVC ID='Optical density_48', QUANTITY='OPTICAL DENSITY',
SPEC_ID='Smoke', XYZ=1.3,0.0,0.11, ORIENTATION=0.0,-1.0,0.0/
&DEVC ID='Optical Density_49', QUANTITY='OPTICAL DENSITY',
SPEC_ID='Smoke', XYZ=2.8,0.0,0.26/
&DEVC ID='Optical Density_5', QUANTITY='OPTICAL DENSITY',
SPEC_ID='Smoke', XYZ=0.2,0.0,0.31/
&DEVC ID='Optical Density_50', QUANTITY='OPTICAL DENSITY',
SPEC_ID='Smoke', XYZ=2.8,0.0,0.21/
&DEVC ID='Optical Density_51', QUANTITY='OPTICAL DENSITY',
SPEC_ID='Smoke', XYZ=2.8,0.0,0.16/
&DEVC ID='Optical Density_52', QUANTITY='OPTICAL DENSITY',
SPEC_ID='Smoke', XYZ=2.8,0.0,0.11/
&DEVC ID='Optical Density_53', QUANTITY='OPTICAL DENSITY',
SPEC_ID='Smoke', XYZ=-1.3,0.0,0.26/
&DEVC ID='Optical Density_54', QUANTITY='OPTICAL DENSITY',
SPEC_ID='Smoke', XYZ=-1.3,0.0,0.21/
&DEVC ID='Optical Density_55', QUANTITY='OPTICAL DENSITY',
SPEC_ID='Smoke', XYZ=-1.3,0.0,0.16/
&DEVC ID='Optical Density_56', QUANTITY='OPTICAL DENSITY',
SPEC_ID='Smoke', XYZ=-1.3,0.0,0.11/
&DEVC ID='Optical Density_6', QUANTITY='OPTICAL DENSITY',
SPEC_ID='Smoke', XYZ=0.0,0.0,0.31/

&DEVC ID='Optical density_69', QUANTITY='OPTICAL DENSITY',
SPEC_ID='Smoke', XYZ=-1.65,0.0,0.45, ORIENTATION=0.0,-1.0,0.0/
&DEVC ID='Optical Density_7', QUANTITY='OPTICAL DENSITY',
SPEC_ID='Smoke', XYZ=-0.2,0.0,0.31/
&DEVC ID='Optical Density_70', QUANTITY='OPTICAL DENSITY',
SPEC_ID='Smoke', XYZ=0.6,0.0,0.31/
&DEVC ID='Optical Density_8', QUANTITY='OPTICAL DENSITY',
SPEC_ID='Smoke', XYZ=-0.4,0.0,0.31/
&DEVC ID='Optical Density_9', QUANTITY='OPTICAL DENSITY',
SPEC_ID='Smoke', XYZ=-0.8,0.0,0.31/
&DEVC ID='THCP_1', QUANTITY='THERMOCOUPLE', XYZ=1.6,0.0,0.279/
&DEVC ID='THCP_10', QUANTITY='THERMOCOUPLE', XYZ=-1.3,0.0,0.279/
&DEVC ID='THCP_11', QUANTITY='THERMOCOUPLE', XYZ=-1.5,0.0,0.279/
&DEVC ID='THCP_12', QUANTITY='THERMOCOUPLE', XYZ=-1.6,0.0,0.279/
&DEVC ID='THCP_13', QUANTITY='THERMOCOUPLE', XYZ=-2.5,0.0,0.279/
&DEVC ID='THCP_14', QUANTITY='THERMOCOUPLE', XYZ=-2.6,0.0,0.279/
&DEVC ID='THCP_15', QUANTITY='THERMOCOUPLE', XYZ=-3.0,0.0,0.279/
&DEVC ID='THCP_16', QUANTITY='THERMOCOUPLE', XYZ=-3.6,0.0,0.279/
&DEVC ID='THCP_17', QUANTITY='THERMOCOUPLE', XYZ=-2.35,0.0,0.45/
&DEVC ID='THCP_18', QUANTITY='THERMOCOUPLE', XYZ=-2.0,0.0,0.45/
&DEVC ID='THCP_19', QUANTITY='THERMOCOUPLE', XYZ=-1.65,0.0,0.45/
&DEVC ID='THCP_2', QUANTITY='THERMOCOUPLE', XYZ=1.5,0.0,0.279/
&DEVC ID='THCP_21', QUANTITY='THERMOCOUPLE', XYZ=2.5,0.0,0.279,
ORIENTATION=0.0,-1.0,0.0/
&DEVC ID='THCP_22', QUANTITY='THERMOCOUPLE', XYZ=2.6,0.0,0.279,
ORIENTATION=0.0,-1.0,0.0/
&DEVC ID='THCP_23', QUANTITY='THERMOCOUPLE', XYZ=2.8,0.0,0.279/
&DEVC ID='THCP_24', QUANTITY='THERMOCOUPLE', XYZ=3.6,0.0,0.279/
&DEVC ID='THCP_25', QUANTITY='THERMOCOUPLE', XYZ=4.4,0.0,0.279/
&DEVC ID='THCP_26', QUANTITY='THERMOCOUPLE', XYZ=5.2,0.0,0.279/
&DEVC ID='THCP_27', QUANTITY='THERMOCOUPLE', XYZ=5.4,0.0,0.279/
&DEVC ID='THCP_28', QUANTITY='THERMOCOUPLE', XYZ=5.6,0.0,0.279/
&DEVC ID='THCP_29', QUANTITY='THERMOCOUPLE', XYZ=6.4,0.0,0.31/
&DEVC ID='THCP_3', QUANTITY='THERMOCOUPLE', XYZ=1.3,0.0,0.279/
&DEVC ID='THCP_30', QUANTITY='THERMOCOUPLE', XYZ=6.6,0.0,0.279/
&DEVC ID='THCP_31', QUANTITY='THERMOCOUPLE', XYZ=6.8,0.0,0.279/
&DEVC ID='THCP_32', QUANTITY='THERMOCOUPLE', XYZ=7.0,0.0,0.279/
&DEVC ID='THCP_33', QUANTITY='THERMOCOUPLE', XYZ=7.2,0.0,0.279/
&DEVC ID='THCP_34', QUANTITY='THERMOCOUPLE', XYZ=2.35,0.0,0.45/
&DEVC ID='THCP_35', QUANTITY='THERMOCOUPLE', XYZ=2.0,0.0,0.45/
&DEVC ID='THCP_36', QUANTITY='THERMOCOUPLE', XYZ=1.65,0.0,0.45/
&DEVC ID='THCP_37', QUANTITY='THERMOCOUPLE', XYZ=6.35,0.0,0.45/
&DEVC ID='THCP_38', QUANTITY='THERMOCOUPLE', XYZ=6.0,0.0,0.45/
&DEVC ID='THCP_39', QUANTITY='THERMOCOUPLE', XYZ=5.65,0.0,0.45/

&DEVC ID='THCP_4', QUANTITY='THERMOCOUPLE', XYZ=0.8,0.0,0.279,
ORIENTATION=0.0,-1.0,0.0/
&DEVC ID='THCP_40', QUANTITY='THERMOCOUPLE', XYZ=0.4,0.0,0.279,
ORIENTATION=0.0,-1.0,0.0/
&DEVC ID='THCP_41', QUANTITY='THERMOCOUPLE', XYZ=0.0,0.0,0.26,
ORIENTATION=0.0,-1.0,0.0/
&DEVC ID='THCP_42', QUANTITY='THERMOCOUPLE', XYZ=0.0,0.0,0.21,
ORIENTATION=0.0,-1.0,0.0/
&DEVC ID='THCP_43', QUANTITY='THERMOCOUPLE', XYZ=0.0,0.0,0.16,
ORIENTATION=0.0,-1.0,0.0/
&DEVC ID='THCP_44', QUANTITY='THERMOCOUPLE', XYZ=0.0,0.0,0.11,
ORIENTATION=0.0,-1.0,0.0/
&DEVC ID='THCP_45', QUANTITY='THERMOCOUPLE', XYZ=1.3,0.0,0.26,
ORIENTATION=0.0,-1.0,0.0/
&DEVC ID='THCP_46', QUANTITY='THERMOCOUPLE', XYZ=1.3,0.0,0.21,
ORIENTATION=0.0,-1.0,0.0/
&DEVC ID='THCP_47', QUANTITY='THERMOCOUPLE', XYZ=1.3,0.0,0.16,
ORIENTATION=0.0,-1.0,0.0/
&DEVC ID='THCP_48', QUANTITY='THERMOCOUPLE', XYZ=1.3,0.0,0.11,
ORIENTATION=0.0,-1.0,0.0/
&DEVC ID='THCP_49', QUANTITY='THERMOCOUPLE', XYZ=2.8,0.0,0.26,
ORIENTATION=0.0,-1.0,0.0/
&DEVC ID='THCP_5', QUANTITY='THERMOCOUPLE', XYZ=0.2,0.0,0.279/
&DEVC ID='THCP_50', QUANTITY='THERMOCOUPLE', XYZ=2.8,0.0,0.21,
ORIENTATION=0.0,-1.0,0.0/
&DEVC ID='THCP_51', QUANTITY='THERMOCOUPLE', XYZ=2.8,0.0,0.16,
ORIENTATION=0.0,-1.0,0.0/
&DEVC ID='THCP_52', QUANTITY='THERMOCOUPLE', XYZ=2.8,0.0,0.11,
ORIENTATION=0.0,-1.0,0.0/
&DEVC ID='THCP_53', QUANTITY='THERMOCOUPLE', XYZ=-1.3,0.0,0.26,
ORIENTATION=0.0,-1.0,0.0/
&DEVC ID='THCP_54', QUANTITY='THERMOCOUPLE', XYZ=-1.3,0.0,0.21,
ORIENTATION=0.0,-1.0,0.0/
&DEVC ID='THCP_55', QUANTITY='THERMOCOUPLE', XYZ=-1.3,0.0,0.16,
ORIENTATION=0.0,-1.0,0.0/
&DEVC ID='THCP_56', QUANTITY='THERMOCOUPLE', XYZ=-1.3,0.0,0.11,
ORIENTATION=0.0,-1.0,0.0/
&DEVC ID='THCP_57', QUANTITY='THERMOCOUPLE', XYZ=-2.6,0.0,0.26,
ORIENTATION=0.0,-1.0,0.0/
&DEVC ID='THCP_58', QUANTITY='THERMOCOUPLE', XYZ=-2.6,0.0,0.21,
ORIENTATION=0.0,-1.0,0.0/
&DEVC ID='THCP_59', QUANTITY='THERMOCOUPLE', XYZ=-2.6,0.0,0.16,
ORIENTATION=0.0,-1.0,0.0/
&DEVC ID='THCP_6', QUANTITY='THERMOCOUPLE', XYZ=0.0,0.0,0.279/

&DEVC ID='THCP_60', QUANTITY='THERMOCOUPLE', XYZ=-2.6,0.0,0.11,
ORIENTATION=0.0,-1.0,0.0/
&DEVC ID='THCP_7', QUANTITY='THERMOCOUPLE', XYZ=-0.2,0.0,0.279/
&DEVC ID='THCP_70', QUANTITY='THERMOCOUPLE', XYZ=0.6,0.0,0.279,
ORIENTATION=0.0,-1.0,0.0/
&DEVC ID='THCP_71', QUANTITY='THERMOCOUPLE', XYZ=-1.0,0.0,0.279/
&DEVC ID='THCP_8', QUANTITY='THERMOCOUPLE', XYZ=-0.4,0.0,0.279/
&DEVC ID='THCP_9', QUANTITY='THERMOCOUPLE', XYZ=-0.8,0.0,0.279/
&DEVC ID='Velocity_64', QUANTITY='VELOCITY', XYZ=-8.4,0.0,0.16,
ORIENTATION=-1.0,0.0,0.0/
&DEVC ID='Velocity_65', QUANTITY='VELOCITY', XYZ=8.4,0.0,0.16,
ORIENTATION=-1.0,0.0,0.0/
&DEVC ID='Velocity_66', QUANTITY='VELOCITY', XYZ=1.65,0.0,0.45,
ORIENTATION=0.0,-1.0,0.0/
&DEVC ID='Velocity_67', QUANTITY='VELOCITY', XYZ=2.35,0.0,0.45,
ORIENTATION=0.0,-1.0,0.0/
&DEVC ID='Velocity_68', QUANTITY='VELOCITY', XYZ=5.65,0.0,0.45,
ORIENTATION=0.0,-1.0,0.0/
&DEVC ID='Velocity_69', QUANTITY='VELOCITY', XYZ=-1.65,0.0,0.45,
ORIENTATION=0.0,-1.0,0.0/
&SURF ID='Burner',
    COLOR='RED',
    HRRPUA=606.91/
&SURF ID='Smoke',
    RGB=26,204,26,
    MASS_FLUX(1)=0.01,
    TAU_MF(1)=1.0/

&OBST XB=-0.02,0.02,-0.02,0.02,0.04,0.08, SURF_IDS='INERT','Smoke','INERT'/
Smoke generator
&VENT SURF_ID='Burner', XB=-0.07,0.07,-0.07,0.07,0.0,0.0/ Burner
&VENT SURF_ID='OPEN', XB=8.48,8.48,-0.35,0.35,0.0,0.32/ +end
&VENT SURF_ID='OPEN', XB=-8.48,-8.48,-0.35,0.35,0.0,0.32/ -end
&VENT SURF_ID='OPEN', XB=1.64,2.36,-0.08,0.08,0.56,0.56/ +1top
&VENT SURF_ID='OPEN', XB=5.64,6.36,-0.08,0.08,0.56,0.56/ +2top
&VENT SURF_ID='OPEN', XB=-2.36,-1.64,-0.08,0.08,0.56,0.56/ -1top
&VENT SURF_ID='OPEN', XB=-6.36,-5.64,-0.08,0.08,0.56,0.56/ -2top

&SLCF QUANTITY='MASS FRACTION', SPEC_ID='Smoke', PBY=0.0/
&SLCF QUANTITY='OPTICAL DENSITY', SPEC_ID='Smoke', PBY=0.0/
&SLCF QUANTITY='TEMPERATURE', PBY=0.0/
&SLCF QUANTITY='VELOCITY', VECTOR=.TRUE., PBY=0.0/

&TAIL /

Tunnel_Helium.fds

&HEAD CHID='Tunnel_Helium'/
&TIME T_END=3000.0/
&DUMP RENDER_FILE='Tunnel_Helium.ge1', DT_RESTART=300.0,
SMOKE3D_QUANTITY='MASS FRACTION', SMOKE3D_SPEC_ID='Smoke'/
&MISC TMPA=19.1, ISOTHERMAL=.TRUE./

&MESH ID='Tunnel_center', FYI='Near burner', IJK=28,36,16, XB=-0.28,0.28,-
0.36,0.36,0.0,0.32/
&MESH ID='Shaft_1', FYI='Shaft_1', IJK=18,4,6, XB=1.64,2.36,-0.08,0.08,0.32,0.56/
&MESH ID='Shaft_2', FYI='Shaft_2', IJK=18,4,6, XB=5.64,6.36,-0.08,0.08,0.32,0.56/
&MESH ID='Tunnel_+1', FYI='Between burner and shaft_1', IJK=50,18,8,
XB=0.28,2.28,-0.36,0.36,0.0,0.32/
&MESH ID='Shaft_-1', FYI='Shaft_-1', IJK=18,4,6, XB=-2.36,-1.64,-
0.08,0.08,0.32,0.56/
&MESH ID='Shaft_-2', FYI='Shaft_-2', IJK=18,4,6, XB=-6.36,-5.64,-
0.08,0.08,0.32,0.56/
&MESH ID='Tunnel_-1', FYI='Between burner and shaft_-1', IJK=50,18,8, XB=-2.28,-
0.28,-0.36,0.36,0.0,0.32/
&MESH ID='+2', IJK=50,18,8, XB=2.28,4.28,-0.36,0.36,0.0,0.32/
&MESH ID='+3', IJK=50,18,8, XB=4.28,6.28,-0.36,0.36,0.0,0.32/
&MESH ID='+4', IJK=55,18,8, XB=6.28,8.48,-0.36,0.36,0.0,0.32/
&MESH ID='-2', IJK=50,18,8, XB=-4.28,-2.28,-0.36,0.36,0.0,0.32/
&MESH ID='-3', IJK=50,18,8, XB=-6.28,-4.28,-0.36,0.36,0.0,0.32/
&MESH ID='-4', IJK=55,18,8, XB=-8.48,-6.28,-0.36,0.36,0.0,0.32/

&SPEC ID='Smoke', FYI='artificial smoke',
MASS_EXTINCTION_COEFFICIENT=8700.0/
&SPEC ID='HELIUM'/

&DEVC ID='LAYER', QUANTITY='LAYER HEIGHT', XB=1.6,1.6,0.0,0.0,0.0,0.31/
&DEVC ID='LAYER02', QUANTITY='LAYER HEIGHT', XB=5.6,5.6,0.0,0.0,0.0,0.31/
&DEVC ID='LAYER03', QUANTITY='LAYER HEIGHT', XB=2.5,2.5,0.0,0.0,0.0,0.31/
&DEVC ID='LAYER04', QUANTITY='LAYER HEIGHT', XB=1.3,1.3,0.0,0.0,0.0,0.31/
&DEVC ID='LAYER05', QUANTITY='LAYER HEIGHT', XB=2.8,2.8,0.0,0.0,0.0,0.31/
&DEVC ID='LAYER06', QUANTITY='LAYER HEIGHT', XB=5.3,5.3,0.0,0.0,0.0,0.31/
&DEVC ID='Optical Density_1', QUANTITY='OPTICAL DENSITY',
SPEC_ID='Smoke', XYZ=1.6,0.0,0.31/
&DEVC ID='Optical Density_10', QUANTITY='OPTICAL DENSITY',
SPEC_ID='Smoke', XYZ=-1.3,0.0,0.31/
&DEVC ID='Optical Density_11', QUANTITY='OPTICAL DENSITY',
SPEC_ID='Smoke', XYZ=-1.5,0.0,0.31/
&DEVC ID='Optical Density_12', QUANTITY='OPTICAL DENSITY',
SPEC_ID='Smoke', XYZ=-1.6,0.0,0.31/

&DEVC ID='Optical Density_13', QUANTITY='OPTICAL DENSITY',
SPEC_ID='Smoke', XYZ=-2.5,0.0,0.31/
&DEVC ID='Optical Density_14', QUANTITY='OPTICAL DENSITY',
SPEC_ID='Smoke', XYZ=-2.6,0.0,0.31/
&DEVC ID='Optical Density_15', QUANTITY='OPTICAL DENSITY',
SPEC_ID='Smoke', XYZ=-3.0,0.0,0.31/
&DEVC ID='Optical Density_16', QUANTITY='OPTICAL DENSITY',
SPEC_ID='Smoke', XYZ=-3.6,0.0,0.31/
&DEVC ID='Optical Density_2', QUANTITY='OPTICAL DENSITY',
SPEC_ID='Smoke', XYZ=1.5,0.0,0.31/
&DEVC ID='Optical density_21', QUANTITY='OPTICAL DENSITY',
SPEC_ID='Smoke', XYZ=2.5,0.0,0.31, ORIENTATION=0.0,-1.0,0.0/
&DEVC ID='Optical Density_22', QUANTITY='OPTICAL DENSITY',
SPEC_ID='Smoke', XYZ=2.6,0.0,0.31/
&DEVC ID='Optical Density_23', QUANTITY='OPTICAL DENSITY',
SPEC_ID='Smoke', XYZ=2.8,0.0,0.31/
&DEVC ID='Optical Density_24', QUANTITY='OPTICAL DENSITY',
SPEC_ID='Smoke', XYZ=3.6,0.0,0.31/
&DEVC ID='Optical Density_25', QUANTITY='OPTICAL DENSITY',
SPEC_ID='Smoke', XYZ=4.4,0.0,0.31/
&DEVC ID='Optical Density_26', QUANTITY='OPTICAL DENSITY',
SPEC_ID='Smoke', XYZ=5.2,0.0,0.31/
&DEVC ID='Optical Density_27', QUANTITY='OPTICAL DENSITY',
SPEC_ID='Smoke', XYZ=5.4,0.0,0.31/
&DEVC ID='Optical density_28', QUANTITY='OPTICAL DENSITY',
SPEC_ID='Smoke', XYZ=5.6,0.0,0.31, ORIENTATION=0.0,-1.0,0.0/
&DEVC ID='Optical density_29', QUANTITY='OPTICAL DENSITY',
SPEC_ID='Smoke', XYZ=6.4,0.0,0.31, ORIENTATION=0.0,-1.0,0.0/
&DEVC ID='Optical density_3', QUANTITY='OPTICAL DENSITY',
SPEC_ID='Smoke', XYZ=1.3,0.0,0.31, ORIENTATION=0.0,-1.0,0.0/
&DEVC ID='Optical density_30', QUANTITY='OPTICAL DENSITY',
SPEC_ID='Smoke', XYZ=6.6,0.0,0.31, ORIENTATION=0.0,-1.0,0.0/
&DEVC ID='Optical density_31', QUANTITY='OPTICAL DENSITY',
SPEC_ID='Smoke', XYZ=6.8,0.0,0.31, ORIENTATION=0.0,-1.0,0.0/
&DEVC ID='Optical density_32', QUANTITY='OPTICAL DENSITY',
SPEC_ID='Smoke', XYZ=7.0,0.0,0.31, ORIENTATION=0.0,-1.0,0.0/
&DEVC ID='Optical density_33', QUANTITY='OPTICAL DENSITY',
SPEC_ID='Smoke', XYZ=7.2,0.0,0.31, ORIENTATION=0.0,-1.0,0.0/
&DEVC ID='Optical density_35', QUANTITY='OPTICAL DENSITY',
SPEC_ID='Smoke', XYZ=2.0,0.0,0.45, ORIENTATION=0.0,-1.0,0.0/
&DEVC ID='Optical density_36', QUANTITY='OPTICAL DENSITY',
SPEC_ID='Smoke', XYZ=1.65,0.0,0.45, ORIENTATION=0.0,-1.0,0.0/
&DEVC ID='Optical density_38', QUANTITY='OPTICAL DENSITY',
SPEC_ID='Smoke', XYZ=6.0,0.0,0.45, ORIENTATION=0.0,-1.0,0.0/

&DEVC ID='Optical density_39', QUANTITY='OPTICAL DENSITY',
SPEC_ID='Smoke', XYZ=5.65,0.0,0.45, ORIENTATION=0.0,-1.0,0.0/
&DEVC ID='Optical Density_4', QUANTITY='OPTICAL DENSITY',
SPEC_ID='Smoke', XYZ=0.8,0.0,0.31/
&DEVC ID='Optical Density_40', QUANTITY='OPTICAL DENSITY',
SPEC_ID='Smoke', XYZ=0.4,0.0,0.31/
&DEVC ID='Optical Density_41', QUANTITY='OPTICAL DENSITY',
SPEC_ID='Smoke', XYZ=0.0,0.0,0.26/
&DEVC ID='Optical Density_42', QUANTITY='OPTICAL DENSITY',
SPEC_ID='Smoke', XYZ=0.0,0.0,0.21/
&DEVC ID='Optical Density_43', QUANTITY='OPTICAL DENSITY',
SPEC_ID='Smoke', XYZ=0.0,0.0,0.16/
&DEVC ID='Optical Density_44', QUANTITY='OPTICAL DENSITY',
SPEC_ID='Smoke', XYZ=0.0,0.0,0.11/
&DEVC ID='Optical density_45', QUANTITY='OPTICAL DENSITY',
SPEC_ID='Smoke', XYZ=1.3,0.0,0.26, ORIENTATION=0.0,-1.0,0.0/
&DEVC ID='Optical density_46', QUANTITY='OPTICAL DENSITY',
SPEC_ID='Smoke', XYZ=1.3,0.0,0.21, ORIENTATION=0.0,-1.0,0.0/
&DEVC ID='Optical density_47', QUANTITY='OPTICAL DENSITY',
SPEC_ID='Smoke', XYZ=1.3,0.0,0.16, ORIENTATION=0.0,-1.0,0.0/
&DEVC ID='Optical density_48', QUANTITY='OPTICAL DENSITY',
SPEC_ID='Smoke', XYZ=1.3,0.0,0.11, ORIENTATION=0.0,-1.0,0.0/
&DEVC ID='Optical Density_49', QUANTITY='OPTICAL DENSITY',
SPEC_ID='Smoke', XYZ=2.8,0.0,0.26/
&DEVC ID='Optical Density_5', QUANTITY='OPTICAL DENSITY',
SPEC_ID='Smoke', XYZ=0.2,0.0,0.31/
&DEVC ID='Optical Density_50', QUANTITY='OPTICAL DENSITY',
SPEC_ID='Smoke', XYZ=2.8,0.0,0.21/
&DEVC ID='Optical Density_51', QUANTITY='OPTICAL DENSITY',
SPEC_ID='Smoke', XYZ=2.8,0.0,0.16/
&DEVC ID='Optical Density_52', QUANTITY='OPTICAL DENSITY',
SPEC_ID='Smoke', XYZ=2.8,0.0,0.11/
&DEVC ID='Optical Density_53', QUANTITY='OPTICAL DENSITY',
SPEC_ID='Smoke', XYZ=-1.3,0.0,0.26/
&DEVC ID='Optical Density_54', QUANTITY='OPTICAL DENSITY',
SPEC_ID='Smoke', XYZ=-1.3,0.0,0.21/
&DEVC ID='Optical Density_55', QUANTITY='OPTICAL DENSITY',
SPEC_ID='Smoke', XYZ=-1.3,0.0,0.16/
&DEVC ID='Optical Density_56', QUANTITY='OPTICAL DENSITY',
SPEC_ID='Smoke', XYZ=-1.3,0.0,0.11/
&DEVC ID='Optical Density_6', QUANTITY='OPTICAL DENSITY',
SPEC_ID='Smoke', XYZ=0.0,0.0,0.31/
&DEVC ID='Optical density_69', QUANTITY='OPTICAL DENSITY',
SPEC_ID='Smoke', XYZ=-1.65,0.0,0.45, ORIENTATION=0.0,-1.0,0.0/

&DEVC ID='Optical Density_7', QUANTITY='OPTICAL DENSITY',
SPEC_ID='Smoke', XYZ=-0.2,0.0,0.31/
&DEVC ID='Optical Density_70', QUANTITY='OPTICAL DENSITY',
SPEC_ID='Smoke', XYZ=0.6,0.0,0.31/
&DEVC ID='Optical Density_8', QUANTITY='OPTICAL DENSITY',
SPEC_ID='Smoke', XYZ=-0.4,0.0,0.31/
&DEVC ID='Optical Density_9', QUANTITY='OPTICAL DENSITY',
SPEC_ID='Smoke', XYZ=-0.8,0.0,0.31/
&DEVC ID='Velocity_64', QUANTITY='VELOCITY', XYZ=-8.4,0.0,0.16,
ORIENTATION=-1.0,0.0,0.0/
&DEVC ID='Velocity_65', QUANTITY='VELOCITY', XYZ=8.4,0.0,0.16,
ORIENTATION=-1.0,0.0,0.0/
&DEVC ID='Velocity_66', QUANTITY='VELOCITY', XYZ=1.65,0.0,0.45,
ORIENTATION=0.0,-1.0,0.0/
&DEVC ID='Velocity_67', QUANTITY='VELOCITY', XYZ=2.35,0.0,0.45,
ORIENTATION=0.0,-1.0,0.0/
&DEVC ID='Velocity_68', QUANTITY='VELOCITY', XYZ=5.65,0.0,0.45,
ORIENTATION=0.0,-1.0,0.0/
&DEVC ID='Velocity_69', QUANTITY='VELOCITY', XYZ=-1.65,0.0,0.45,
ORIENTATION=0.0,-1.0,0.0/
&DEVC ID='VF_1', QUANTITY='VOLUME FRACTION', SPEC_ID='HELIUM',
XYZ=1.6,0.0,0.31/
&DEVC ID='VF_10', QUANTITY='VOLUME FRACTION', SPEC_ID='HELIUM',
XYZ=-1.3,0.0,0.31/
&DEVC ID='VF_11', QUANTITY='VOLUME FRACTION', SPEC_ID='HELIUM',
XYZ=-1.5,0.0,0.31/
&DEVC ID='VF_12', QUANTITY='VOLUME FRACTION', SPEC_ID='HELIUM',
XYZ=-1.6,0.0,0.31/
&DEVC ID='VF_13', QUANTITY='VOLUME FRACTION', SPEC_ID='HELIUM',
XYZ=-2.5,0.0,0.31/
&DEVC ID='VF_14', QUANTITY='VOLUME FRACTION', SPEC_ID='HELIUM',
XYZ=2.6,0.0,0.31/
&DEVC ID='VF_15', QUANTITY='VOLUME FRACTION', SPEC_ID='HELIUM',
XYZ=-3.0,0.0,0.31/
&DEVC ID='VF_16', QUANTITY='VOLUME FRACTION', SPEC_ID='HELIUM',
XYZ=-3.6,0.0,0.31/
&DEVC ID='VF_2', QUANTITY='VOLUME FRACTION', SPEC_ID='HELIUM',
XYZ=1.5,0.0,0.31/
&DEVC ID='VF_21', QUANTITY='VOLUME FRACTION', SPEC_ID='HELIUM',
XYZ=2.5,0.0,0.31/
&DEVC ID='VF_22', QUANTITY='VOLUME FRACTION', SPEC_ID='HELIUM',
XYZ=2.6,0.0,0.31/
&DEVC ID='VF_23', QUANTITY='VOLUME FRACTION', SPEC_ID='HELIUM',
XYZ=-2.8,0.0,0.31/

&DEVC ID='VF_24', QUANTITY='VOLUME FRACTION', SPEC_ID='HELIUM',
XYZ=3.6,0.0,0.31/
&DEVC ID='VF_25', QUANTITY='VOLUME FRACTION', SPEC_ID='HELIUM',
XYZ=4.4,0.0,0.31/
&DEVC ID='VF_26', QUANTITY='VOLUME FRACTION', SPEC_ID='HELIUM',
XYZ=5.2,0.0,0.31/
&DEVC ID='VF_27', QUANTITY='VOLUME FRACTION', SPEC_ID='HELIUM',
XYZ=5.4,0.0,0.31/
&DEVC ID='VF_28', QUANTITY='VOLUME FRACTION', SPEC_ID='HELIUM',
XYZ=5.6,0.0,0.31/
&DEVC ID='VF_29', QUANTITY='VOLUME FRACTION', SPEC_ID='HELIUM',
XYZ=6.4,0.0,0.31/
&DEVC ID='VF_3', QUANTITY='VOLUME FRACTION', SPEC_ID='HELIUM',
XYZ=1.3,0.0,0.31/
&DEVC ID='VF_30', QUANTITY='VOLUME FRACTION', SPEC_ID='HELIUM',
XYZ=6.6,0.0,0.31/
&DEVC ID='VF_31', QUANTITY='VOLUME FRACTION', SPEC_ID='HELIUM',
XYZ=6.8,0.0,0.31/
&DEVC ID='VF_32', QUANTITY='VOLUME FRACTION', SPEC_ID='HELIUM',
XYZ=7.0,0.0,0.31/
&DEVC ID='VF_33', QUANTITY='VOLUME FRACTION', SPEC_ID='HELIUM',
XYZ=7.2,0.0,0.31/
&DEVC ID='VF_35', QUANTITY='VOLUME FRACTION', SPEC_ID='HELIUM',
XYZ=2.0,0.0,0.45/
&DEVC ID='VF_36', QUANTITY='VOLUME FRACTION', SPEC_ID='HELIUM',
XYZ=1.65,0.0,0.45/
&DEVC ID='VF_38', QUANTITY='VOLUME FRACTION', SPEC_ID='HELIUM',
XYZ=6.0,0.0,0.45/
&DEVC ID='VF_39', QUANTITY='VOLUME FRACTION', SPEC_ID='HELIUM',
XYZ=5.65,0.0,0.45/
&DEVC ID='VF_4', QUANTITY='VOLUME FRACTION', SPEC_ID='HELIUM',
XYZ=0.8,0.0,0.31/
&DEVC ID='VF_40', QUANTITY='VOLUME FRACTION', SPEC_ID='HELIUM',
XYZ=0.4,0.0,0.31/
&DEVC ID='VF_41', QUANTITY='VOLUME FRACTION', SPEC_ID='HELIUM',
XYZ=0.0,0.0,0.26/
&DEVC ID='VF_42', QUANTITY='VOLUME FRACTION', SPEC_ID='HELIUM',
XYZ=0.0,0.0,0.21/
&DEVC ID='VF_43', QUANTITY='VOLUME FRACTION', SPEC_ID='HELIUM',
XYZ=0.0,0.0,0.16/
&DEVC ID='VF_44', QUANTITY='VOLUME FRACTION', SPEC_ID='HELIUM',
XYZ=0.0,0.0,0.11/
&DEVC ID='VF_45', QUANTITY='VOLUME FRACTION', SPEC_ID='HELIUM',
XYZ=1.3,0.0,0.26/

```
&DEVC ID='VF_46', QUANTITY='VOLUME FRACTION', SPEC_ID='HELIUM',
   XYZ=1.3,0.0,0.21/
&DEVC ID='VF_47', QUANTITY='VOLUME FRACTION', SPEC_ID='HELIUM',
   XYZ=1.3,0.0,0.16/
&DEVC ID='VF_48', QUANTITY='VOLUME FRACTION', SPEC_ID='HELIUM',
   XYZ=1.3,0.0,0.11/
&DEVC ID='VF_49', QUANTITY='VOLUME FRACTION', SPEC_ID='HELIUM',
   XYZ=-2.8,0.0,0.26/
&DEVC ID='VF_5', QUANTITY='VOLUME FRACTION', SPEC_ID='HELIUM',
   XYZ=0.2,0.0,0.31/
&DEVC ID='VF_50', QUANTITY='VOLUME FRACTION', SPEC_ID='HELIUM',
   XYZ=-2.8,0.0,0.21/
&DEVC ID='VF_51', QUANTITY='VOLUME FRACTION', SPEC_ID='HELIUM',
   XYZ=-2.8,0.0,0.16/
&DEVC ID='VF_52', QUANTITY='VOLUME FRACTION', SPEC_ID='HELIUM',
   XYZ=-2.8,0.0,0.11/
&DEVC ID='VF_53', QUANTITY='VOLUME FRACTION', SPEC_ID='HELIUM',
   XYZ=-1.3,0.0,0.26/
&DEVC ID='VF_54', QUANTITY='VOLUME FRACTION', SPEC_ID='HELIUM',
   XYZ=-1.3,0.0,0.21/
&DEVC ID='VF_55', QUANTITY='VOLUME FRACTION', SPEC_ID='HELIUM',
   XYZ=-1.3,0.0,0.16/
&DEVC ID='VF_56', QUANTITY='VOLUME FRACTION', SPEC_ID='HELIUM',
   XYZ=-1.3,0.0,0.11/
&DEVC ID='VF_57', QUANTITY='VOLUME FRACTION', SPEC_ID='HELIUM',
   XYZ=2.6,0.0,0.26/
&DEVC ID='VF_58', QUANTITY='VOLUME FRACTION', SPEC_ID='HELIUM',
   XYZ=2.6,0.0,0.21/
&DEVC ID='VF_59', QUANTITY='VOLUME FRACTION', SPEC_ID='HELIUM',
   XYZ=2.6,0.0,0.16/
&DEVC ID='VF_6', QUANTITY='VOLUME FRACTION', SPEC_ID='HELIUM',
   XYZ=0.0,0.0,0.31/
&DEVC ID='VF_60', QUANTITY='VOLUME FRACTION', SPEC_ID='HELIUM',
   XYZ=2.6,0.0,0.11/
&DEVC ID='VF_7', QUANTITY='VOLUME FRACTION', SPEC_ID='HELIUM',
   XYZ=-0.2,0.0,0.31/
&DEVC ID='VF_70', QUANTITY='VOLUME FRACTION', SPEC_ID='HELIUM',
   XYZ=-0.6,0.0,0.31/
&DEVC ID='VF_8', QUANTITY='VOLUME FRACTION', SPEC_ID='HELIUM',
   XYZ=-0.4,0.0,0.31/
&DEVC ID='VF_9', QUANTITY='VOLUME FRACTION', SPEC_ID='HELIUM',
   XYZ=-0.8,0.0,0.31/
&SURF ID='Helium_Source',
   COLOR='RED',
   MASS_FLUX(2)=0.2245,
```

```
      TAU_MF(2)=1.0/
&SURF ID='Smoke',
     RGB=26,204,26,
     MASS_FLUX(1)=0.01,
     TAU_MF(1)=1.0/

&OBST XB=-0.02,0.02,-0.02,0.02,0.04,0.08, SURF_IDS='INERT','Smoke','INERT'/
Smoke generator

&HOLE XB=1.64,2.36,-0.08,0.08,0.31,0.35/ Hole+1
&HOLE XB=5.64,6.36,-0.08,0.08,0.31,0.35/ Hole+2
&HOLE XB=-2.36,-1.64,-0.08,0.08,0.31,0.35/ Hole-1
&HOLE XB=-6.36,-5.64,-0.08,0.08,0.31,0.35/ Hole-2

&VENT SURF_ID='Helium_Source', XB=-0.07,0.07,-0.07,0.07,0.0,0.0/ Burner
&VENT SURF_ID='OPEN', XB=8.48,8.48,-0.35,0.35,0.0,0.32/ +end
&VENT SURF_ID='OPEN', XB=-8.48,-8.48,-0.35,0.35,0.0,0.32/ -end
&VENT SURF_ID='OPEN', XB=1.64,2.36,-0.08,0.08,0.56,0.56/ +1top
&VENT SURF_ID='OPEN', XB=5.64,6.36,-0.08,0.08,0.56,0.56/ +2top
&VENT SURF_ID='OPEN', XB=-2.36,-1.64,-0.08,0.08,0.56,0.56/ -1top
&VENT SURF_ID='OPEN', XB=-6.36,-5.64,-0.08,0.08,0.56,0.56/ -2top

&SLCF QUANTITY='MASS FRACTION', SPEC_ID='Smoke', PBY=0.0/
&SLCF QUANTITY='OPTICAL DENSITY', SPEC_ID='Smoke', PBY=0.0/
&SLCF QUANTITY='TEMPERATURE', PBY=0.0/
&SLCF QUANTITY='VELOCITY', VECTOR=.TRUE., PBY=0.0/


&TAIL /
```
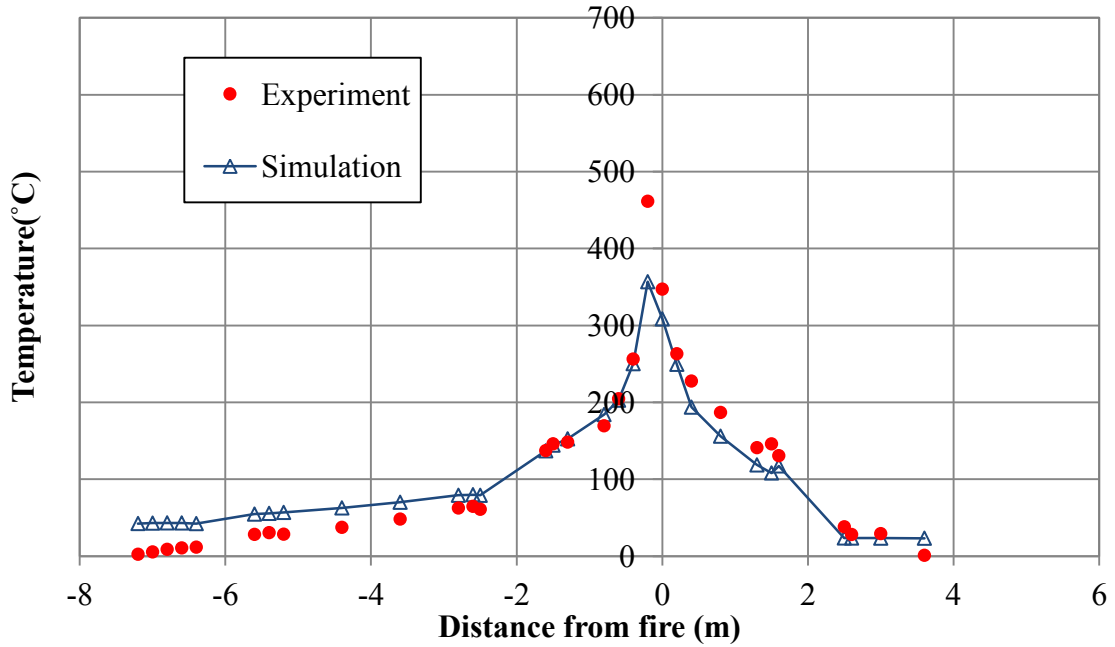
APPENDIX F – TUNNEL MODEL DATA COMPARISON

1. Temperature results

Comparison of temperature results for case 2.
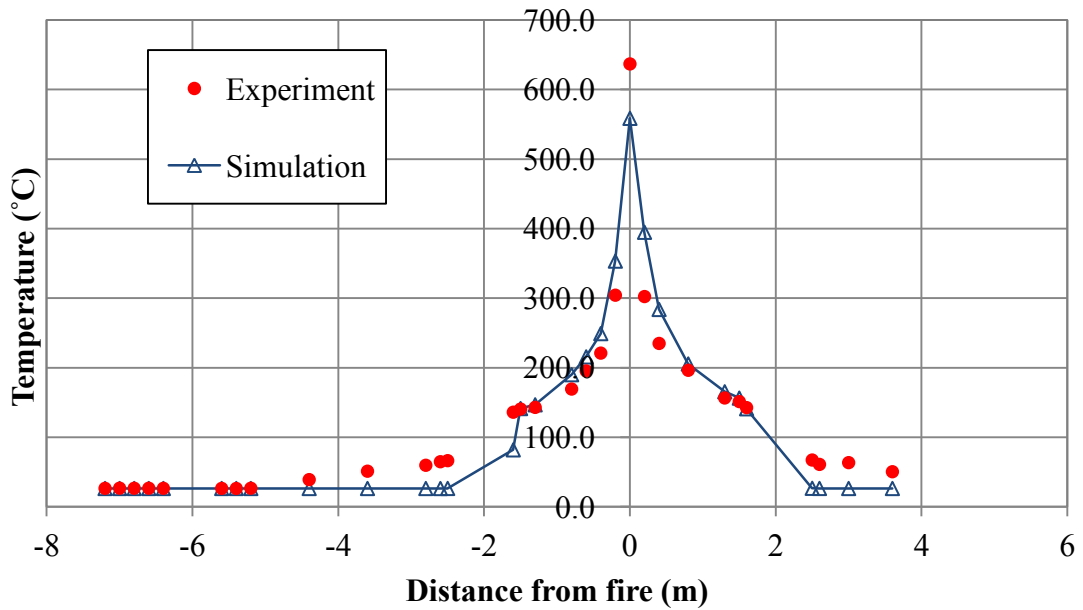
Comparison of temperature results for case 3.
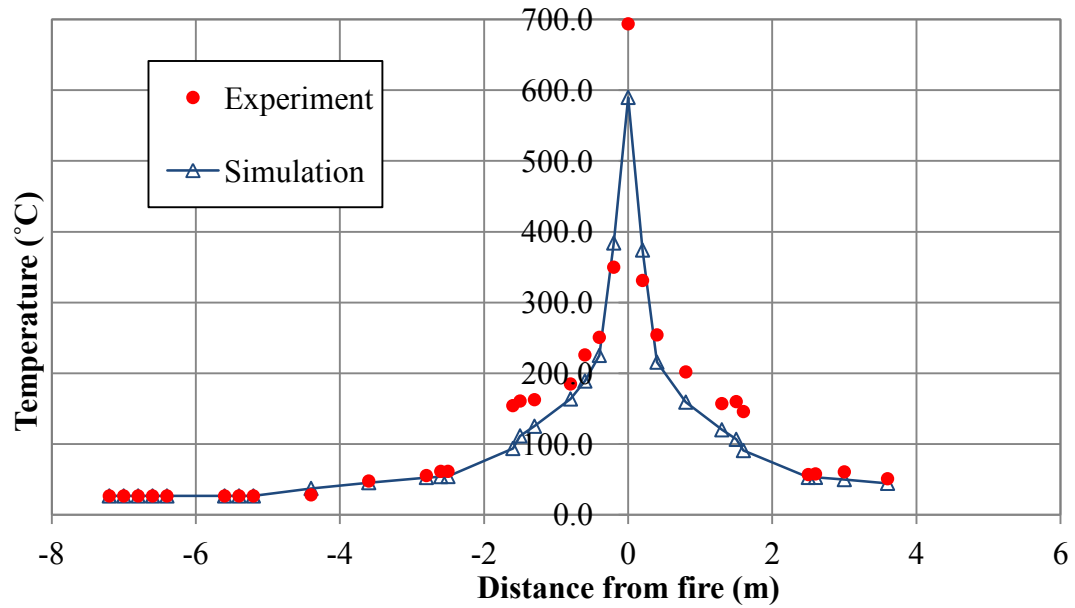
Comparison of temperature results for case 4.

2. Smoke optical density results
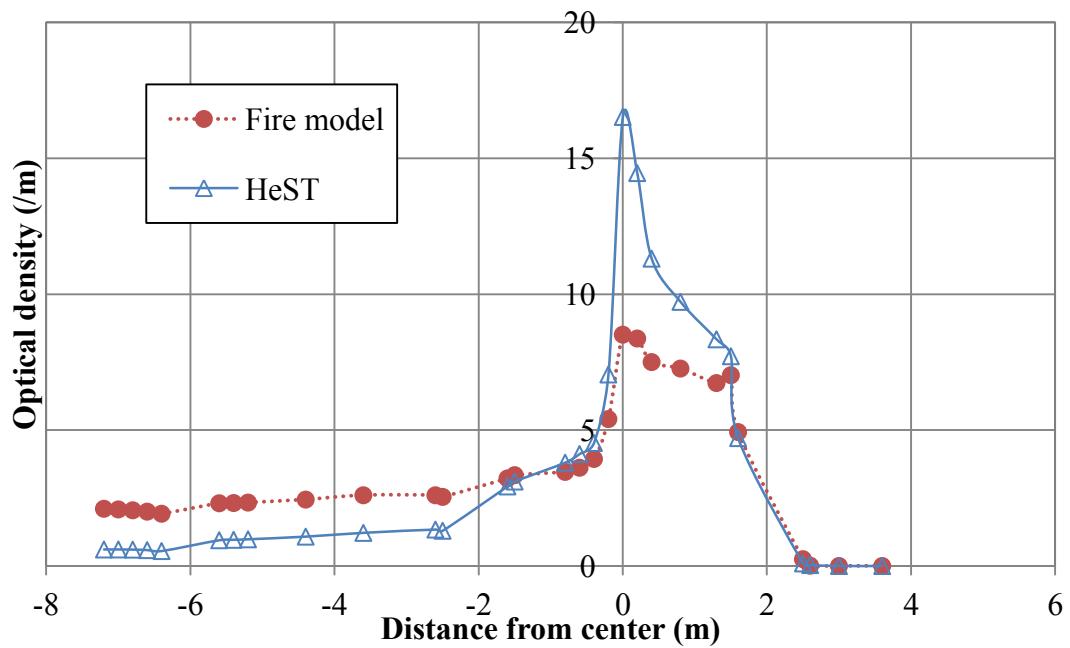
Comparison of smoke optical density between HST model and HeST model for case 2.
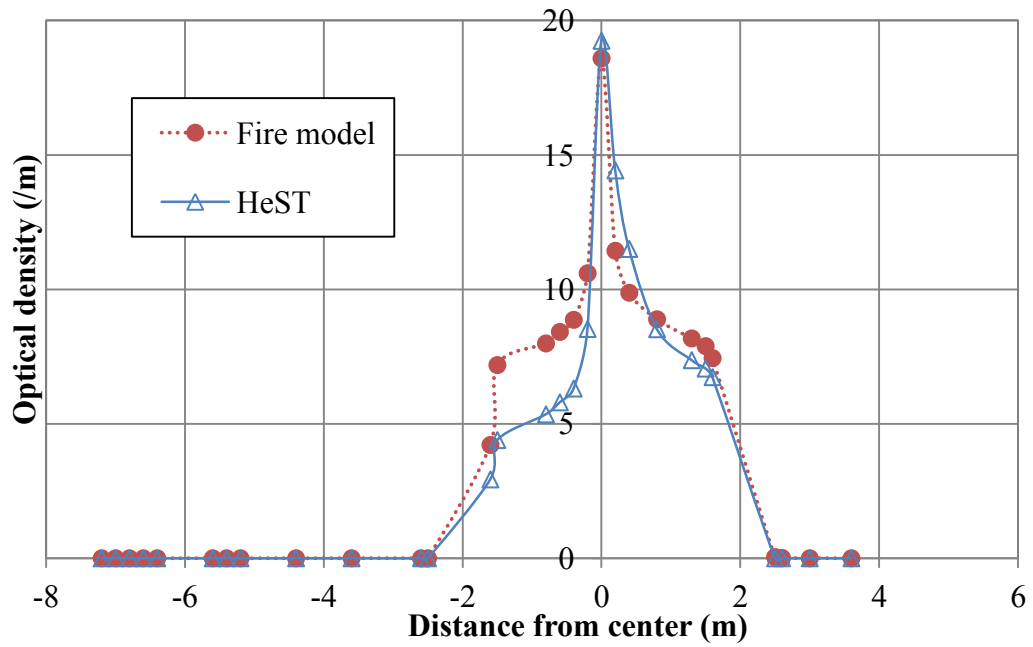
Comparison of smoke optical density between HST model and HeST model for case 3.
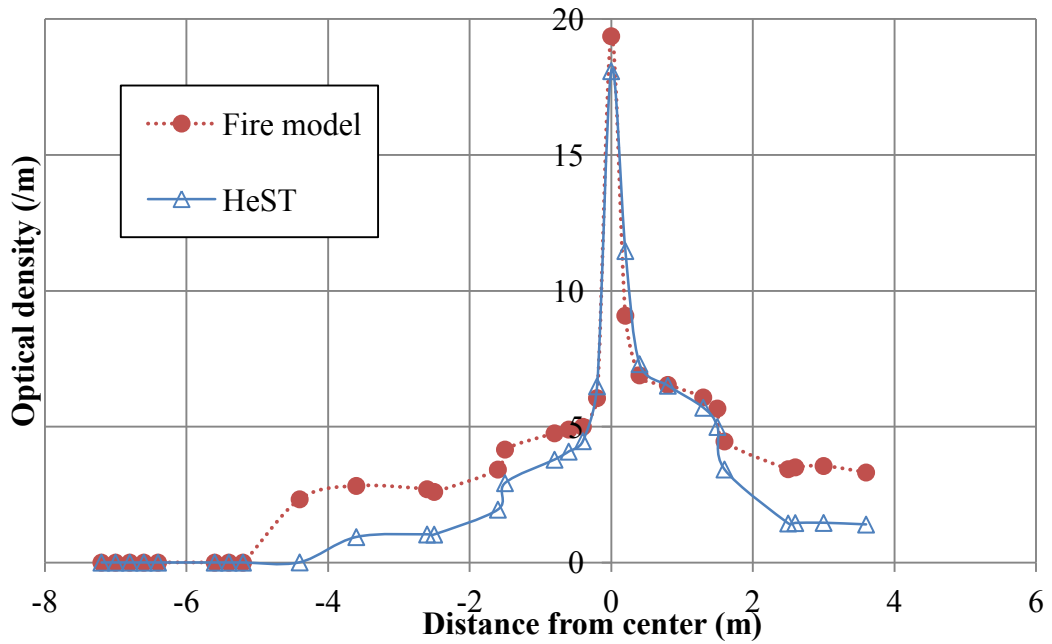
Comparison of smoke optical density between HST model and HeST model for case 4.

3. Smoke layer height results
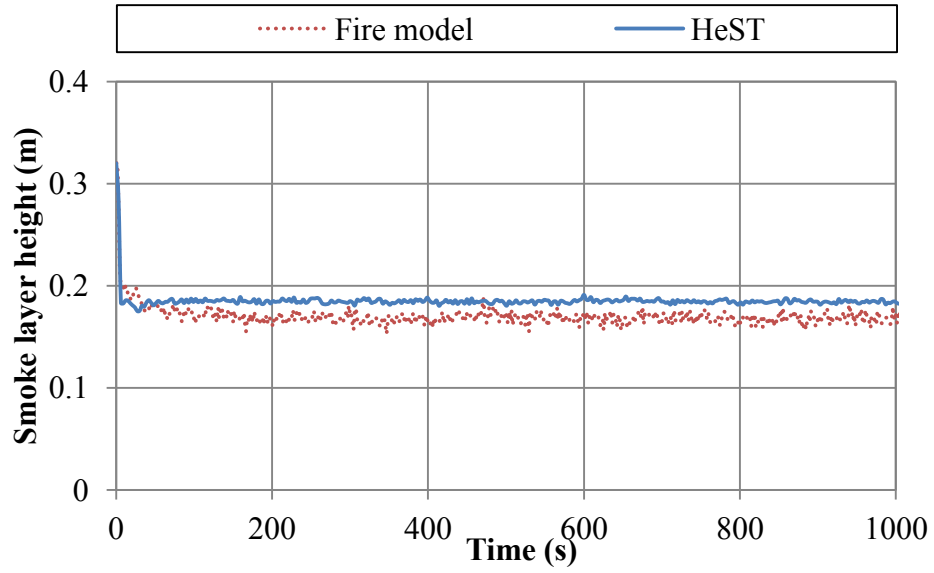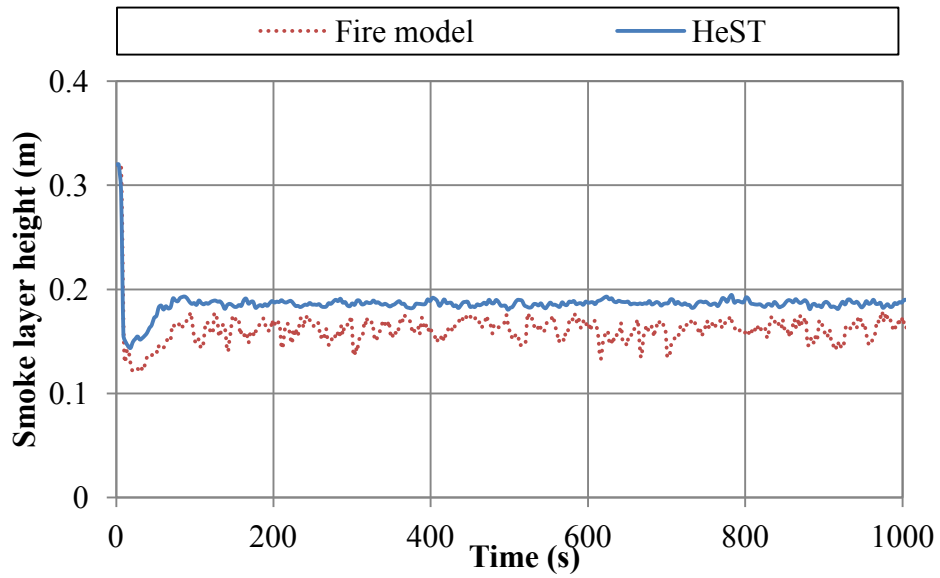
Comparison of smoke layer height in HST model and HeST model at location 01 (before first shaft) in case 2.

Comparison of smoke layer height in HST model and HeST model at location 02 (after first shaft) in case 2.

139
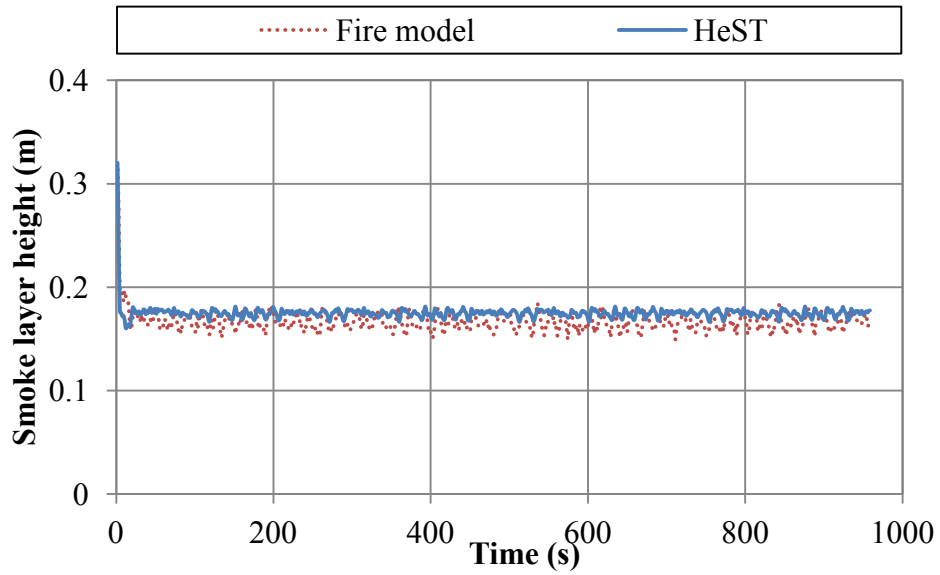
Comparison of smoke layer height in HST model and HeST model at location 01 (before first shaft) in case 3.
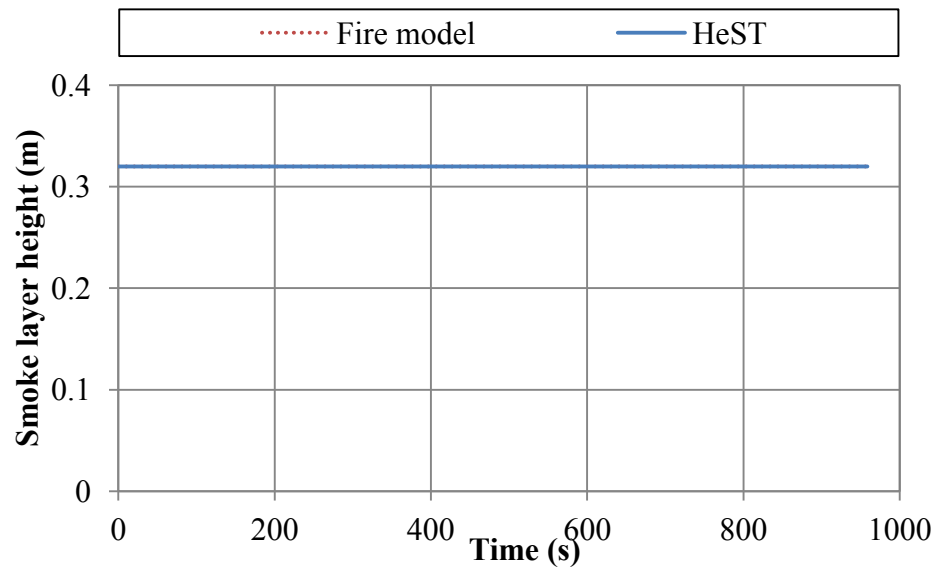
Comparison of smoke layer height in HST model and HeST model at location 02 (after first shaft) in case 3.
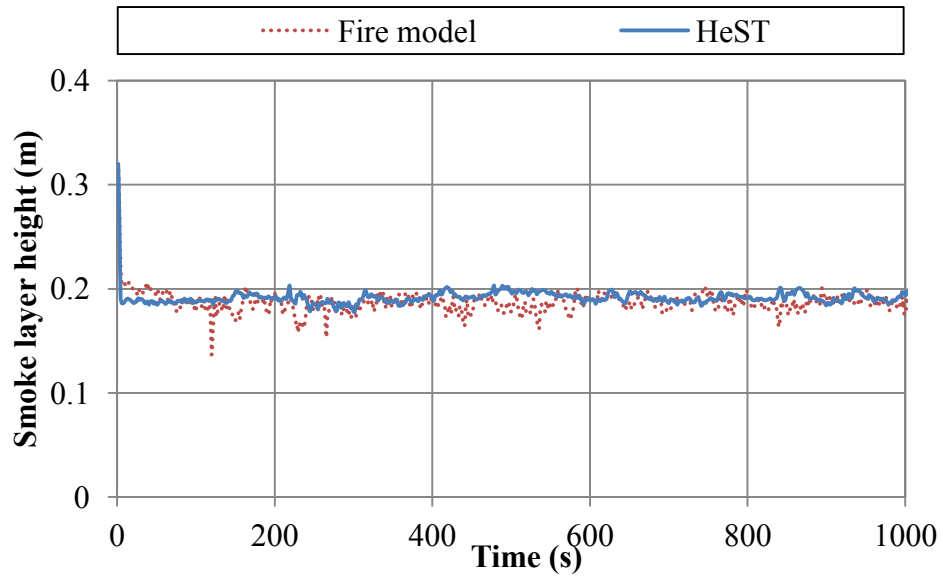
Comparison of smoke layer height in HST model and HeST model at location 01 (before first shaft) in case 4.
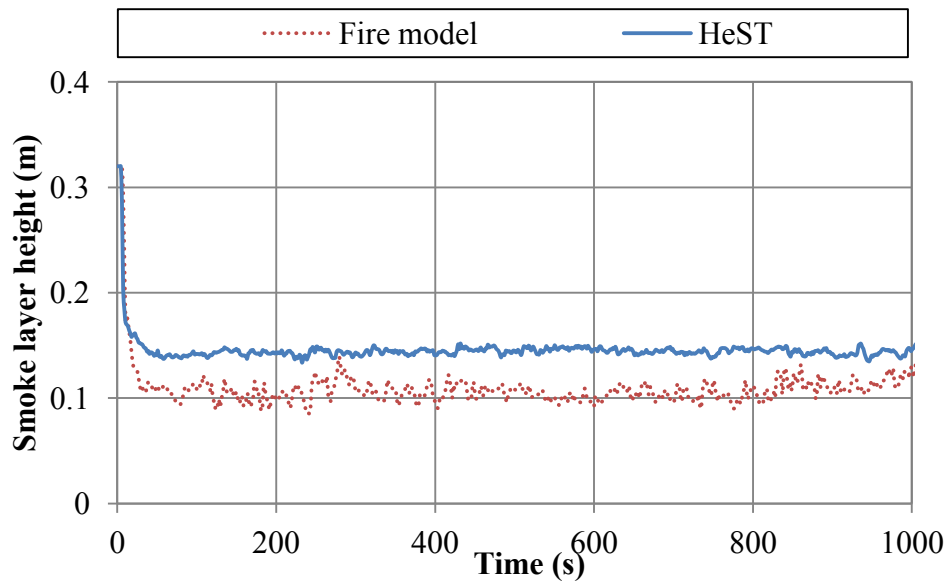
Comparison of smoke layer height in HST model and HeST model at location 02 (after first shaft) in case 4.

APPENDIX G – FDS INPUT OF 3-STOREY BUILDING MODEL

NRC_Fire1.fds

&HEAD CHID='NRC_Fire1'/
&TIME T_END=1.0000000E003/
&DUMP RENDER_FILE='NRC_Fire1.ge1', DT_RESTART=300.00,
SMOKE3D_QUANTITY='MASS FRACTION', SMOKE3D_SPEC_ID='MySmoke'/

&MESH ID='MESH', IJK=42,35,30, XB=0.00,10.57,0.00,9.00,0.00,7.64/

&SPEC ID='MySmoke', FYI='SmokeGenerator',
MASS_EXTINCTION_COEFFICIENT=8.7000000E003/

&PROP ID='Cleary Ionization I102',
    QUANTITY='CHAMBER OBSCURATION',
    SPEC_ID='MySmoke',
    ALPHA_E=2.50,
    BETA_E=-0.70,
    ALPHA_C=0.80,
    BETA_C=-0.90/
&PROP ID='Cleary Photoelectric P102',
    QUANTITY='CHAMBER OBSCURATION',
    SPEC_ID='MySmoke',
   ALPHA_E=1.80,
    BETA_E=-1.00,
    ALPHA_C=1.00,
    BETA_C=-0.80/
&DEVC ID='GAS_1_01', QUANTITY='OPTICAL DENSITY', SPEC_ID='MySmoke',
XYZ=9.50,8.00,2.40/
&DEVC ID='GAS_1_02', QUANTITY='OPTICAL DENSITY', SPEC_ID='MySmoke',
XYZ=9.50,8.00,1.90/
&DEVC ID='GAS_1_03', QUANTITY='OPTICAL DENSITY', SPEC_ID='MySmoke',
XYZ=9.50,8.00,1.40/
&DEVC ID='GAS_1_04', QUANTITY='OPTICAL DENSITY', SPEC_ID='MySmoke',
XYZ=9.50,8.00,0.90/
&DEVC ID='GAS_1_05', QUANTITY='OPTICAL DENSITY', SPEC_ID='MySmoke',
XYZ=9.50,8.00,0.4000/
&DEVC ID='GAS_1_11', QUANTITY='OPTICAL DENSITY', SPEC_ID='MySmoke',
XYZ=6.50,8.00,2.40/
&DEVC ID='GAS_1_12', QUANTITY='OPTICAL DENSITY', SPEC_ID='MySmoke',
XYZ=6.50,8.00,1.90/
&DEVC ID='GAS_1_13', QUANTITY='OPTICAL DENSITY', SPEC_ID='MySmoke',
XYZ=6.50,8.00,1.40/

&DEVC ID='GAS_1_14', QUANTITY='OPTICAL DENSITY', SPEC_ID='MySmoke',
XYZ=6.50,8.00,0.90/
&DEVC ID='GAS_1_15', QUANTITY='OPTICAL DENSITY', SPEC_ID='MySmoke',
XYZ=6.50,8.00,0.4000/
&DEVC ID='GAS_1_21', QUANTITY='OPTICAL DENSITY', SPEC_ID='MySmoke',
XYZ=6.50,4.80,2.40/
&DEVC ID='GAS_2_01', QUANTITY='OPTICAL DENSITY', SPEC_ID='MySmoke',
XYZ=5.50,5.00,5.00/
&DEVC ID='GAS_2_11', QUANTITY='OPTICAL DENSITY', SPEC_ID='MySmoke',
XYZ=8.00,2.00,5.00/
&DEVC ID='GAS_2_21', QUANTITY='OPTICAL DENSITY', SPEC_ID='MySmoke',
XYZ=2.60,2.00,5.00/
&DEVC ID='GAS_2_31', QUANTITY='OPTICAL DENSITY', SPEC_ID='MySmoke',
XYZ=2.60,7.00,5.00/
&DEVC ID='GAS_2_41', QUANTITY='OPTICAL DENSITY', SPEC_ID='MySmoke',
XYZ=8.00,7.00,5.00/
&DEVC ID='GAS_3_01', QUANTITY='OPTICAL DENSITY', SPEC_ID='MySmoke',
XYZ=8.00,7.00,7.60/
&DEVC ID='GAS_3_11', QUANTITY='OPTICAL DENSITY', SPEC_ID='MySmoke',
XYZ=8.00,2.00,7.60/
&DEVC ID='LAYER 1-1', QUANTITY='LAYER HEIGHT',
XB=8.00,8.00,2.00,2.00,2.60,5.04/
&DEVC ID='LAYER 1-2', QUANTITY='LAYER HEIGHT',
XB=8.00,8.00,7.00,7.00,2.60,5.04/
&DEVC ID='LAYER 3-1', QUANTITY='LAYER HEIGHT',
XB=9.50,9.50,8.00,8.00,5.20,7.64/
&DEVC ID='LAYER 3-2', QUANTITY='LAYER HEIGHT',
XB=9.50,9.50,1.00,1.00,5.20,7.64/
&DEVC ID='LAYER basement1', QUANTITY='LAYER HEIGHT',
XB=9.50,9.50,8.00,8.00,0.00,2.44/
&DEVC ID='LAYER basement2', QUANTITY='LAYER HEIGHT',
XB=6.50,6.50,8.00,8.00,0.00,2.44/
&DEVC ID='Smoke detector1-1', PROP_ID='Cleary Ionization I102',
XYZ=5.50,5.00,2.43/
&DEVC ID='Smoke detector2-1', PROP_ID='Cleary Ionization I102',
XYZ=5.70,5.00,5.00/
&DEVC ID='Smoke detector2-2', PROP_ID='Cleary Photoelectric P102',
XYZ=8.10,7.00,5.00/
&DEVC ID='Smoke detector3-1', PROP_ID='Cleary Ionization I102',
XYZ=8.10,7.00,7.60/
&DEVC ID='Smoke detector3-2', PROP_ID='Cleary Ionization I102',
XYZ=8.10,2.00,7.60/
&DEVC ID='TC_tree1_01', QUANTITY='THERMOCOUPLE', XYZ=9.50,8.00,2.40/
&DEVC ID='TC_tree1_02', QUANTITY='THERMOCOUPLE', XYZ=9.50,8.00,1.90/
&DEVC ID='TC_tree1_03', QUANTITY='THERMOCOUPLE', XYZ=9.50,8.00,1.40/

```
&DEVC ID='TC_tree1_04', QUANTITY='THERMOCOUPLE', XYZ=9.50,8.00,0.90/
&DEVC ID='TC_tree1_05', QUANTITY='THERMOCOUPLE', XYZ=9.50,8.00,0.4000/
&DEVC ID='TC_tree1_11', QUANTITY='THERMOCOUPLE', XYZ=6.50,8.00,2.40/
&DEVC ID='TC_tree1_12', QUANTITY='THERMOCOUPLE', XYZ=6.50,8.00,1.90/
&DEVC ID='TC_tree1_13', QUANTITY='THERMOCOUPLE', XYZ=6.50,8.00,1.40/
&DEVC ID='TC_tree1_14', QUANTITY='THERMOCOUPLE', XYZ=6.50,8.00,0.90/
&DEVC ID='TC_tree1_15', QUANTITY='THERMOCOUPLE', XYZ=6.50,8.00,0.4000/
&DEVC ID='TC_tree1_21', QUANTITY='THERMOCOUPLE', XYZ=6.50,4.80,2.40/
&DEVC ID='TC_tree2_01', QUANTITY='THERMOCOUPLE', XYZ=5.50,5.00,5.00/
&DEVC ID='TC_tree2_11', QUANTITY='THERMOCOUPLE', XYZ=8.00,2.00,5.00/
&DEVC ID='TC_tree2_21', QUANTITY='THERMOCOUPLE', XYZ=2.60,2.00,5.00/
&DEVC ID='TC_tree2_31', QUANTITY='THERMOCOUPLE', XYZ=2.60,7.00,5.00/
&DEVC ID='TC_tree2_41', QUANTITY='THERMOCOUPLE', XYZ=8.00,7.00,5.00/
&DEVC ID='TC_tree3_01', QUANTITY='THERMOCOUPLE', XYZ=8.00,7.00,7.60/
&DEVC ID='TC_tree3_11', QUANTITY='THERMOCOUPLE', XYZ=8.00,2.00,7.60/

&MATL ID='CONCRETE',
    FYI='NBSIR 88-3752 - ATF NIST Multi-Floor Validation',
    SPECIFIC_HEAT=1.04,
    CONDUCTIVITY=1.80,
    DENSITY=2.2800000E003/
&MATL ID='STEEL',
    FYI='Drysdale, Intro to Fire Dynamics - ATF NIST Multi-Floor Validation',
    SPECIFIC_HEAT=0.4600,
    CONDUCTIVITY=45.80,
    DENSITY=7.8500000E003,
    EMISSIVITY=0.95/
&MATL ID='GYPSUM',
    FYI='NBSIR 88-3752 - ATF NIST Multi-Floor Validation',
    SPECIFIC_HEAT=1.09,
    CONDUCTIVITY=0.1700,
    DENSITY=930.00/

&SURF ID='cement board',
    COLOR='GRAY 60',
    MATL_ID(1,1)='CONCRETE',
    MATL_MASS_FRACTION(1,1)=1.00,
    THICKNESS(1)=0.0800/
&SURF ID='steel',
    RGB=255,153,153,
    MATL_ID(1,1)='STEEL',
    MATL_MASS_FRACTION(1,1)=1.00,
    THICKNESS(1)=5.0000000E-003/
&SURF ID='gypsum *2',
    COLOR='WHITE',
```

```
    MATL_ID(1,1)='GYPSUM',
    MATL_ID(2,1)='GYPSUM',
    MATL_MASS_FRACTION(1,1)=1.00,
    MATL_MASS_FRACTION(2,1)=1.00,
    THICKNESS(1:2)=0.0160,0.0160/
&SURF ID='MySmoke',
    FYI='Helium mixture/pure helium',
    RGB=26,204,26,
    MASS_FLUX(1)=1.0000000E-004,
    TAU_MF(1)=1.00/
&SURF ID='BURNER',
    COLOR='RED',
    HRRPUA=300.00,
    TAU_Q=-80.00/


&OBST XB=2.88,5.24,5.45,5.53,2.60,5.04, SURF_ID='cement board'/ stair wall[1]
&OBST XB=2.88,5.24,4.46,4.54,2.60,5.04, SURF_ID='cement board'/ stair wall 2[1]
&OBST XB=5.24,5.32,4.46,5.53,2.60,5.04, SURF_ID='cement board'/ stair wall 4
&OBST XB=2.80,2.88,4.46,5.53,5.20,7.64, SURF_ID='cement board'/ stair wall 3
&OBST XB=5.24,5.32,5.45,6.25,5.20,7.64, SURF_ID='cement board'/ Wall[1][1]
&OBST XB=6.74,6.82,0.00,9.00,5.20,7.64, SURF_ID='cement board'/ Wall[1][1]
&OBST XB=5.24,5.32,0.00,4.54,5.20,7.64, SURF_ID='cement board'/ Wall[1]
&OBST XB=5.24,5.32,5.45,9.00,0.00,2.44, SURF_ID='cement board'/ Wall[1]
&OBST XB=2.88,5.24,5.45,5.53,5.20,7.64, SURF_ID='cement board'/ stair wall[2]
&OBST XB=2.88,5.24,4.46,4.54,5.20,7.64, SURF_ID='cement board'/ stair wall 2[2]
&OBST XB=6.82,10.57,4.46,4.54,5.20,7.64, SURF_ID='cement board'/ wall
&OBST XB=5.24,6.74,6.25,6.33,5.20,7.64, SURF_ID='cement board'/ stair wall[2][1]
&OBST XB=5.24,6.74,1.72,1.80,5.20,7.64, SURF_ID='cement board'/ stair wall[2][1][1]
&OBST XB=2.80,2.88,4.46,5.53,0.00,2.44, SURF_ID='cement board'/ stair wall 3[1]
&OBST XB=5.24,5.32,0.00,4.54,0.00,2.44, SURF_ID='cement board'/ Wall
&OBST XB=2.88,5.24,5.45,5.53,0.00,2.44, SURF_ID='cement board'/ stair wall
&OBST XB=2.88,5.24,4.46,4.54,0.00,2.44, SURF_ID='cement board'/ stair wall 2
&OBST XB=5.32,10.57,3.70,3.78,0.00,2.44, SURF_ID='cement board'/ wall3
&OBST XB=-0.0500,10.62,-0.0500,0.00,0.00,7.64, COLOR='INVISIBLE',
SURF_ID6='steel','steel','steel','cement board','steel','steel'/ Bottom Wall (Min X)
&OBST XB=10.57,10.62,-0.0500,9.05,0.00,7.64, COLOR='INVISIBLE',
SURF_ID6='cement board','steel','steel','steel','steel','steel'/ Right Wall (Max Y)
&OBST XB=-0.0500,10.62,9.00,9.05,0.00,7.64, COLOR='INVISIBLE',
SURF_ID6='steel','steel','cement board','steel','steel','steel'/ Top Wall (Max X)
&OBST XB=-0.0500,0.00,-0.0500,9.05,0.00,7.64, COLOR='INVISIBLE',
SURF_ID6='steel','cement board','steel','steel','steel','steel'/ Left Wall (Min Y)
&OBST XB=0.00,10.57,0.00,9.00,2.44,2.60, SURF_IDS='cement board','cement
board','gypsum *2'/ ceiling1
&OBST XB=0.00,10.57,0.00,9.00,-0.1600,0.00, SURF_ID='cement board'/ floor
```

&OBST XB=0.00,10.57,0.00,9.00,5.04,5.20, SURF_IDS='cement board','cement board','gypsum *2'/ ceiling1[1]
&OBST XB=0.00,10.57,0.00,9.00,7.64,7.80, COLOR='INVISIBLE', SURF_IDS='steel','steel','gypsum *2'/ ceiling1[2]
&OBST XB=8.20,8.60,6.20,6.60,0.50,0.80, SURF_IDS='INERT','MySmoke','INERT'/ Smoke generator
&OBST XB=2.77,3.02,4.63,5.40,2.55,2.55, SURF_ID='steel'/ Slab[1]
&OBST XB=3.02,3.27,4.63,5.40,2.80,2.80, SURF_ID='steel'/ Slab[1]
&OBST XB=3.27,3.52,4.63,5.40,3.06,3.06, SURF_ID='steel'/ Slab[1]
&OBST XB=3.52,3.78,4.63,5.40,3.31,3.31, SURF_ID='steel'/ Slab[1]
&OBST XB=3.78,4.03,4.63,5.40,3.57,3.57, SURF_ID='steel'/ Slab[1]
&OBST XB=4.03,4.28,4.63,5.40,3.82,3.82, SURF_ID='steel'/ Slab[1]
&OBST XB=4.28,4.53,4.63,5.40,4.07,4.07, SURF_ID='steel'/ Slab[1]
&OBST XB=4.53,4.78,4.63,5.40,4.33,4.33, SURF_ID='steel'/ Slab[1]
&OBST XB=4.78,5.03,4.63,5.40,4.58,4.58, SURF_ID='steel'/ Slab[1]
&OBST XB=5.03,5.28,4.63,5.40,4.84,4.84, SURF_ID='steel'/ Slab[1]
&OBST XB=3.02,3.02,4.63,5.40,2.55,2.80, SURF_ID='steel'/ Slab[1]
&OBST XB=3.27,3.27,4.63,5.40,2.80,3.06, SURF_ID='steel'/ Slab[1]
&OBST XB=3.52,3.52,4.63,5.40,3.06,3.31, SURF_ID='steel'/ Slab[1]
&OBST XB=3.78,3.78,4.63,5.40,3.31,3.57, SURF_ID='steel'/ Slab[1]
&OBST XB=4.03,4.03,4.63,5.40,3.57,3.82, SURF_ID='steel'/ Slab[1]
&OBST XB=4.28,4.28,4.63,5.40,3.82,4.07, SURF_ID='steel'/ Slab[1]
&OBST XB=4.53,4.53,4.63,5.40,4.07,4.33, SURF_ID='steel'/ Slab[1]
&OBST XB=4.78,4.78,4.63,5.40,4.33,4.58, SURF_ID='steel'/ Slab[1]
&OBST XB=5.03,5.03,4.63,5.40,4.58,4.84, SURF_ID='steel'/ Slab[1]
&OBST XB=5.28,5.28,4.63,5.40,4.84,5.09, SURF_ID='steel'/ Slab[1]

&HOLE
XB=5.2450000E000,5.3250000E000,4.5900000E000,5.4000000E000,2.6000000E000,4.6500000E000/ stair door
&HOLE
XB=2.0000000E000,2.8900000E000,8.9000000E000,9.1000000E000,2.6000000E000,4.6700000E000/ door
&HOLE
XB=6.7400000E000,6.8200000E000,2.5000000E000,3.3100000E000,5.2000000E000,7.2500000E000/ stair door[1]
&HOLE
XB=6.7400000E000,6.8200000E000,4.8000000E000,5.6100000E000,5.2000000E000,7.2500000E000/ stair door[1][1]
&HOLE
XB=1.0500000E001,1.0700000E001,5.3500000E000,7.3500000E000,1.8000000E000,2.3000000E000/ basement opening
&HOLE
XB=2.8850000E000,5.3250000E000,4.5400000E000,5.4500000E000,2.4400000E000,2.6000000E000/ Hole

&HOLE
XB=2.8850000E000,5.3250000E000,4.5400000E000,5.4500000E000,5.0400000E000,5.
2000000E000/ Hole[1]

&VENT SURF_ID='BURNER', XB=7.90,8.90,5.90,6.90,0.00,0.00/ Burner
&VENT SURF_ID='OPEN', XB=2.00,2.89,9.00,9.00,2.60,4.67/ door
&VENT SURF_ID='OPEN', XB=10.57,10.57,5.35,7.35,1.80,2.30/ window

&SLCF QUANTITY='DENSITY', PBY=2.00/
&SLCF QUANTITY='PRESSURE', PBY=2.00/
&SLCF QUANTITY='TEMPERATURE', VECTOR=.TRUE., PBY=2.00/
&SLCF QUANTITY='VELOCITY', VECTOR=.TRUE., PBY=2.00/
&SLCF QUANTITY='PRESSURE', PBY=5.00/
&SLCF QUANTITY='TEMPERATURE', PBY=5.00/
&SLCF QUANTITY='VELOCITY', VECTOR=.TRUE., PBY=5.00/
&SLCF QUANTITY='DENSITY', PBY=6.40/
&SLCF QUANTITY='PRESSURE', PBY=6.40/
&SLCF QUANTITY='TEMPERATURE', PBY=6.40/
&SLCF QUANTITY='VELOCITY', VECTOR=.TRUE., PBY=6.40/
&SLCF QUANTITY='TEMPERATURE', PBY=7.00/

&TAIL /

NRC_Helium1.fds

&HEAD CHID='NRC_Helium1'/
&TIME T_END=1.0000000E003/
&DUMP RENDER_FILE='NRC_Helium1.ge1', DT_RESTART=300.00,
SMOKE3D_QUANTITY='MASS FRACTION', SMOKE3D_SPEC_ID='MySmoke'/
&MISC RADIATION=.FALSE./

&MESH ID='MESH', IJK=42,35,30, XB=0.00,10.57,0.00,9.00,0.00,7.64/

&SPEC ID='MySmoke', FYI='SmokeGenerator',
MASS_EXTINCTION_COEFFICIENT=8.7000000E003/
&SPEC ID='HELIUM'/

&PROP ID='Cleary Ionization I102',
    QUANTITY='CHAMBER OBSCURATION',
    SPEC_ID='MySmoke',
    ALPHA_E=2.50,
    BETA_E=-0.70,
    ALPHA_C=0.80,
    BETA_C=-0.90/
&PROP ID='Cleary Photoelectric P102',
    QUANTITY='CHAMBER OBSCURATION',
    SPEC_ID='MySmoke',
    ALPHA_E=1.80,
    BETA_E=-1.00,
    ALPHA_C=1.00,
    BETA_C=-0.80/
&DEVC ID='GAS_1_01', QUANTITY='OPTICAL DENSITY', SPEC_ID='MySmoke',
XYZ=9.50,8.00,2.40/
&DEVC ID='GAS_1_02', QUANTITY='OPTICAL DENSITY', SPEC_ID='MySmoke',
XYZ=9.50,8.00,1.90/
&DEVC ID='GAS_1_03', QUANTITY='OPTICAL DENSITY', SPEC_ID='MySmoke',
XYZ=9.50,8.00,1.40/
&DEVC ID='GAS_1_04', QUANTITY='OPTICAL DENSITY', SPEC_ID='MySmoke',
XYZ=9.50,8.00,0.90/
&DEVC ID='GAS_1_05', QUANTITY='OPTICAL DENSITY', SPEC_ID='MySmoke',
XYZ=9.50,8.00,0.4000/
&DEVC ID='GAS_1_11', QUANTITY='OPTICAL DENSITY', SPEC_ID='MySmoke',
XYZ=6.50,8.00,2.40/
&DEVC ID='GAS_1_12', QUANTITY='OPTICAL DENSITY', SPEC_ID='MySmoke',
XYZ=6.50,8.00,1.90/
&DEVC ID='GAS_1_13', QUANTITY='OPTICAL DENSITY', SPEC_ID='MySmoke',
XYZ=6.50,8.00,1.40/

&DEVC ID='GAS_1_14', QUANTITY='OPTICAL DENSITY', SPEC_ID='MySmoke',
XYZ=6.50,8.00,0.90/
&DEVC ID='GAS_1_15', QUANTITY='OPTICAL DENSITY', SPEC_ID='MySmoke',
XYZ=6.50,8.00,0.4000/
&DEVC ID='GAS_1_21', QUANTITY='OPTICAL DENSITY', SPEC_ID='MySmoke',
XYZ=6.50,4.80,2.40/
&DEVC ID='GAS_2_01', QUANTITY='OPTICAL DENSITY', SPEC_ID='MySmoke',
XYZ=5.50,5.00,5.00/
&DEVC ID='GAS_2_11', QUANTITY='OPTICAL DENSITY', SPEC_ID='MySmoke',
XYZ=8.00,2.00,5.00/
&DEVC ID='GAS_2_21', QUANTITY='OPTICAL DENSITY', SPEC_ID='MySmoke',
XYZ=2.60,2.00,5.00/
&DEVC ID='GAS_2_31', QUANTITY='OPTICAL DENSITY', SPEC_ID='MySmoke',
XYZ=2.60,7.00,5.00/
&DEVC ID='GAS_2_41', QUANTITY='OPTICAL DENSITY', SPEC_ID='MySmoke',
XYZ=8.00,7.00,5.00/
&DEVC ID='GAS_3_01', QUANTITY='OPTICAL DENSITY', SPEC_ID='MySmoke',
XYZ=8.00,7.00,7.60/
&DEVC ID='GAS_3_11', QUANTITY='OPTICAL DENSITY', SPEC_ID='MySmoke',
XYZ=8.00,2.00,7.60/
&DEVC ID='LAYER 1-1', QUANTITY='LAYER HEIGHT',
XB=8.00,8.00,2.00,2.00,2.60,5.04/
&DEVC ID='LAYER 1-2', QUANTITY='LAYER HEIGHT',
XB=8.00,8.00,7.00,7.00,2.60,5.04/
&DEVC ID='LAYER 3-1', QUANTITY='LAYER HEIGHT',
XB=9.50,9.50,8.00,8.00,5.20,7.64/
&DEVC ID='LAYER 3-2', QUANTITY='LAYER HEIGHT',
XB=9.50,9.50,1.00,1.00,5.20,7.64/
&DEVC ID='LAYER basement1', QUANTITY='LAYER HEIGHT',
XB=9.50,9.50,8.00,8.00,0.00,2.44/
&DEVC ID='LAYER basement2', QUANTITY='LAYER HEIGHT',
XB=6.50,6.50,8.00,8.00,0.00,2.44/
&DEVC ID='Smoke detector1-1', PROP_ID='Cleary Ionization I102',
XYZ=5.50,5.00,2.43/
&DEVC ID='Smoke detector2-1', PROP_ID='Cleary Ionization I102',
XYZ=5.70,5.00,5.00/
&DEVC ID='Smoke detector2-2', PROP_ID='Cleary Photoelectric P102',
XYZ=8.10,7.00,5.00/
&DEVC ID='Smoke detector3-1', PROP_ID='Cleary Ionization I102',
XYZ=8.10,7.00,7.60/
&DEVC ID='Smoke detector3-2', PROP_ID='Cleary Ionization I102',
XYZ=8.10,2.00,7.60/
&DEVC ID='VF_1_01', QUANTITY='VOLUME FRACTION', SPEC_ID='HELIUM',
XYZ=9.50,8.00,2.40/

&DEVC ID='VF_1_02', QUANTITY='VOLUME FRACTION', SPEC_ID='HELIUM',
XYZ=9.50,8.00,1.90/
&DEVC ID='VF_1_03', QUANTITY='VOLUME FRACTION', SPEC_ID='HELIUM',
XYZ=9.50,8.00,1.40/
&DEVC ID='VF_1_04', QUANTITY='VOLUME FRACTION', SPEC_ID='HELIUM',
XYZ=9.50,8.00,0.90/
&DEVC ID='VF_1_05', QUANTITY='VOLUME FRACTION', SPEC_ID='HELIUM',
XYZ=9.50,8.00,0.4000/
&DEVC ID='VF_1_11', QUANTITY='VOLUME FRACTION', SPEC_ID='HELIUM',
XYZ=6.50,8.00,2.40/
&DEVC ID='VF_1_12', QUANTITY='VOLUME FRACTION', SPEC_ID='HELIUM',
XYZ=6.50,8.00,1.90/
&DEVC ID='VF_1_13', QUANTITY='VOLUME FRACTION', SPEC_ID='HELIUM',
XYZ=6.50,8.00,1.40/
&DEVC ID='VF_1_14', QUANTITY='VOLUME FRACTION', SPEC_ID='HELIUM',
XYZ=6.50,8.00,0.90/
&DEVC ID='VF_1_15', QUANTITY='VOLUME FRACTION', SPEC_ID='HELIUM',
XYZ=6.50,8.00,0.4000/
&DEVC ID='VF_1_21', QUANTITY='VOLUME FRACTION', SPEC_ID='HELIUM',
XYZ=6.50,4.80,2.40/
&DEVC ID='VF_2_01', QUANTITY='VOLUME FRACTION', SPEC_ID='HELIUM',
XYZ=5.50,5.00,5.00/
&DEVC ID='VF_2_11', QUANTITY='VOLUME FRACTION', SPEC_ID='HELIUM',
XYZ=8.00,2.00,5.00/
&DEVC ID='VF_2_21', QUANTITY='VOLUME FRACTION', SPEC_ID='HELIUM',
XYZ=2.60,2.00,5.00/
&DEVC ID='VF_2_31', QUANTITY='VOLUME FRACTION', SPEC_ID='HELIUM',
XYZ=2.60,7.00,5.00/
&DEVC ID='VF_2_41', QUANTITY='VOLUME FRACTION', SPEC_ID='HELIUM',
XYZ=8.00,7.00,5.00/
&DEVC ID='VF_3_01', QUANTITY='VOLUME FRACTION', SPEC_ID='HELIUM',
XYZ=8.00,7.00,7.60/
&DEVC ID='VF_3_11', QUANTITY='VOLUME FRACTION', SPEC_ID='HELIUM',
XYZ=8.00,2.00,7.60/

&MATL ID='CONCRETE',
    FYI='NBSIR 88-3752 - ATF NIST Multi-Floor Validation',
    SPECIFIC_HEAT=1.04,
    CONDUCTIVITY=1.80,
    DENSITY=2.2800000E003/
&MATL ID='STEEL',
    FYI='Drysdale, Intro to Fire Dynamics - ATF NIST Multi-Floor Validation',
    SPECIFIC_HEAT=0.4600,
    CONDUCTIVITY=45.80,
    DENSITY=7.8500000E003,

```
        EMISSIVITY=0.95/
&MATL ID='GYPSUM',
    FYI='NBSIR 88-3752 - ATF NIST Multi-Floor Validation',
    SPECIFIC_HEAT=1.09,
    CONDUCTIVITY=0.1700,
    DENSITY=930.00/

&SURF ID='cement board',
    COLOR='GRAY 60',
    MATL_ID(1,1)='CONCRETE',
    MATL_MASS_FRACTION(1,1)=1.00,
    THICKNESS(1)=0.0800/
&SURF ID='steel',
    RGB=255,153,153,
    MATL_ID(1,1)='STEEL',
    MATL_MASS_FRACTION(1,1)=1.00,
    THICKNESS(1)=5.0000000E-003/
&SURF ID='gypsum *2',
    COLOR='WHITE',
    MATL_ID(1,1)='GYPSUM',
    MATL_ID(2,1)='GYPSUM',
    MATL_MASS_FRACTION(1,1)=1.00,
    MATL_MASS_FRACTION(2,1)=1.00,
    THICKNESS(1:2)=0.0160,0.0160/
&SURF ID='MySmoke',
    FYI='Helium mixture/pure helium',
    RGB=26,204,26,
    MASS_FLUX(1)=1.0000000E-004,
    TAU_MF(1)=1.00/
&SURF ID='Helium',
    COLOR='RED',
    MASS_FLUX(2)=0.1100,
    TAU_MF(2)=-80.00/
&SURF ID='INERT_FIRE',
    FYI='Forcefully invoke the mixture fraction model.',
    HRRPUA=1.0000000E-003/

&OBST XB=2.88,5.24,5.45,5.53,2.60,5.04, SURF_ID='cement board'/ stair wall[1]
&OBST XB=2.88,5.24,4.46,4.54,2.60,5.04, SURF_ID='cement board'/ stair wall 2[1]
&OBST XB=5.24,5.32,4.46,5.53,2.60,5.04, SURF_ID='cement board'/ stair wall 4
&OBST XB=2.80,2.88,4.46,5.53,5.20,7.64, SURF_ID='cement board'/ stair wall 3
&OBST XB=5.24,5.32,5.45,6.25,5.20,7.64, SURF_ID='cement board'/ Wall[1][1]
&OBST XB=6.74,6.82,0.00,9.00,5.20,7.64, SURF_ID='cement board'/ Wall[1][1]
&OBST XB=5.24,5.32,0.00,4.54,5.20,7.64, SURF_ID='cement board'/ Wall[1]
&OBST XB=5.24,5.32,5.45,9.00,0.00,2.44, SURF_ID='cement board'/ Wall[1]
```

&OBST XB=2.88,5.24,5.45,5.53,5.20,7.64, SURF_ID='cement board'/ stair wall[2]
&OBST XB=2.88,5.24,4.46,4.54,5.20,7.64, SURF_ID='cement board'/ stair wall 2[2]
&OBST XB=6.82,10.57,4.46,4.54,5.20,7.64, SURF_ID='cement board'/ wall
&OBST XB=5.24,6.74,6.25,6.33,5.20,7.64, SURF_ID='cement board'/ stair wall[2][1]
&OBST XB=5.24,6.74,1.72,1.80,5.20,7.64, SURF_ID='cement board'/ stair wall[2][1][1]
&OBST XB=2.80,2.88,4.46,5.53,0.00,2.44, SURF_ID='cement board'/ stair wall 3[1]
&OBST XB=5.24,5.32,0.00,4.54,0.00,2.44, SURF_ID='cement board'/ Wall
&OBST XB=2.88,5.24,5.45,5.53,0.00,2.44, SURF_ID='cement board'/ stair wall
&OBST XB=2.88,5.24,4.46,4.54,0.00,2.44, SURF_ID='cement board'/ stair wall 2
&OBST XB=5.32,10.57,3.70,3.78,0.00,2.44, SURF_ID='cement board'/ wall3
&OBST XB=-0.0500,10.62,-0.0500,0.00,0.00,7.64, COLOR='INVISIBLE',
SURF_ID6='steel','steel','steel','cement board','steel','steel'/ Bottom Wall (Min X)
&OBST XB=10.57,10.62,-0.0500,9.05,0.00,7.64, COLOR='INVISIBLE',
SURF_ID6='cement board','steel','steel','steel','steel','steel'/ Right Wall (Max Y)
&OBST XB=-0.0500,10.62,9.00,9.05,0.00,7.64, COLOR='INVISIBLE',
SURF_ID6='steel','steel','cement board','steel','steel','steel'/ Top Wall (Max X)
&OBST XB=-0.0500,0.00,-0.0500,9.05,0.00,7.64, COLOR='INVISIBLE',
SURF_ID6='steel','cement board','steel','steel','steel','steel'/ Left Wall (Min Y)
&OBST XB=0.00,10.57,0.00,9.00,2.44,2.60, SURF_IDS='cement board','cement
board','gypsum *2'/ ceiling1
&OBST XB=0.00,10.57,0.00,9.00,-0.1600,0.00, SURF_ID='cement board'/ floor
&OBST XB=0.00,10.57,0.00,9.00,5.04,5.20, SURF_IDS='cement board','cement
board','gypsum *2'/ ceiling1[1]
&OBST XB=0.00,10.57,0.00,9.00,7.64,7.80, COLOR='INVISIBLE',
SURF_IDS='steel','steel','gypsum *2'/ ceiling1[2]
&OBST XB=8.20,8.60,6.20,6.60,0.50,0.80, SURF_IDS='INERT','MySmoke','INERT'/
Smoke generator
&OBST XB=2.77,3.02,4.63,5.40,2.55,2.55, SURF_ID='steel'/ Slab[1]
&OBST XB=3.02,3.27,4.63,5.40,2.80,2.80, SURF_ID='steel'/ Slab[1]
&OBST XB=3.27,3.52,4.63,5.40,3.06,3.06, SURF_ID='steel'/ Slab[1]
&OBST XB=3.52,3.78,4.63,5.40,3.31,3.31, SURF_ID='steel'/ Slab[1]
&OBST XB=3.78,4.03,4.63,5.40,3.57,3.57, SURF_ID='steel'/ Slab[1]
&OBST XB=4.03,4.28,4.63,5.40,3.82,3.82, SURF_ID='steel'/ Slab[1]
&OBST XB=4.28,4.53,4.63,5.40,4.07,4.07, SURF_ID='steel'/ Slab[1]
&OBST XB=4.53,4.78,4.63,5.40,4.33,4.33, SURF_ID='steel'/ Slab[1]
&OBST XB=4.78,5.03,4.63,5.40,4.58,4.58, SURF_ID='steel'/ Slab[1]
&OBST XB=5.03,5.28,4.63,5.40,4.84,4.84, SURF_ID='steel'/ Slab[1]
&OBST XB=3.02,3.02,4.63,5.40,2.55,2.80, SURF_ID='steel'/ Slab[1]
&OBST XB=3.27,3.27,4.63,5.40,2.80,3.06, SURF_ID='steel'/ Slab[1]
&OBST XB=3.52,3.52,4.63,5.40,3.06,3.31, SURF_ID='steel'/ Slab[1]
&OBST XB=3.78,3.78,4.63,5.40,3.31,3.57, SURF_ID='steel'/ Slab[1]
&OBST XB=4.03,4.03,4.63,5.40,3.57,3.82, SURF_ID='steel'/ Slab[1]
&OBST XB=4.28,4.28,4.63,5.40,3.82,4.07, SURF_ID='steel'/ Slab[1]
&OBST XB=4.53,4.53,4.63,5.40,4.07,4.33, SURF_ID='steel'/ Slab[1]
&OBST XB=4.78,4.78,4.63,5.40,4.33,4.58, SURF_ID='steel'/ Slab[1]

&OBST XB=5.03,5.03,4.63,5.40,4.58,4.84, SURF_ID='steel'/ Slab[1]
&OBST XB=5.28,5.28,4.63,5.40,4.84,5.09, SURF_ID='steel'/ Slab[1]

&HOLE
XB=5.2450000E000,5.3250000E000,4.5900000E000,5.4000000E000,2.6000000E000,4.6500000E000/ stair door
&HOLE
XB=6.7400000E000,6.8200000E000,2.5000000E000,3.3100000E000,5.2000000E000,7.2500000E000/ stair door[1]
&HOLE
XB=6.7400000E000,6.8200000E000,4.8000000E000,5.6100000E000,5.2000000E000,7.2500000E000/ stair door[1][1]
&HOLE
XB=2.8850000E000,5.3250000E000,4.5400000E000,5.4500000E000,2.4400000E000,2.6000000E000/ Hole
&HOLE
XB=2.8850000E000,5.3250000E000,4.5400000E000,5.4500000E000,5.0400000E000,5.2000000E000/ Hole[1]
&HOLE
XB=2.0000000E000,2.8900000E000,8.9000000E000,9.1000000E000,2.6000000E000,4.6700000E000/ door
&HOLE
XB=1.0500000E001,1.0700000E001,5.3500000E000,7.3500000E000,1.8000000E000,2.3000000E000/ basement opening

&VENT SURF_ID='Helium', XB=7.90,8.90,5.90,6.90,0.00,0.00/ Burner
&VENT SURF_ID='OPEN', XB=2.00,2.89,9.00,9.00,2.60,4.67/ door
&VENT SURF_ID='OPEN', XB=10.57,10.57,5.35,7.35,1.80,2.30/ window

&SLCF QUANTITY='VOLUME FRACTION', SPEC_ID='HELIUM', VECTOR=.TRUE., PBY=2.00/
&SLCF QUANTITY='MASS FRACTION', SPEC_ID='MySmoke', PBY=2.00/
&SLCF QUANTITY='DENSITY', PBY=2.00/
&SLCF QUANTITY='VELOCITY', VECTOR=.TRUE., PBY=2.00/
&SLCF QUANTITY='VOLUME FRACTION', SPEC_ID='HELIUM', PBY=5.00/
&SLCF QUANTITY='MASS FRACTION', SPEC_ID='MySmoke', PBY=5.00/
&SLCF QUANTITY='VELOCITY', VECTOR=.TRUE., PBY=5.00/
&SLCF QUANTITY='VOLUME FRACTION', SPEC_ID='HELIUM', PBY=6.40/
&SLCF QUANTITY='MASS FRACTION', SPEC_ID='MySmoke', PBY=6.40/
&SLCF QUANTITY='DENSITY', PBY=6.40/
&SLCF QUANTITY='VELOCITY', VECTOR=.TRUE., PBY=6.40/
&SLCF QUANTITY='VOLUME FRACTION', SPEC_ID='HELIUM', PBY=7.00/

&TAIL /